

fachhochschule hamburg

FACHBEREICH FAHRZEUGTECHNIK

Studiengang Flugzeugbau

Berliner Tor 5  
D - 20099 Hamburg

in Zusammenarbeit mit:

University of Limerick  
Department of Mechanical & Aeronautical Engineering  
Limerick, Ireland

Diplomarbeit  
- Flugzeugbau -

## Performance Assessment of Hybrid Laminar Flow Control (HLFC) Aircraft

Verfasser: Conny Schmidt

Abgabedatum: 06.07.01

Betreuer: Trevor Young, Lecturer

1. Prüfer: Prof. Dr.-Ing. Dieter Scholz, MSME
2. Prüfer: Prof. Dr.-Ing. Hartmut Zingel



## **Abstract**

The application of Hybrid Laminar Flow Control (HLFC) offers the potential of significant fuel savings due to drag reduction. Since practical explorations during flights are very expensive, computer software, which models the en-route performance of jet transport aircraft, has been established. This report describes this software in detail. Furthermore the document deals with a modification of this program by entering performance data of a typical jet transport aircraft in the general class of the Airbus A330. Of particular importance is how the information is processed and how it is made compatible to the software.

After assuring the reliability of the modified program by comparing its results with information from published sources, a sensitivity study is performed to investigate the possible impact of HLFC on fuel usage. These results are discussed and evaluated, and some conclusions are given.

The necessary background for all applied calculations is provided in the form of basic explanations at the beginning of this report.



## Performance Assessment of HLFC (Hybrid Laminar Flow Control) Aircraft

*Diplomarbeit* (diplom thesis) in compliance with § 21 of „Ordnung der staatlichen Zwischen- und Diplomprüfung in den Studiengängen Fahrzeugbau und Flugzeugbau an der Fachhochschule Hamburg“.

### Background

Hybrid Laminar Flow Control (HLFC) is an drag reduction technique that permits extended laminar flow control on an aircraft surface at chord Reynolds numbers normally associated with turbulent flow. The delay in transition of the boundary layer is usually achieved by the application of suction over the first 10 to 20% of the chord (i.e. ahead the front spar of the wing). With HLFC a correctly profiled wing, empennage or nacelle could permit laminar flow to extend back to about 50% of the chord. This is however at the expense of an increase in system weight, maintenance costs and increased Specific Fuel Consumption. A computer performance model of a twin engine aircraft in the class of the Boeing 757 has been developed at the University of Limerick to study the potential fuel saving of a HLFC aircraft, taking into account the possible increase in the SFC (Specific Fuel Consumption) of the engines due to the energy required for the suction system. In calculating the fuel required for a specific mission, the program uses a series of “lookup” tables that define the primary aerodynamic characteristics of the aircraft and the fuel flow versus thrust relationships (as a function of height and air-speed).

### Task

It is required that the candidate develops a second series of „lookup“ tables for a generic aircraft of greater size and longer range, in the class of the Airbus A330-200. Partial performance information on this aircraft is available. It is required that the candidate works backwards from the given performance results to derive the basic aerodynamic characteristics and the fuel relationships for this aircraft, using the existing twin jet data as a model. Having established the input data for the second aircraft, it will be necessary to validate the model against published operational data for this aircraft. If necessary the input data will be adjusted to improve the accuracy of the results. The computer model will then be used to perform a sensitivity study to investigate the impact on fuel burn of various levels of Drag reduction, SFC penalty, and OEW increase.



# Contents

	Page
List of figures.....	9
List of tables .....	11
Nomenclature.....	13
List of abbreviations.....	15
List of terms and definitions .....	16
<b>1 Introduction.....</b>	<b>18</b>
1.1 Motivation.....	18
1.3 Objectives.....	20
1.4 Literature review.....	21
1.5 Structure arranged of work .....	22
<b>2 Aerodynamics and Performance .....</b>	<b>23</b>
2.1 The Flight Profile.....	23
2.2 Fuel Planning.....	24
2.3 The Atmosphere .....	28
2.4 Flight Level.....	28
2.5 Lift and Drag .....	28
2.5.1 Basic Information .....	30
2.5.2 The Lift .....	30
2.5.3 The Drag .....	31
2.5.4 The Drag Polar and L/D ratio .....	31
2.6 General Cruise Calculations .....	34
2.6.1 Level Flight .....	34
2.6.2 Fuel Consumption.....	36
2.6.3 Range Cruise Calculations .....	37
2.6.4 Time Cruise Calculations .....	39
2.6.5 Integrated Range and Integrated Time .....	40
2.7 Climb and Descent.....	41
2.7.1 Climb angle and Rate of Climb (ROC) .....	42
2.7.2 The acceleration factor .....	44
2.7.3 Climb schedule .....	45
2.7.4 Time to Climb.....	46
2.7.5 Descent Calculations.....	48
2.7.6 Glide angle .....	48

<b>3</b>	<b>Hybrid Laminar Flow Control (HLFC)</b> .....	50
3.1	Structure and Function of HLFC.....	51
3.2	Reasons for HLFC System failures.....	51
3.3	HLFC Research undertaken .....	53
3.4	Other Drag Reducing Devices.....	55
<b>4</b>	<b>Performance Calculation Software</b> .....	58
4.1	The Structure of the Young's Program .....	58
4.2	The Function of the Young's Program .....	59
4.2.1	The Cruise Calculation Table .....	61
4.2.2	The Climb Calculation Table.....	63
4.2.3	The Macros .....	65
4.2.4	Remark on Young's Program .....	67
4.3	Specification of Straubinger's Program .....	67
4.4	Comparison of Results from both Programs .....	69
<b>5</b>	<b>Modification for a long-range class Aircraft</b> .....	71
5.1	Flight Test Data.....	71
5.1.1	Corrected Fuel flow tables .....	72
5.1.2	The Drag Polar.....	75
5.1.3	Maximum Climb and in-flight idle Thrust .....	78
5.2	Data of the Operating Manual A330.....	81
5.2.1	Example of Operating Manual for Long Range Speed.....	82
5.2.2	Example for a fixed Mach number.....	84
5.5	Comparison to an Airbus Briefing .....	85
<b>6</b>	<b>The Sensitivity Study</b> .....	86
6.1	Study 1 - Impact on Block fuel.....	86
6.2	Results of Study 1.....	87
6.2	Study 2 - Modification based on Practical Information .....	90
6.4	Results of Study 2.....	90
6.5	Study 3 - General Statement .....	93
<b>7</b>	<b>Discussion</b> .....	94
<b>8</b>	<b>Conclusion</b> .....	98
	<b>References</b> .....	99
	Acknowledgement .....	102

<b>Appendix A (Configuration Tables of the modified Program)</b> .....	103
<b>Appendix B (Flowcharts of the Programs)</b> .....	115
B.1 Flowcharts of Straubinger’s Program.....	115
B.2 Simple Flowchart of Young’s Program .....	124
<b>Appendix C (Original example of Operating Manual A330)</b> .....	125
C.1 Original Example for LR speed.....	125
C.2 Comparison with computed Results of the modified Program .....	142
<b>Appendix D (Example according to the Operating Manual A330)</b> .....	143
D.1 Example for a fixed Mach number .....	143
D.2 Comparison with computed Results of the modified Program .....	149
<b>Appendix E (Airspeed Conversations)</b> .....	150
<b>Appendix F (Units Conversations)</b> .....	152
<b>Appendix G (ISA Table and Basic Data)</b> .....	153



## List of figures

<b>Figure 2.1</b>	Complete mission of an aircraft .....	23
<b>Figure 2.2</b>	Typical pressure pattern surrounding an airfoil .....	29
<b>Figure 2.3</b>	Lift and drag .....	29
<b>Figure 2.4</b>	Relationship between lift coefficient and angle of attack .....	30
<b>Figure 2.5</b>	Drag breakdown .....	31
<b>Figure 2.6</b>	The drag polar .....	32
<b>Figure 2.7</b>	Influence of Mach number on drag .....	33
<b>Figure 2.8</b>	Drag polars for several Mach numbers .....	34
<b>Figure 2.9</b>	General forces acting on an aircraft .....	34
<b>Figure 2.10</b>	Speed schedule for minimum drag .....	35
<b>Figure 2.11</b>	Specific Air Range .....	40
<b>Figure 2.12</b>	Integrated Range .....	41
<b>Figure 2.13</b>	Forces acting on an aircraft performing a climb .....	41
<b>Figure 2.14</b>	Best ROC speed compared to constant EAS and Mach number.....	45
<b>Figure 2.15</b>	Typical climb schedule .....	46
<b>Figure 2.16</b>	Rate of climb .....	47
<b>Figure 2.17</b>	Simple scheme for a weight determination method .....	47
<b>Figure 2.18</b>	Minimum glide angle consideration .....	49
<b>Figure 3.1</b>	Comparison of laminar flow techniques .....	50
<b>Figure 3.2</b>	Location of HLFC applied on a wing .....	51
<b>Figure 3.3</b>	Overview of laminar flow control projects.....	53
<b>Figure 3.4</b>	Laminar flow extend obtained on Boeing 757 HLFC flight test.....	54
<b>Figure 3.5</b>	Enlarged model of the sharkskin.....	55
<b>Figure 3.6</b>	Slotted wing-tips of a bird.....	56
<b>Figure 3.7</b>	Multi-Wing-Loop .....	56
<b>Figure 3.8</b>	Model of an adaptive wing based on memory wires.....	57
<b>Figure 4.1</b>	The control and input box .....	59
<b>Figure 4.2</b>	Input Box for HLFC data.....	60
<b>Figure 4.3</b>	Hierarchy of macros.....	68
<b>Figure 4.4</b>	Input box of Straubinger's program containing the input parameters .....	69
<b>Figure 5.1</b>	Corrected fuel flow curves for several Mach numbers at 35000 ft.....	73
<b>Figure 5.2</b>	Intersection point at 30000 ft .....	74
<b>Figure 5.3</b>	Intersection point at 29000 ft .....	74
<b>Figure 5.4</b>	Comparison of available drag polar data with parabolic deviation .....	76
<b>Figure 5.5</b>	Extrapolation of drag polar data.....	77
<b>Figure 5.6</b>	Net thrust for several heights .....	79
<b>Figure 5.7</b>	payload range diagram of A330-200 .....	85

<b>Figure 6.1</b>	Block fuel affected by the particular impacts (study 1).....	87
<b>Figure 6.2</b>	Block fuel savings due to the particular impacts (study 1).....	88
<b>Figure 6.3</b>	Comparison of block fuel savings (study 1) .....	89
<b>Figure 6.4</b>	Block fuel savings due to the particular impacts (study 2).....	91
<b>Figure 6.5</b>	Comparison of block fuel savings (study 2) .....	92
<b>Figure 6.6</b>	Cross-reading of block fuel savings .....	93
<b>Figure B.1</b>	Flowchart of main macro (Diversion for fuel and range calculation) .....	115
<b>Figure B.2</b>	Flowchart of main macro (Fuel and range calculation).....	116
<b>Figure B.3</b>	Flowchart of main macro (Calculation of payload) .....	117
<b>Figure B.4</b>	Flowchart of macro for cruise calculation <i>subcruise</i> .....	118
<b>Figure B.5</b>	Flowchart of macro for cruise calculation <i>subcruise</i> .....	119
<b>Figure B.6</b>	Flowchart of macro for climb and descent <i>subclides</i> .....	120
<b>Figure B.7</b>	Flowchart of macro for climb and descent <i>subclides</i> .....	121
<b>Figure B.8</b>	Flowchart of <i>subfuel</i> (controls the interpolation of fuel flow) .....	122
<b>Figure B.9</b>	Flowchart of Newton's interpolation <i>subnewton</i> .....	123
<b>Figure B.10</b>	Flowchart of calculations .....	124
<b>Figure C.1</b>	Description of cruise fuel and time determination (part 1).....	125
<b>Figure C.2</b>	Description of cruise fuel and time determination (part 2).....	126
<b>Figure C.3</b>	Table for cruise fuel and time determination .....	127
<b>Figure C.4</b>	Description of corrections and determination of end results .....	128
<b>Figure C.5</b>	Table of corrections and determination of end results .....	129
<b>Figure C.6</b>	Table for corrections due to wind effects.....	130
<b>Figure C.7</b>	Integrated cruise table for LR at FL310 (part 1).....	131
<b>Figure C.8</b>	Integrated cruise table for LR at FL310 (part 2).....	132
<b>Figure C.9</b>	Integrated cruise table for LR at FL310 (part 3).....	133
<b>Figure C.10</b>	Integrated cruise table for LR at FL350 (part 1).....	134
<b>Figure C.11</b>	Integrated cruise table for LR at FL350 (part 2).....	135
<b>Figure C.12</b>	Integrated cruise table for LR at FL390 (part 1).....	136
<b>Figure C.13</b>	Integrated cruise table for LR at FL390 (part 2).....	137
<b>Figure C.14</b>	Climb correction tables .....	138
<b>Figure C.15</b>	Descent correction tables .....	139
<b>Figure C.16</b>	Alternate determination tables .....	140
<b>Figure C.17</b>	General information of constants.....	141
<b>Figure D.1</b>	Integrated cruise table for M0.80 opt. FL (part 1) .....	146
<b>Figure D.2</b>	Integrated cruise table for M0.80 opt. FL (part 2) .....	147
<b>Figure D.3</b>	Integrated cruise table for M0.80 opt. FL (part 3) .....	148

## List of tables

<b>Table 3.1</b>	Events which impact fuel usage on HLFC aircraft .....	52
<b>Table 4.1</b>	The contents of the particular pages .....	59
<b>Table 4.2</b>	Types of input.....	68
<b>Table 4.3</b>	Comparison of results from the programs of Straubinger and Young .....	70
<b>Table 5.1</b>	Comparison of input data of both versions .....	71
<b>Table 5.2</b>	Corrected fuel flow data for rounded thrust values .....	72
<b>Table 5.3</b>	High-speed drag polar data .....	75
<b>Table 5.4</b>	The applied factors for the different Mach numbers.....	77
<b>Table 5.5</b>	Thrust over delta data of Boeing 757 class aircraft (PEM).....	78
<b>Table 5.6</b>	Calculation table of the exponent n.....	80
<b>Table 5.7</b>	Integrated range of the program and of the Operating Manual.....	83
<b>Table 5.8</b>	Input parameters of the fixed Mach number example.....	84
<b>Table 5.9</b>	Comparison of payload range data .....	85
<b>Table 6.1</b>	Cases of study 1.....	86
<b>Table 6.2</b>	Results for block fuel (study 1) .....	87
<b>Table 6.3</b>	Change in block fuel (study 1).....	88
<b>Table 6.4</b>	Block fuel savings (study 1) .....	89
<b>Table 6.5</b>	Cases of study 2.....	90
<b>Table 6.6</b>	Results for block fuel (study 2) .....	90
<b>Table 6.7</b>	Block fuel savings (study 2) .....	92
<b>Table A.1</b>	Corrected Fuel Flow, altitude 0 ft (part 1).....	103
<b>Table A.2</b>	Corrected Fuel Flow, altitude 0 ft (part 2).....	103
<b>Table A.3</b>	Corrected Fuel Flow, altitude 1500 ft (part 1) .....	103
<b>Table A.4</b>	Corrected Fuel Flow, altitude 1500 ft (part 2) .....	104
<b>Table A.5</b>	Corrected Fuel Flow, altitude 5000 ft (part 1) .....	104
<b>Table A.6</b>	Corrected Fuel Flow, altitude 5000 ft (part 2) .....	104
<b>Table A.7</b>	Corrected Fuel Flow, altitude 10000 ft (part 1) .....	104
<b>Table A.8</b>	Corrected Fuel Flow, altitude 10000 ft (part 2) .....	105
<b>Table A.9</b>	Corrected Fuel Flow, altitude 15000 ft (part 1) .....	105
<b>Table A.10</b>	Corrected Fuel Flow, altitude 15000 ft (part 2) .....	105
<b>Table A.11</b>	Corrected Fuel Flow, altitude 20000 ft (part 1) .....	105
<b>Table A.12</b>	Corrected Fuel Flow, altitude 20000 ft (part 2) .....	105
<b>Table A.13</b>	Corrected Fuel Flow, altitude 25000 ft (part 1) .....	106
<b>Table A.14</b>	Corrected Fuel Flow, altitude 25000 ft (part 2) .....	106
<b>Table A.15</b>	Corrected Fuel Flow, altitude 29000 ft.....	106

<b>Table A.16</b>	Corrected Fuel Flow, altitude 30000 ft.....	106
<b>Table A.17</b>	Corrected Fuel Flow, altitude 31000 ft.....	107
<b>Table A.18</b>	Corrected Fuel Flow, altitude 32000 ft.....	107
<b>Table A.19</b>	Corrected Fuel Flow, altitude 33000 ft.....	107
<b>Table A.20</b>	Corrected Fuel Flow, altitude 34000 ft.....	107
<b>Table A.21</b>	Corrected Fuel Flow, altitude 35000 ft.....	108
<b>Table A.22</b>	Corrected Fuel Flow, altitude 36000 ft.....	108
<b>Table A.23</b>	Corrected Fuel Flow, altitude 37000 ft.....	108
<b>Table A.24</b>	Corrected Fuel Flow, altitude 38000 ft.....	108
<b>Table A.25</b>	Corrected Fuel Flow, altitude 39000 ft.....	109
<b>Table A.26</b>	Corrected Fuel Flow, altitude 40000 ft.....	109
<b>Table A.27</b>	Corrected Fuel Flow, altitude 41000 ft.....	109
<b>Table A.28</b>	Maximum climb thrust .....	110
<b>Table A.29</b>	Minimum idle in-flight thrust.....	111
<b>Table A.30</b>	Minimum idle fuel flow .....	111
<b>Table A.31</b>	Data for brake release to 1500 ft.....	112
<b>Table A.32</b>	Recommended holding speed at 1500 ft .....	112
<b>Table A.33</b>	High-speed drag polar (part 1) .....	113
<b>Table A.34</b>	High-speed drag polar (part 2) .....	114
<b>Table A.35</b>	High-speed drag polar (part 3).....	114
<b>Table C.1</b>	Comparison of results of LR speed example.....	142
<b>Table D.1</b>	Cruise fuel and time calculation.....	143
<b>Table D.2</b>	Corrections and calculation of block fuel, payload and flight time.....	144
<b>Table D.3</b>	Comparison of results of fixed Mach number example.....	149
<b>Table G.1</b>	ISA Table .....	153
<b>Table G.2</b>	Basic data for ISA-Table Calculation .....	154

# Nomenclature

$a$	acceleration
$a$	speed of sound
$b$	constant
$A$	aspect ratio
$c$	specific fuel consumption (also SFC)
$CAS$	Calibrated Airspeed
$c_D$	drag coefficient
$c_L$	lift coefficient
$D$	drag
$e$	Euler constant
$e$	Oswald efficiency factor
$E$	lift-to-drag ratio
$EAS$	Equivalent Airspeed
$F$	force
$FN$	net thrust per engine
$f_{acc}$	acceleration factor
$g$	acceleration due to gravity
$h$	height
$k$	factor
$L$	lapse rate of temperature in ISA
$L$	lift
$m$	aircraft mass
$m$	slope
$M$	Mach number
$n$	exponent
$p$	pressure
$Q$	fuel flow
$q$	dynamic pressure
$r_a$	specific air range (also SAR)
$R$	gas constant of air
$R$	range
$R$	resultant (force)
$S$	wing reference area
$t$	time
$T$	thrust
$T$	temperature
$v$	velocity (also TAS)
$v_v$	vertical airspeed (also ROC)

$W$	weight (force)
$x$	coordinate in forward direction
$x$	engine dependent exponent
$x$	still air distance
$y$	coordinate in starboard direction
$y$	exponent for drag polar deviation
$z$	coordinate in downward direction

## Greek

$\acute{\alpha}$	angle of attack
$\tilde{\alpha}$	ratio of specific heat of air
$\tilde{\alpha}$	still air climb angle
$\ddot{\alpha}$	pressure ratio referred to sea level
$\grave{\epsilon}$	temperature ratio referred to sea level
$\ddot{\epsilon}$	engine dependent factor
$\tilde{n}$	mass density
$\acute{o}$	density ratio referred to sea level
$\emptyset$	velocity dependent factor for acceleration factor

## Subscripts

$a$	air speed
$acc$	acceleration
$est$	estimated value
$corr$	corrected
$D$	referred to drag
$i$	induced
$i$	interval
$I$	inertia
$F$	Fuel
$L$	referred to lift
$M$	Mach number effect
$n$	designation of an interval
$T$	total values
$trop$	referred to Troposphere
$0$	zero lift
$0, SL$	sea level values

## List of abbreviations

A/C	Aircraft
ATA	Air Transport Association
BRW	Brake Release Weight (also OTOW)
CAS	Calibrated Air Speed
C.P.	Centre of Pressure
DIN	Deutsche Industrienormen
DLR	Deutsche Forschungsanstalt für Luft- und Raumfahrt
DVA	Deutsche Verlags-Anstalt
EAS	Equivalent Air Speed
FL	Flight Level
HLFC	Hybrid Laminar Flow Control
ICAO	International Civil Aviation Association
ISA	International Standard Atmosphere
JAR	Joint Airworthiness Requirements
LFC	Laminar Flow Control
LR	Long Range
MPL	Maximum Payload
MTOW	Maximum Take-Off Weight
MZFW	Maximum Zero Fuel Weight
NLF	Natural Laminar Flow
OEW	Operating Empty Weight
PEM	Performance Engineer's Manual
P/L	Payload
ROC	Rate Of Climb
ROD	Rate Of Descent
ROS	Rate Of Sink
SAR	Specific Air Range
SFC	Specific Fuel Consumption
TAS	True Air Speed
TOC	Top Of Climb
TOD	Top Of Descent
UK	United Kingdom
URL	Universal Resource Locator
ZFW	Zero Fuel Weight

# List of Terms and Definitions

## Airspeeds

The airspeed definitions are according to **Young (1999) and Boeing (1989)**.

### Ground Speed

The velocity of the aeroplane relative to the ground.

### True airspeed (TAS, $v$ )

The velocity of the airplane relative to the surrounding air.

### Equivalent airspeed (EAS)

The velocity the airplane would have at sea level when developing the same dynamic pressure.

### Calibrated airspeed (CAS)

The airspeed reading on a calibrated air speed indicator, which is corrected for position and ambient atmospheric conditions.

In appendix E can be found the necessary equations for the airspeed conversions.

## Weights

The Weights are defined according to the **ATA-Chapter, Specification 100**.

### Operating Empty Weight (OEW)

Basic empty weight or fleet empty weight plus operational items.

### Maximum Design Take-Off Weight (MTOW)

Maximum Weight for takeoff as limited by aircraft strength and airworthiness requirements. (This is the maximum weight at start of takeoff run).

### Operational Take-Off Weight (OTOW) or Brake Release Weight (BRW)

Maximum authorized weight for takeoff. (It is subject to airport, operational, and related restrictions. This is the weight at the start of takeoff run and must not exceed maximum design takeoff weight)



**Maximum Design Zero Fuel Weight (MZFW)**

Maximum weight allowed before usable fuel and other specified usable agents must be loaded in defined sections of the aircraft as limited by strength and airworthiness requirements.

**Actual Zero Fuel Weight (AZFW) or Zero Fuel Weight (ZFW)**

Operational empty weight plus payload. (It must not exceed maximum design zero fuel weight)

**Maximum Payload (MPL)**

Maximum design zero fuel weight minus operational empty weight.

**Payload (P/L)**

Weight of passengers, cargo, and baggage. (These may be revenue and/or nonrevenue)

**Coordinate system**

The coordinates are defined according to the **Young (1999)**.

This report is based on a conventional coordinate system, which is a right-handed set of rectangular axes through the centre of gravity. The axes are fixed in the aircraft and move with it. Point 0 is the centre of gravity,  $O_x$  is in a forward direction,  $O_y$  is starboard and  $O_z$  downwards.

The aircraft is considered as a rigid body.

# 1 Introduction

## 1.1 Motivation

Throughout the history of aeronautics it has always been an important task to improve the aerodynamic properties of aircraft. While in the early years of aircraft construction main purpose was to gain more powerful designs, the current research generally aims to achieve lower fuel consumption. As the shape of conventional aircraft has been optimized over the decades drag reducing is of particular interest these days. Research in this area has flourished since 1970 because of the shortage and, therefore higher fuel prices, due to the oil crisis. Nowadays, the hard competition between the airlines with lots of dumping prices for the flights is rather a topic than the fuel price.

Additionally the exhaustion of worldwide oil reserves is foreseeable and newly developed techniques are usually less efficient in the first years of their usage. Therefore, optimized aerodynamic characteristics are indispensable to keep up current air traffic in the future. This is of great significance, since mobility is one of the most important pillars of modern economy.

Presently, Hydrogen is the propellant, which presents the most promising possibilities as a replacement for kerosene. However, this would still entail some problems, which are not properly solved yet. Steady low temperatures are needed to keep it in its liquid state and it is very voluminous. Therefore, an at least cylindrical structure is required to keep the outer surface and thus the weight as low as possible, which brings with it the disadvantage that the wings cannot be used anymore to store fuel. Nevertheless, the developing explosive mixture in contact with Oxygen is problematic and demands high safety requirements regarding the tanks.

The environmental implications have to be considered from two points of view. On one hand, air traffic is a way to bring high numbers of passengers from A to B, which causes less environmental damage than all other means of transportation by taking into account, that it has to be within an acceptable time. Because of the meanwhile gigantic dimensions of transport jets, like for instance the new A380, the fuel burned per person is similar to that burned on an average car journey. In addition, an aeroplane can take the direct and, therefore, the shortest route without needing many en-route ground facilities. On the other hand, this occurs at the expense of the ozone layer due to damaging emissions like Nitrogen oxides because most transport jets operate at altitudes within the stratosphere for efficiency reasons. Another dangerous substance, which develops while fuel is being burned, is carbon dioxide. This is one of the gases, which is most responsible for the greenhouse effect. Since water vapour, which comes into existence by using Hydrogen, has also an adverse influence, the greenhouse effect will continue to be a source of concern in the future.

Several other possibilities also exist to improve the efficiency of an aircraft, for instance a reduction of weight or an increase in the engine's efficiency. The latter can be achieved by increasing the bypass ratio, which defines how much air passes through the engine's core in relation to the actual air used to burn the fuel. A crude rule is that the higher this ratio, the higher the engine's efficiency, which is, of course, limited by the fact that a combustion chamber of a certain size is needed to gain enough power. On the other hand the fan cannot, even unducted, get an arbitrary large radius as this produces additional drag and results in lower velocities being reached by the aeroplane.

Other possible solutions include the boundary layer suction from turbine blades in order to reduce drag peaks affected by sonic velocities of the passing air, or blade cooling, to allow higher rotation speeds.

Weight reduction is a subject that gains high importance due to the possibility of replacing aluminium alloys with much lighter composite materials, made of carbon fibre. It is not yet possible to use them for all aircraft structures, because, in the majority of cases, the required reliability cannot be assured. However, these materials are becoming more technologically advanced so that more and more parts of the aircraft will be made of composites prospective, and in aircraft construction every kilogram counts.

Here it may also be cited, that in the remote future the shape of aircraft might change. A study concerning an oblique flying wing is being carried out by DASA and NASA is already conducting flight tests with flying wings. First results show that they possess favourable low speed properties and that their in-flight behaviour is very stable, although they have no empennages. The interference drag could nearly disappear, as the structure contains no fuselage and the wider wings offer the opportunity to integrate the engines. Therefore, a potential of 25 to 40% fuel saving is estimated. **(DVA, 2001), (Schmidt, 1998)**

However, today's attempts concentrate mainly on drag reduction. Here, the profile drag is the centre of interest, as it depends on the transition of the boundary layer in high proportion, which is controllable even though limited at present. One way to achieve this is boundary layer suction. As this is an active device, it offers the opportunity to manipulate airflow in minute detail. Unfortunately, this is connected with an increase in weight and fuel consumption, as some additional equipment and power is needed. The *Break Release Weight* (BRW) of an aeroplane is fixed. Therefore, sensitivity studies have to be carried out to examine the extent to which the gross efficiency is impaired due to the higher *Operational Empty Weight* (OEW) and an increased *Specific Fuel Consumption* (SFC).

## 1.2 Objectives

Software was developed in the context of a research project of the Universities of Limerick, Ireland and Cranfield, UK, to investigate the impact of HLFC system on a medium range twin jet aircraft in the Boeing 757 class. This software models the en-route performance of an entire flight mission according to requirements of the International Civil Aviation Organization (ICAO) including the alternate, where HLFC system can be installed virtually. It uses the *Lotus 1-2-3* software package and essentially determines the fuel required for a specific flight mission. The calculations are based on data, which defines the main aerodynamic and engine characteristics for the aircraft.

Computed results were crosschecked against results of another program, based on the same data set, and high accuracy could be ascertained. Comparisons with independent information were made beforehand and were found to be acceptable

In order to extend the spectrum of studies, the software has been modified by substituting data for another aircraft, a larger one with a longer range, in the general class of the Airbus A330. For that reason it was required to develop input tables, which was achieved by making assumptions based on theoretical mathematical analysis applied to extend the available performance information provided by the University of Limerick.

After the input data was established, the results computed by the software were crosschecked against published information, such as a flight crew operating manual for fuel planning, which is supplied by the manufacturer to the airlines to enable them to carry out en-route calculations quickly. Another check against an advertising document of Airbus was done. Both comparisons led to acceptable results.

Once sufficient accuracy was assured, the software was used to perform a sensitivity study to investigate the possible impact of HLFC system on the fuel usage. By considering the change in block fuel, the single impacts of such systems were obtained and their sum was compared to answers computed for a virtual full installation. These results are discussed and evaluated.

### 1.3 Literature review

The Boeing Notes “Jet Transport Performance Methods” (**Boeing, 1989**) provided the necessary background since they contain basics of aeronautical engineering like aerodynamics, power plant and aircraft performance in a very comprehensive form. Since the origin of nearly all parameters is derived, it offered an extension of the knowledge attained by the previous study. In addition the notes include a summary of useful information for performance engineers, which was also very helpful as information needed could be found quickly.

In the Boeing Notes No. 1 and No. 2 (**Boeing, 1996**) many descriptive pages can be found, which make it more apparent how the theory given in release No. 1 is used in practice. Furthermore, some examples are worked out in detail. These all enable a reader with some engineering background to understand the derivations and to use the given equations properly.

Some further information was found in the lecture notes for flight mechanics of **Young (1999)**. Their use was very helpful, since difficult topics are elaborated in a way that a student is able to understand them. In addition, these notes provide much information about the practical use of this theory, which makes them easier and more interesting to read and gives an idea of the meaning of it all.

Also both notes of Scholz used for this work may be cited, the “Skript zur Vorlesung – Flugzeugentwurf” (**Scholz, 1999**) and “Normgerechtes Verfassen von Diplomarbeiten mit Hilfe einer Word-Musterdatei” (**Scholz, 2001**). The former deals with the complete design of an airplane and gives all necessary information to work out ones own design, which leads to amazing close results compared to a re-designed aircraft, which already exists.

The other notes describe how to compose a scientific report based on the DIN norms. In addition a scheme is given, which can be practically used in Microsoft Word to achieve these normalized formats. Whoever had to write a report knows how much time, otherwise needed for research and realization of the desired form, can be saved, if such a tool is available. This has recently been published in book form.

To understand the functions of the Lotus 1-2-3 software package some literature was reviewed. However, good one could not be found as the most are based on business backgrounds, and it was hard to pick out the necessary information in adequate time. The help function of the package provided the more efficient tool.

In the documents of **Young/Fielding (2000)** and **Young/Fielding (2001)** the necessary background about the application of HLFC system could be found. The advantages and disadvantages are explained and some studies are described, which made the task easier to solve.

## 1.5 Structure arranged of Work

Several different working steps had to carry out in order to solve the problems given in the task. Therefore, the report will have the subsequent structure. After explaining the necessary theoretical background in **chapter 2** and the specification of HLFC system by taking into account its advantages and disadvantages, as well as other drag reducing devices in **chapter 3**, it deals in the main part with the following topics:

- Chapter 4** describes the structure and the function of the original software in detail and compares computed answers to other results based on the same data set
- Chapter 5** explains how the available performance data is dealt with to modify the software for a second aircraft of another class and how the calculated results compare to results from published sources
- Chapter 6** contains the sensitivity studies, their results in tables form, illustrations and the descriptions of the illustrations
- Chapter 7** discusses the experiences, gained from the research, the application of the software, and its modification, as well as the results of the studies
- Chapter 8** gives the conclusions resulting from the previous experiences made in handling the software and the data, and in working out the studies
- Appendix A** includes the developed tables, which define the main aerodynamic properties and engine parameters
- Appendix B** contains flowcharts of both the applied software and the program based on the same data set used to compare the results
- Appendix C** contains the original example together with all necessary data pages of the Operating Manual of A330 for the fuel planning
- Appendix D** gives a further example, which was worked out to achieve more similarity to the basic conditions of the software, where all steps are described in detail
- Appendix E** provides the necessary equations for airspeed conversions
- Appendix F** provides data, which is useful for unit's conversions
- Appendix G** contains the used table of values for the International Standard Atmosphere

## 2 Aerodynamics and Performance

### 2.1 Flight Profile

The profile of any flight mission basically includes steps 1 to 5, as well as the steps 12 and 13 as shown in figure 2.1. However, unpredictable contingencies may occur, whereby additional operations are necessary to ensure that an aeroplane is able to reach an alternate aerodrome. These, for safety reasons required operations are defined by the International Civil Aviation Organization (ICAO):

ICAO Annex 6-4.3.6.3 (Boeing 1996):

4.3.6.3 Aeroplanes equipped with turbo-jet engines.

4.3.6.3.2. A) When an alternate aerodrome is required:  
To fly to and execute an approach, and a missed approach, at the aerodrome to which the flight is planned, and thereafter:

- a) To fly to the alternate aerodrome specified in the flight plan; and then
- b) To fly for 30 minutes at holding speed at 450 m (1500 ft) above the alternate aerodrome under standard temperature conditions, and approach and land; ...

According to these requirements a complete flight profile of aircraft equipped with turbo-jet engines may be pictured as follows:

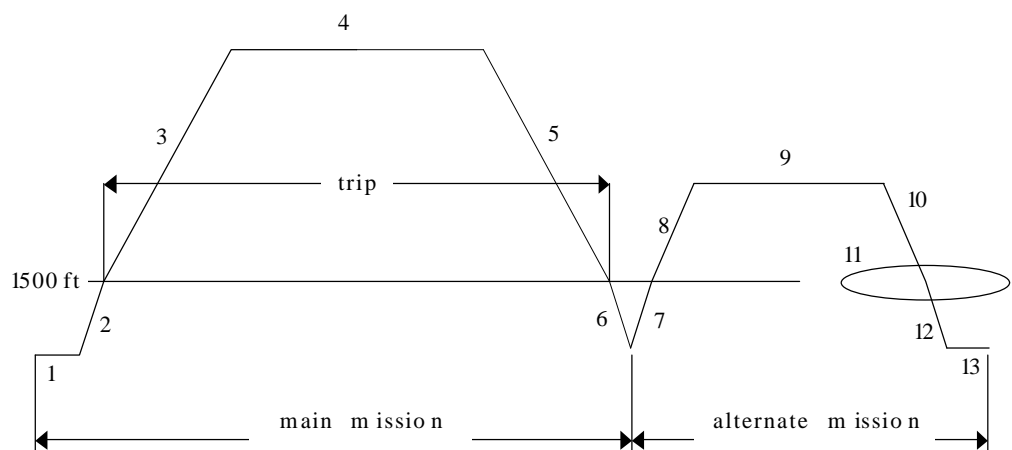


Figure 2.1 Complete mission of an aircraft, based on Sraubinger (2000a)

- 1 Engine start-up, taxi and line-up
- 2 Take-off and climb to 1500 ft
- 3 Climb to cruise altitude
- 4 Cruise
- 5 Descent to 1500 ft
- 6 Approach
- 7 Overshoot, climb to 1500 ft
- 8 Climb to alternate cruise altitude
- 9 Alternate cruise
- 10 Descent to 1500 ft
- 11 Hold for 30 minutes
- 12 Approach and land
- 13 Taxi and shutdown

## 2.2 Fuel Planning

There must be enough fuel onboard to be able to perform the entire mission as described in the previous chapter. According to **JAR-OPS 1**, Subpart D, an additional amount of fuel must be taken onboard, denoted as *contingency fuel*. This is regarded as necessary, because the alternate mission does not cover all possible occurrences, especially during trip-time. Therefore the following modes must be able to compensate:

- (1) Deviations of an individual aeroplane from the expected fuel consumption data;
- (2) Deviations from forecast meteorological conditions;
- (3) Deviations from planned routings and/or cruising levels/altitudes

The amount of the contingency fuel is regulated as follows according to **Young/Fielding (2000)**:

*“The contingency fuel may be either 5 % of the planned trip fuel, or 3 % of the planned trip fuel provided that an en-route alternate aerodrome is available.”*

This may be insufficient for the use of HLFC devices, since a lower operational reliability than other aircraft systems is expected. In addition most of the conceivable failures that might cause impacts result in a complete loss of laminar flow for the entire remaining mission. Therefore an amount of about 10 % is proposed to cover HLFC system failures. (**Young/Fielding, 2000**)



Furthermore, it is sometimes necessary to provide so-called *additional fuel* to cover a possible failure of a power unit or loss of pressurization for certain aircraft or specific missions. This is only required if such a failure cannot be compensated by the contingency fuel as described above, and has to be based on the assumption that it occurs at the most critical point along the route. **(Young/Fielding, 2000)**

Under certain circumstances it may be efficient for an airline to take more fuel onboard than required. This depends on the difference between the fuel prices of departure and destination. Since, for example kerosene is very expensive in South America, it is more economical to burn more fuel due to the additional weight of this *tankered fuel*. **(Young, 2001a)**

*Total fuel* is the entire sum of all fuel parts described above and is therefore the amount, which is to be taken onboard.

It may be also cited the *block fuel*, since this is often used in this report. It consists of the needed fuel for the main mission inclusive of the necessary taxes at depart and destination.

## 2.3 The Atmosphere

To be able to compare the different aeroplane and engine performances it was necessary to establish a standard for the ambient conditions in the atmosphere. Therefore, the atmospheric properties like temperature, density and pressure were observed for several years and at the end of the day it was possible to provide approximate definitions for an average day in the temperate latitudes of Europe and Northern America, called International Standard Atmosphere (ISA). This is defined as follows:

The atmosphere is divided into two regions, the troposphere up to 11000 m (36089 ft) and the stratosphere above this height. The border between both regions is called the tropopause.

The temperature at sea level,  $T_0$  equal to 15 degrees above zero (288.15 K) succumbs to a lapse rate,  $L$  (linear reduction in temperature with height), of 6.5 degrees per 1000 m up to the tropopause. In the stratosphere it is assumed that the temperature is a constant of  $-56.5$  °C.

The standard sea level pressure,  $p_0$  amounts to 101325 Pa and the corresponding mass density,  $\tilde{n}_0$ , of dry air equal to  $1.225$  kg/m<sup>3</sup>.

Knowing these values makes it possible to perform a complete model for the whole atmosphere by using the Equation of State for gases, since the following constants are generally known:

$$\begin{array}{ll}
 R & = 3089.81 \text{ ft}^2/\text{s}^2\text{K} & \text{(gas constant of air)} \\
 \tilde{a} & = 1.40 & \text{(ratio of specific heat of air)}
 \end{array}$$

In order to identify them, the sea level values are designated with the subscript,  $_0$ . The Equation of State shows that they depend on each other:

$$p_0 = R \cdot T_0 \cdot r_0 \quad (2.3-1)$$

By using the same equation for an arbitrary height and dividing this by the sea level related term above, the constant R cancels, and the parameters appear as ratios:

$$\frac{p}{p_0} = \frac{T}{T_0} \cdot \frac{r}{r_0} \quad (2.3-2)$$

Because these ratios are used quite frequently they each have a specific symbol:

For the temperature: 
$$q = \frac{T}{T_0} \quad (2.3-3)$$

For the pressure: 
$$d = \frac{p}{p_0} \quad (2.3-4)$$

For the density: 
$$s = \frac{r}{r_0} \quad (2.3-5)$$

Set into equation [2.3-2], it leads to the following expression, which shows that the ratios are not independent:

$$d = sq \quad \text{or more commonly:} \quad s = \frac{d}{q} \quad (2.3-6)$$

The temperature,  $T$ , at a certain height up to the tropopause may be obtained by the following equation.

$$T = T_0 - Lh \quad (2.3-7)$$

In the troposphere the temperature is assumed as a constant as previously discussed. Set in the known values, where the lapse rate is converted to a value given in feet, because of the pressure height is commonly measured in this unit, leads to:

Below the tropopause:  $T = 15^{\circ}\text{C} - 0.0019812 \frac{\text{C}}{\text{ft}} h$  and (2.3-8)

Above the tropopause:  $T_{\text{trop}} = \text{constant} = -56,5^{\circ}\text{C}$  (2.3-9)

Using the basic equations of hydrostatics and the gas laws, the following equation to determine the pressure,  $p$ , at an arbitrary height in the stratosphere can be derived.

$$p = p_0 \left( \frac{T}{T_0} \right)^{\frac{1}{LR}} \quad (2.3-10)$$

Since the pressure continues to decrease whilst the temperature remains constant in the stratosphere a further equation for heights above 36,089.24 ft can be deduced:

$$p = p_0 \left( \frac{T_{\text{Trop}}}{T_0} \right)^{\frac{1}{LR}} e^{-\left( \frac{h-36,089.24 \text{ ft}}{RT_{\text{trop}}} \right)} \quad (2.3-11)$$

It is convenient to express the equations above as follows as several terms are known and constant:

Below the tropopause:  $p = 101325 \text{ Pa} \left( \frac{T}{288.15 \text{ K}} \right)^{5.25588}$  (2.3-12)

Above the tropopause:  $p = 101325 \text{ Pa} \cdot 0.22336 \cdot e^{1.73158 - 4.8063 \cdot 10^{-5} \cdot h}$  (2.3-13)

Note that the temperature is used in units of Kelvin in the terms above. Combining equations [2.3-12] and [2.3-13] with [2.3-2] yields expressions, which enable one to obtain the mass density of any height of the atmosphere.

Below the tropopause:  $\mathbf{r} = 1,225 \text{ kg/m}^3 \left( \frac{T}{288.15 \text{ K}} \right)^{4.25588}$  (2.3-14)

Above the tropopause:  $\mathbf{r} = 1,225 \text{ kg/m}^3 \cdot 0.29707 \cdot e^{1.73158 - 4.8063 \cdot 10^{-5} \cdot h}$  (2.3-15)

By dividing the derived equations above by the corresponding sea level values, results in the useful expressions of the ratios for temperature, pressure, and mass density, respectively, referred to sea level conditions.

The equations derived in this chapter, valid for the standard atmosphere only, enable one to make a table of the atmospheric properties at any altitude. These tables can be found in several publications however slight differences occur occasionally due to the impact of rounding errors. For that reason the table used for the research this report is dealing with is attached in appendix G.

## 2.4 Flight Level

Airspace is subdivided into different flight levels for air traffic. They are denoted as FL and a number, which corresponds to the measured pressure height in feet divided by 100. So an aeroplane, which is flying at a pressure height of 35000 ft, would use the FL350. In order to have enough space between the flight levels to intercept eventual approximations, the difference between two flight levels amounts to 2000 ft. (Young, 1999)

The pressure height is the altitude, where the actual outer pressure, which can be measured, equals that of the international standard atmosphere. In reality the aeroplane can be situated at another height at this time, dependent on the atmospheric conditions on a specific day. For the reason that all aircraft are conducted by the same system there is no risk of encounters.

Of course, this is insufficient for operations at lower altitudes near ground level, e.g. start and landing manoeuvres at an aerodrome. Therefore, the pilot is able to adjust the altimeter with knowledge of the outside conditions on a specific day for the area she is acting in to get the true height value.

## 2.5 Lift and drag

### 2.5.1 Basic information

A typical pressure pattern surrounding a common airfoil experienced by fluid motion may be pictured as shown in figure 2.2. It can be seen clearly, that the change of flow, which has to take place in order to pass the shape, induces a force. The magnitude of this *resultant*, acting at the centre of pressure, is influenced by the difference of pressure between upper and lower surface of the wing. This increases with the chamber or the angle of attack, á up to a certain peak.

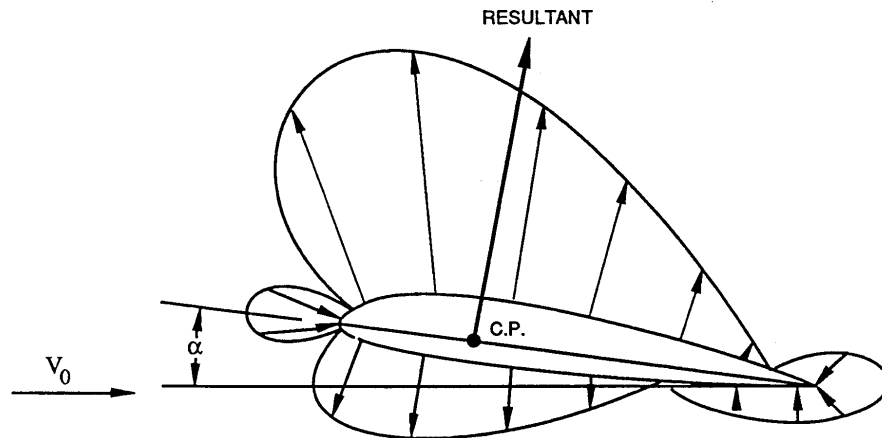


**Figure 2.2** Typical pressure pattern surrounding an airfoil (Boeing, 1989)

By replacing this *resultant* into its two components it bears a force perpendicular to the free stream velocity, called lift,  $L$ , and another one parallel to it, denoted as drag,  $D$  (See figure 2.3). These are defined as follows:

$$\text{Lift:} \quad L = c_L q S \quad (2.5-1)$$

$$\text{Drag:} \quad D = c_D q S \quad (2.5-2)$$

Where,

- $q$  is dynamic pressure
- $S$  is wing area
- $c_L$  lift coefficient
- $c_D$  drag coefficient

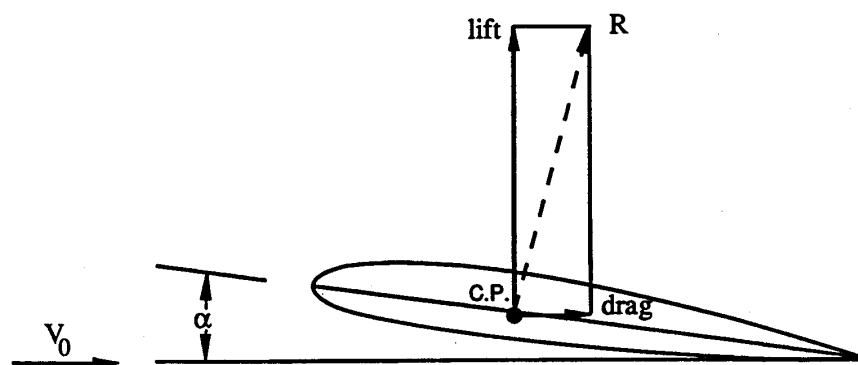


**Figure 2.3** Lift and drag (Boeing, 1989)

## 2.5.2 The Lift

Since the lift can be replaced for most calculations through the weight of the aeroplane and nearly all considerations are made with respect to the lift coefficient, equation [2.5-1] may be written:

$$c_L = \frac{L}{\frac{1}{2} \rho v^2 S} \quad (2.5-3)$$

by using:

$$q = \frac{1}{2} \rho v^2 \quad (2.5-4)$$

Furthermore, the lift coefficient depends on the angle of attack,  $\alpha$ . This relationship is shown in figure 2.4.

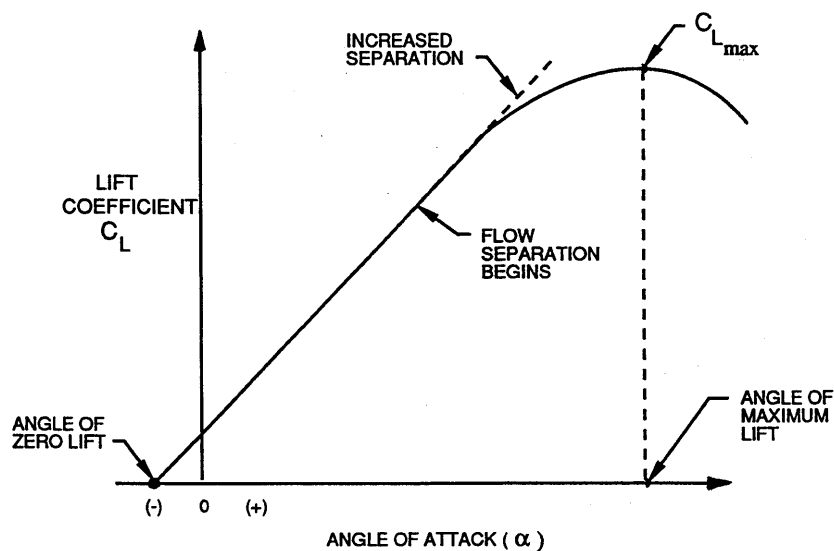


**Figure 2.4** Relationship between lift coefficient and angle of attack (Boeing, 1989)

## 2.5.3 The Drag

Also, most analysis regarding the drag is based on the corresponding coefficient. Therefore, it is convenient to express equation [2.5-2] as follows by using term [2.5-4] for the dynamic pressure again:

$$c_D = \frac{D}{\frac{1}{2} \rho v^2 S} \quad (2.5-5)$$

This coefficient is the sum of several drag proportion coefficients, as is evident from figure 2.5. Reducing the zero-lift drag is of special importance in current research to achieve lower fuel consumption.

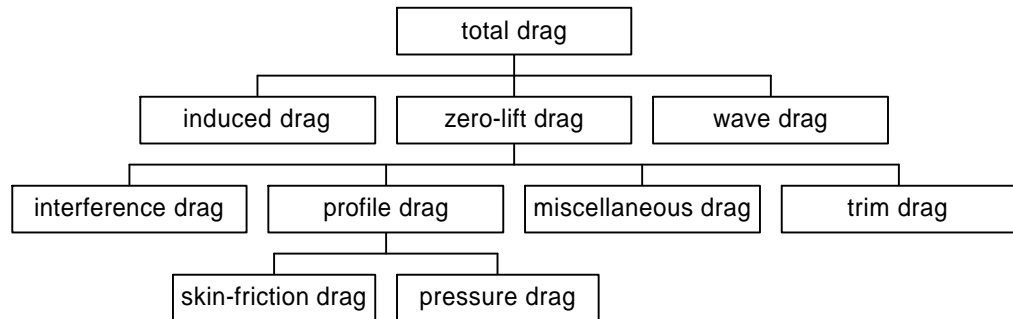


**Figure 2.5** Drag breakdown, based on **Scholz (1999)**

The induced drag develops due to lift and equals zero if no lift is produced. In this case the zero-lift drag is equivalent to the total drag and therefore independent of the lift, which is clear from equation [2.5-6]. It depends on the friction, the shape of the boundary layer, mutual influence to flow around adjacent components, the level of slats, flaps and rudders and miscellaneous drag causing impacts like, for example, the landing gears, respectively.

The wave drag appears at Mach numbers greater than about 0.6. It can be considered separate or proportionate to the zero-lift drag and the induced drag (**Scholz, 1999**). Thus, by using the latter, the total drag coefficient may be also expressed as follows:

$$c_D = c_{D,0} + c_{D,i} \quad (2.5-6)$$

## 2.5.4 The Drag Polar and L/D ratio

As is explained in chapter 2.5.1, the coefficients are dependent on each other. A relationship exists because of the lift-dependent proportion, which is discussed in the previous chapter. This relation is commonly given in the form of the drag polar and provides a comprehensive statement about the aerodynamic properties of an airplane. Therefore, the manufacturers keep them as a secret, at least for their current competitive models.

However, it is possible to apply the following parabolic equation in order to provide a drag polar for low Mach numbers with sufficient accuracy:

$$c_D = c_{D,0} + k c_L^2 \quad (2.5-7)$$

where,

$$k = \frac{1}{\rho A e} \quad (2.5-8)$$

where:  
 A is the aspect ratio  
 e is the Oswald efficiency factor  
 e = 0.85 for most airplanes in cruise performance (**Scholz, 1999**)

The factor  $k$  can vary away from the statement above in order to achieve matching results to from flight test data calculated values, as will be shown later in this report. Using equations [2.5-7] and [2.5-8] a drag polar may be depicted as follows:

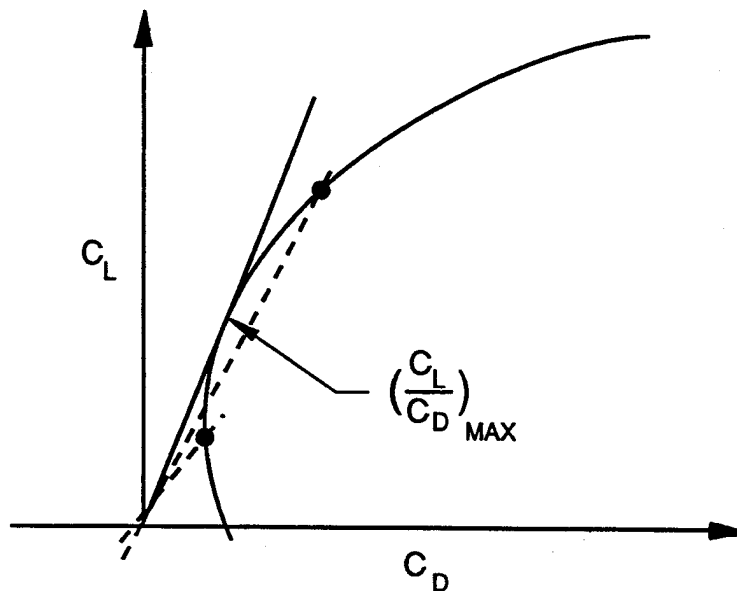


**Figure 2.6** The drag polar (**Boeing, 1989**)

In addition, figure 2.6 shows how the most efficient operational state of an airfoil can be determined. It is the maximum of the ratio of lift,  $L$ , and drag,  $D$ , so the point at the curvature with the most lift for the smallest drag. This ratio is called  $L$  over  $D$  and is denoted as  $E$ . It is derived by dividing equation [2.5-3] by equation [2.5-5], which results in the following term, since  $q$  and  $S$  cancel:

$$E = \frac{c_L}{c_D} = \frac{L}{D} \quad (2.5-9)$$



For Mach numbers at which the accelerated air flowing around an airfoil reaches sonic velocity, which leads to a shock wave, equation [2.5-7] is not sufficient anymore. In this case this equation is extended by a further term as follows. The included exponent  $y$  is greater than 2 or may be raised in order to achieve closer approximation. Values of 3 or 4 are generally applied.

$$c_D = c_{D,0} + k_1 c_L^2 + k_2 c_L^y \quad (2.5-10)$$

The influence on drag due to the Mach number may be sketched as shown in figure 2.7 for a given lift coefficient. It can be seen that the drag coefficient suddenly rises at a certain speed, which is called the *critical Mach number*. This is the lowest remote velocity at which a local Mach number of unity is attained and hence a shock wave is produced on any part of an airfoil.

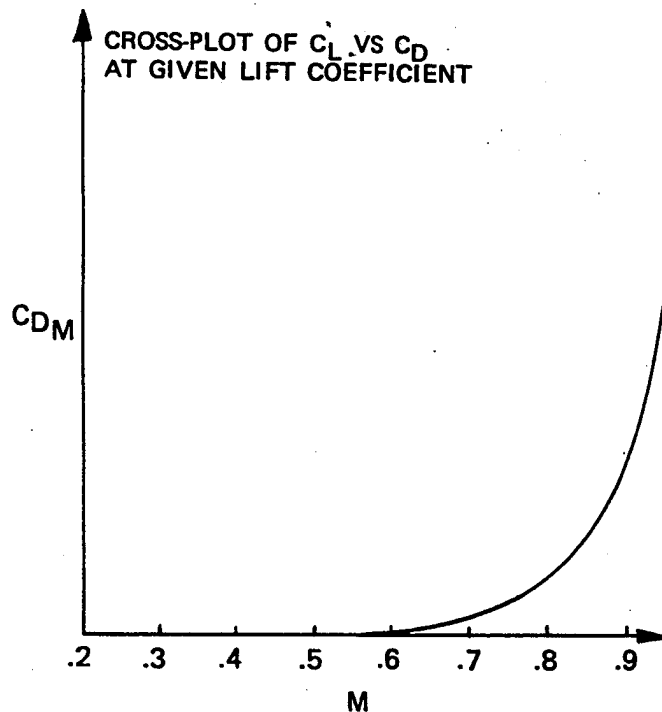


**Figure 2.7** Influence of Mach number on drag (Boeing, 1989)

This correlation leads to several drag polars for higher Mach numbers, as is shown in figure 2.8. The additional drag is the so-called wave drag and will be taken into account in this report through a change of factor  $k$  and the choice of a higher exponent applied on equation [2.5-10], since the actual critical Mach number was unknown.

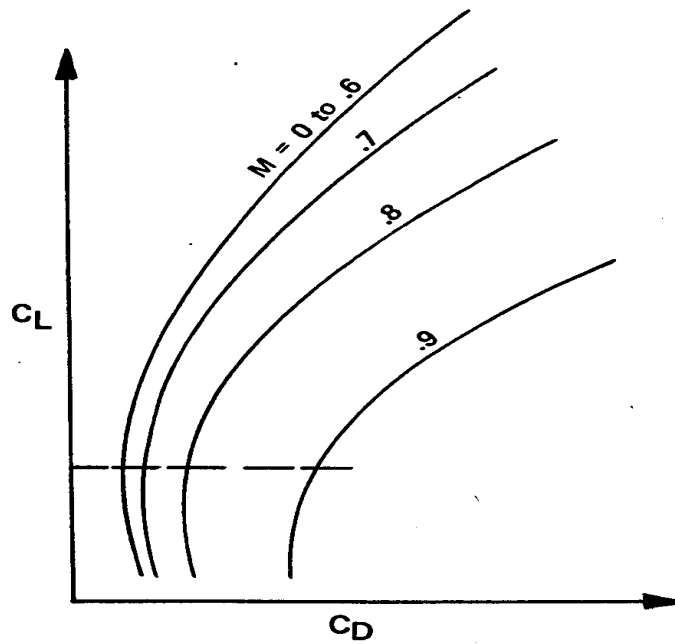


Figure 2.8 Drag polars for several Mach numbers (Boeing, 1989)

## 2.6 General Cruise Calculations

### 2.6.1 Level Flight

The major Forces acting on an airplane are lift,  $L$ , weight,  $W$ , thrust,  $T$ , and drag,  $D$ . Figure 2.6.1 depicts a simplified example of how these forces interact. In order to simplify the cruise calculations, an airplane is frequently considered to perform a straight unaccelerated flight. In this state the lift is equal to the weight, and the thrust is equal to the drag.

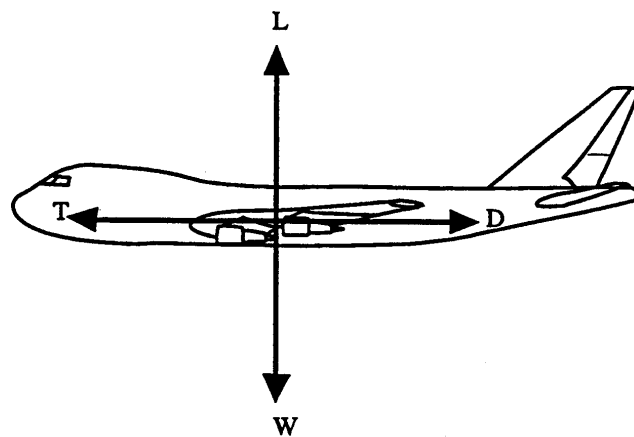


Figure 2.9 General forces acting on an aircraft (Boeing, 1989)

Because engine data is mostly given as thrust over delta, the equations [2.5-1] and [2.5.2] will appear in a modified form in succeeding chapters. This may be derived as follows:

by using  $v = Ma$  (2.6-1)

and  $a = \sqrt{gRT}$  (2.6-2)

By dividing the latter through the sea level related equation and resolving this for  $a$  it leads to:

$$a = a_0 \sqrt{\frac{T}{T_0}} = a_0 \sqrt{q} \tag{2.6-3}$$

Since the true airspeed in equation [2.5-4] appears squared, the root for the temperature ratio cancel and by writing the density as follows, the pressure ratio,  $\bar{r}$ , may be introduced:

$$\bar{r} = r_0 \frac{r}{r_0} = r_0 s \tag{2.6-4}$$

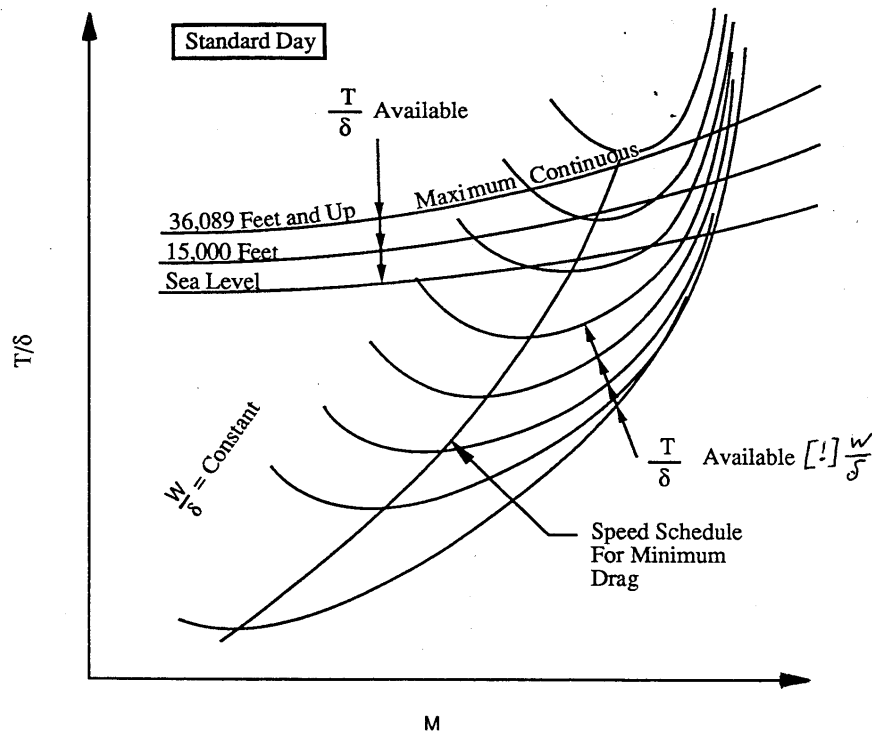


Figure 2.10 Speed schedule for minimum drag (Boeing, 1989)

By using the relationship between the atmospheric ratios  $\rho$  and  $\sigma$  can be replaced by  $\alpha$  (See equation [2.3-6]). If this is placed on the left side, it results for a steady level flight in:

$$\frac{L}{d} = \frac{1}{2} \rho_0 a_0^2 M^2 C_L S = \frac{W}{d} \quad (2.6-5)$$

$$\frac{D}{d} = \frac{1}{2} \rho_0 a_0^2 M^2 C_D S = \frac{T}{d} \quad (2.6-6)$$

By plotting both terms as functions for several heights into one diagram, both the appropriate speed for minimum drag and the availability of thrust for a specific performance can be determined. (See figure 2.10)

## 2.6.2 The Fuel Consumption

Another current information is the fuel flow,  $Q$ . It is dependent on the net thrust per engine, altitude and Mach number and an expression for burned fuel per unit time per engine.

$$Q = -\frac{dm_F}{dt} \quad (2.6-7)$$

Usually, it is given in terms of corrected fuel flow,  $Q_{\text{corr}}$ , which is generalized by dividing by the total pressure ratio and root of the total temperature ratio. These are defined as follows:

$$\text{Total temperature ratio:} \quad q_T = \frac{T_T}{T_0} = q(1 + 0.2 \cdot M^2) \quad (2.6-8)$$

$$\text{Total pressure ratio:} \quad d_T = \frac{p_T}{p_0} = d(1 + 0.2 \cdot M^2)^{3.5} \quad (2.6-9)$$

$$\text{Therefore,} \quad Q_{\text{corr}} = \frac{Q}{d \sqrt{q} (1 + 0.2 \cdot M^2)^4} = \frac{Q}{d_T \sqrt{q_T}} \quad (2.6-10)$$

This is only valid for a complete generalization, where differences between various engines are not considered. To take into account the engines particularities, another factor, called  $\check{e}$ , may be introduced, which is unity in theoretical mathematical analysis and is a function of total temperature ratio. Therefore it can be combined with this as follows:

$$I \sqrt{q_T} = q_T^x \quad (2.6-11)$$

The exponential value of  $x$  can rise up to 0.67, which depends on the specific engine. In the provided software it amounts to 0.6363, which was given by Boeing in the PEM. (**Boeing**)

The calculations concerning the long-haul aircraft are based on the mathematical analysis, since no engine data was available. Therefore  $x$  is equal to 0.5 in this case. For reasons of thoroughness, equation [2.6-10] may be written in its modified form:

$$Q_{\text{corr}} = \frac{Q}{dq^x (1 + 0.2 \cdot M^2)^{3.5+x}} = \frac{Q}{d_T q_T^x} \quad (2.6-12)$$

A further statement about the necessary fuel is the Specific Fuel Consumption (SFC). It develops by dividing the total fuel flow, and thus the sum for all engines by the instantaneous provided thrust. Therefore, it is the burned fuel per unit time per unit thrust. The lower its value the more efficient the power plant of an airplane. It is given the symbol  $c$  and for approximate calculations it is assumed to be constant.

$$c = \frac{Q_{\text{total}}}{T} \quad (2.6-13)$$

### 2.6.3 Range cruise calculations

In order to obtain the distance in still air, which is possible to fly per unit burned fuel; their ratio may be contemplated. It is given the symbol  $r_a$  and called *Specific Air Range* (SAR):

$$r_a = -\frac{dx}{dm_F} \quad (2.6-14)$$

By relating the numerator, as well as the denominator to a certain change of time the equation appears as an expression, where the terms can be replaced by already known ones, which are *True Air Speed* (TAS),  $v$  and total fuel flow,  $Q_{\text{total}}$ :

$$r_a = \frac{dx/dt}{-dm_F/dt} = \frac{v}{Q_{\text{total}}} \quad (2.6-15)$$

Since  $r_a$  is now known, equation [2.6-15] can be resolved for  $dx$ . The actual flown range,  $R$ , answers from its integral, as is shown below. For the analysis of this report the change of the aircraft gross weight is the same as the mass of burned fuel, and so the subscript,  $F$ , can be neglected from now on:

$$R = \int dx = -\int r_a dm = -\int \frac{v}{Q_{\text{total}}} dm \quad (2.6-16)$$

As fuel flow is usually unknown in first design stages it is convenient to replace it with the term [2.6-13]. Furthermore, the unaccelerated level flight, which is considered here, offers the possibility to write drag,  $D$ , for thrust,  $T$ . In addition, the weight equals the produced lift, whereby their ratio is unity and this can be multiplied without changing the result. Hereby, the weight may be written as the product of mass and acceleration:

$$Q_{\text{total}} = cT = c \frac{D}{L} mg \quad (2.6-17)$$

The drag and the lift can be replaced by their corresponding coefficients, which is clear from equation [2.5-9]. Therefore the integral finally appears as follows:

$$R = -\int \frac{v c_L}{c g c_D} \frac{dm}{m} \quad (2.6-18)$$

In order to solve this integral, some parameters have to be considered as being constant. Since the actual SFC shuttles at about an average value, it can be fixed for estimations with sufficient accuracy. For the remaining variables there are three different ways to combine them, as they are dependent on each other, as well as on the operational altitude:

1. Flight at constant altitude and constant lift coefficient
2. Flight at constant airspeed and constant lift coefficient
3. Flight at constant airspeed and constant altitude

**(Young, 1999)**

By using the second all parameters of the first fraction are constant, which results in the following expression, generally known as the *Breguet Range Equation*.

$$R = \frac{v c_L}{c g c_D} \ln \left( \frac{m_1}{m_2} \right) \quad (2.6-19)$$

The application of Breguet leads to the greatest possible range. However, since the weight drops due to fuel being burned, this succumbs to the condition that a slight rise of altitude has to be allowed to keep the lift coefficient constant. It is apparent from equation [2.5-3] that for this reason the density has to drop as well, which decreases with an increase of height according to the ISA.

This is, of course, not practical for classified air traffic. However, to be able to use this potential of increased efficiency, the pilot will usually request for a change of the FL during the cruise. If this is released he will perform a so-called *Step Climb*. (Young, 1999)

## 2.6.4 Time Cruise Calculations

For specific flight missions, it may be more efficient to obtain the conditions, which allow an airplane to stay airborne as long as possible per unit of burned fuel. In performing a hold, due to not receiving the landing permission, the pilot will, for instance, turn into this mode. Other examples are flight missions, which are conducted by the necessity to observe a certain area, e.g. for rescue reasons or the exploration of weather phenomenon.

The derivation of an expression to calculate the time is only slightly different to that for the range. Equation [2.6-7], resolved for the time difference, already supplies the basis for the necessary integral. The fuel flow is replaced as shown in [2.6-17] and drag and lift should be substituted by their coefficients:

$$t = -\int \frac{1}{Q} dm = -\frac{1}{c g} \int \frac{c_L}{c_D} \frac{dm}{m} \quad (2.6-20)$$

This expression, in which the SFC is assumed to be constant again, shows, that an airplane achieves its maximum airborne endurance, while it is flying at maximum  $L/D$ , and at a speed, which is bearing the smallest possible drag.

The integral is solvable by making the same three assumptions for the variables as in the previous chapter. For a constant lift coefficient, this leads to the time equation according to Breguet:

$$t = \frac{c_L}{c_D c g} \ln \left( \frac{m_1}{m_2} \right) \quad (2.6-21)$$

### 2.6.5 Integrated Range and Integrated Time

As discussed in the previous chapters, the Equations of Breguet give approximate results, since some generalizations have to be made and certain conditions have to be complied with. To achieve a more correct answer, the change of altitude and the assumption, that the SFC would be constant, cannot be accepted.

Therefore, another alternative will be introduced here, which is the method of *Integrated Range* and *Integrated Time*. On this occasion, the Mach number and the operational altitude are stated for a certain time interval. As a steady level flight is performed, the thrust has to equal to the drag, which can be obtained from the drag polar by assuming an instantaneous weight and calculating the according lift coefficient. Besides the drag polar, data about the corrected fuel flow has to be available for this method, to be able to obtain the total fuel flow. Now the SAR for any weight within the given limits can be computed and plotted using equation [2.6-15] as is shown in figure 2.11.

$$r_a = \frac{v}{Q_{\text{total}}}$$

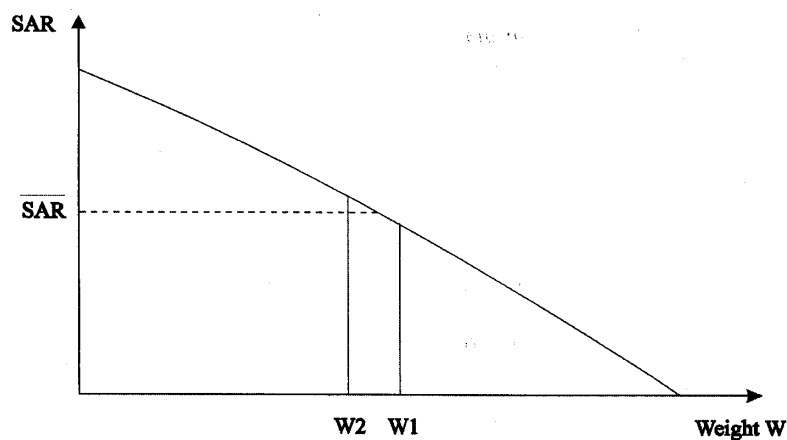


**Figure 2.11** Specific Air Range (Straubinger, 2000a)

In order to determine the distance, which can be flown by an aircraft with a certain amount of fuel  $W_1 - W_2$ , the weight must be subdivided into according intervals and their average SAR, denoted as  $\overline{\text{SAR}}$ , has to be calculated. The product of this, and the weight interval  $W_1 - W_2$  gives the answer, whereby it is apparent from figure 2.10 that this result depends on the momentary gross weight. The summation, or rather the integration of all distances leads to the integrated Range. (See figure 2.12) It is evident that the smaller the chosen intervals, the preciser the ends result.



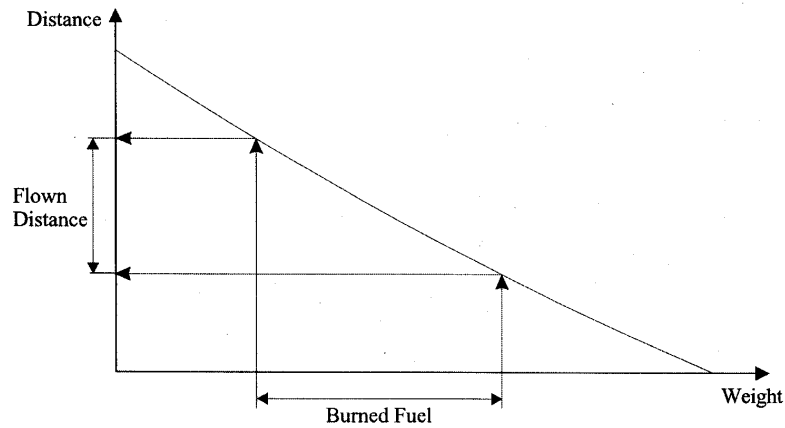


**Figure 2.12** Integrated Range (Straubinger, 2000a)

By dividing the distances through the according TAS, the time needed to fly is obtained, since the following kinematical equation is valid. Their integration results in the Integrated Time.

$$t_i = \frac{x_i}{v_i} \quad (2.6-22)$$

In practice this method is generally applied the other way around. This means that usually the manufacturer supplies data of integrated range and integrated time, determined during flights. This data shall enable the customer to carry out fuel checking. For the reason that the results can be quickly determined, it is very useful for in-flight planning.

## 2.7 Climb and Descent

For climb and descent performance the statements in chapter 2.6 are not valid anymore. In order to derive equations for this, it is necessary to examine the acting forces on an aircraft again.

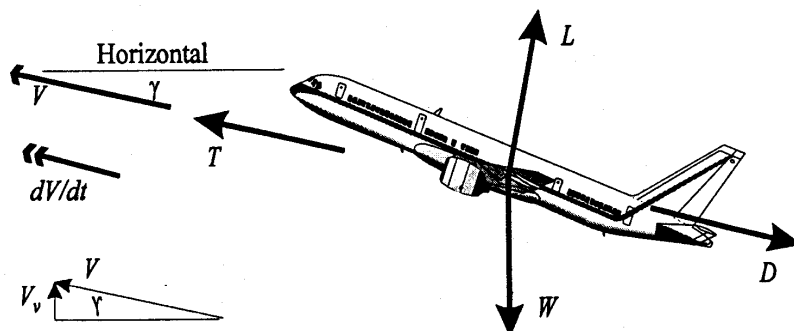


**Figure 2.13** Forces acting on an aircraft performing a climb (Boeing, 1989)

It is apparent from figure 2.13, that the thrust is not equal to the drag anymore. It was increased to enable the airplane to gain height. In addition the weight and the lift no longer act in one line. The flight path of the airplane will have a certain angle now relative to the horizontal. This is called the climb angle,  $\tilde{\alpha}$ , which is used to work out equations for the equilibrium of the acting forces:

$$\text{parallel to the flight path:} \quad \sum F_x = 0 = T - D - W \sin \mathbf{g} - F_I \quad (2.7-1)$$

$$\text{normal to the flight path:} \quad \sum F_y = 0 = L - W \cos \mathbf{g} \quad (2.7-2)$$

Besides the known elements in equation [2.7-1], an additional force,  $F_I$ , can be found, which describes the inertia of the aircraft mass against its acceleration. It is convenient to express this in another form:

$$F_I = m a = \frac{W}{g} \frac{dv}{dt} \quad (2.7-3)$$

Furthermore, it may be stated here, that the climb angle of aircraft considered in this report is generally small (i.e. less than  $15^\circ$ ), therefore the small angle assumptions can be used, which state: (**Young, 1999**)

$$\sin \mathbf{g} \approx \mathbf{g} \approx \tan \mathbf{g} \quad (2.7-4)$$

$$\text{and:} \quad \cos \mathbf{g} \approx 1 \quad (2.7-5)$$

Usually, a further angle exists between the line of thrust and flight path, which is so small and insignificant, that the decision was made to neglect it.

### 2.7.1 Climb angle and Rate of Climb (ROC)

The climb angle,  $\tilde{\alpha}$ , is defined and discussed in the previous chapter. This statement has to be considered as it does not allow for the effect of wind. Since moving air around a flying airplane influences its velocity relative to ground, both head- and tailwind would falsify the results. Therefore,  $\tilde{\alpha}$  is frequently designated as the *still air climb angle* in several publications. Generally, the climb angle is used to obtain the gain in height over a flown distance, given in terms of its tangent and denoted as *climb gradient*. By resolving term [2.7-1] for  $\sin \tilde{\alpha}$  it may be expressed:

$$\sin \mathbf{g} = \frac{T - D}{W} - \frac{1}{g} \frac{dv}{dh} \frac{dh}{dt} \quad (2.7-6)$$

The mathematical trick applied to the last term in the equation above offers the possibility to introduce the vertical airspeed component, since:

$$v_v = \frac{dh}{dt} = v \sin \mathbf{g} \quad (2.7-7)$$

Hence, by substituting this in equation [2.7-6]:

$$\sin \mathbf{g} = \frac{T - D}{W} - \frac{v}{g} \frac{dv}{dh} \sin \mathbf{g} \quad (2.7-8)$$

Herein, a dimensionless factor appears, which is generally known as the acceleration factor. This will be described in detail in the next chapter:

$$f_{acc} = \frac{v}{g} \frac{dv}{dh} \quad (2.7-9)$$

Some further simplifications may be made by applying the small angle assumption to attribute the equation to terms, generally known at this stage:

$$W \cos \mathbf{g} = L \approx W$$

and thus

$$\frac{D}{W} = \frac{D}{L} = \frac{c_D}{c_L}$$

Resolving equation [2.7-8] for  $\sin \tilde{\alpha}$ , and using the other assumption for small angles results in an expression for the climb gradient. This is usually given in percentage form and is one of the take-off requirements, which an airplane has to meet in order to get obstacle clearance.

$$\mathbf{g} \approx \tan \mathbf{g} \approx \sin \mathbf{g} = \frac{\frac{T}{W} - \frac{c_D}{c_L}}{1 + f_{acc}} \quad (2.7-10)$$

For en-route performance, the derivation and use is rather in terms of the *Rate of Climb* (ROC). The ROC equals the vertical speed component, which is given by equation [2.7-7], and can be determined as follows, since  $\sin \tilde{\alpha}$  is now known:

$$ROC = v \sin g = \frac{\frac{T}{W} - \frac{c_D}{c_L}}{1 + f_{acc}} v \quad (2.7-11)$$

### 2.7.2 The acceleration factor

The previously cited acceleration factor may be specified more accurately now. It is dependent on the Mach number and also whether or not the climb is performed below or above the tropopause. Besides this, its amount is highly influenced by the climb speed condition.

For constant TAS, it is apparent from equation [2.7-9] that the factor becomes zero, since the speed does not vary with a change in height. This leads to the following expressions valid for a steady unaccelerated climb only:

$$\text{climb gradient:} \quad \tan g = \frac{T}{W} - \frac{c_D}{c_L} \quad (2.7-12)$$

$$\text{rate of climb:} \quad ROC = v \left( \frac{T}{W} - \frac{c_D}{c_L} \right) \quad (2.7-13)$$

In order to consider the acceleration factor affected by velocities, which are constant in relation to other conditions, it may be stated as follows (**Boeing, 1989**):

$$f_{acc} = \frac{1.4 M^2}{2} \emptyset \quad (2.7-14)$$

Herein,  $\emptyset$  is defined for the different remaining climb speed conditions as follows (**Boeing, 1989**):

$$\text{constant Mach number:} \quad \emptyset = -LR \left( \frac{T_{ISA}}{T} \right) \quad (2.7-15)$$

$$\text{constant EAS:} \quad \emptyset = 1 - LR \left( \frac{T_{ISA}}{T} \right) \quad (2.7-16)$$

$$\text{constant CAS:} \quad \emptyset = f - LR \left( \frac{T_{ISA}}{T} \right) \quad (2.7-17)$$

with: 
$$\ddot{O} = \frac{1}{0.7M^2} \cdot \frac{(1+0.2M^2)^{3.5} - 1}{(1+0.2M^2)^{2.5}} \quad (2.7-18)$$

The temperature ratio offers the opportunity to take non-standard day conditions into account. It is unity for states according to ISA. Since it contains the temperature lapse rate, which is described in chapter 2.3, the factor  $LR$  becomes zero above the tropopause and amounts to 0.190263 for feet related statements at and below it.

### 2.7.3 Climb schedule

In order to reach the required cruise altitude as soon as possible, climbing close to best ROC speed is attempted. This is partially the case at constant CAS below the tropopause and constant Mach number above it, as is shown in figure 2.14. (Boeing, 1989)

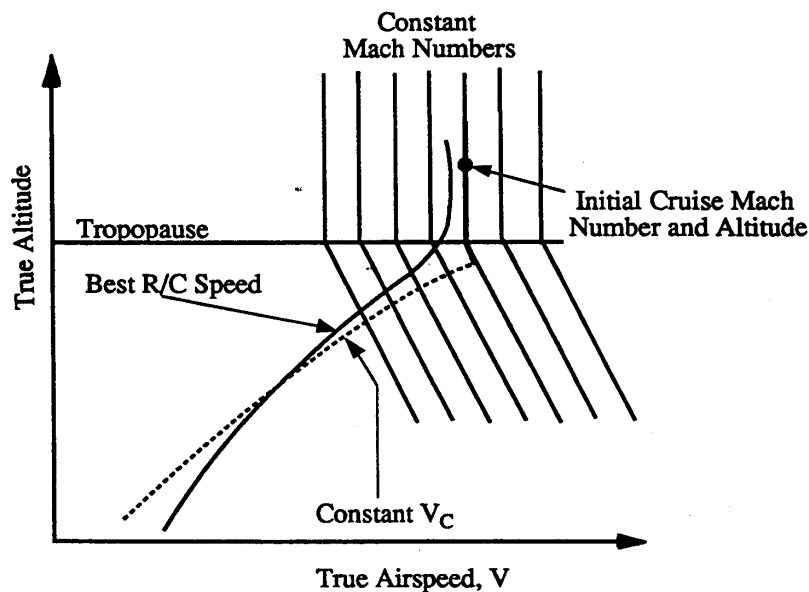


**Figure 2.14** Best ROC speed compared to constant EAS and Mach number (Boeing, 1989)

Therefore, so-called climb schedules are established, which generally consist of three numbers. The first one is the CAS, which should be flown up to 10000 ft, where a change to CAS is proposed equal to the second number until the Mach number is reached, which is given as the third value. This is to hold up to the cruise altitude. A typical example could be the climb schedule 250/300/0.8 and appears as shown in figure 2.15. (Young, 1999)

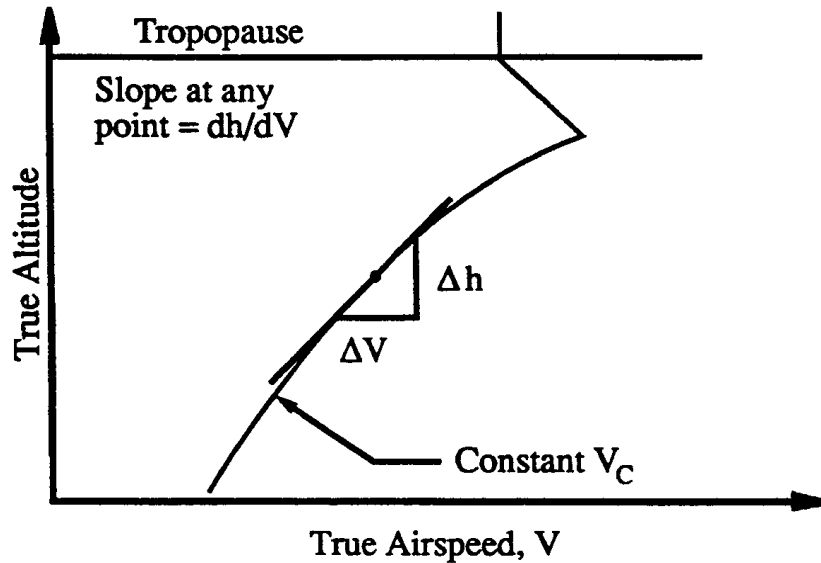


Figure 2.15 Typical climb schedule (Boeing, 1989)

#### 2.7.4 Time to Climb

Equation [2.7-7] supplies the basis for the following integral, since, besides the time, it includes the ROC and the change in height.

$$t = \int dt = \int \frac{1}{v_v} dh \quad (2.7-18)$$

Even if a quasi-steady state is assumed, where TAS is constant and the acceleration factor is neglected, its solution contains some difficulties because of the interdependency of the remaining variables. This becomes clearer through examining the rate of climb again:

$$ROC = v_v = \frac{T - D}{W} v$$

The weight drops due to fuel which is burned, and whose amount is dependent on the fuel flow,  $Q$ . However, this is equal to the product of SFC and thrust,  $T$ . By assuming an ideal jet, SFC is admittedly constant, but still the thrust will decrease with the drop in air density and will vary with changes in throttle settings.

In addition, it is clear from equation [2.5-2] that the drag is also dependent on the weight and the air density and thus the instantaneous operational altitude.

To solve the integral it is therefore necessary to divide the considered climb into vertical intervals. It is recommended to choose a smaller increase at higher altitudes, as ROC is a negative acceleration, which in turn means that the time needed to gain in height increases with altitude. The assumption that the ROC changes linearly with height inside of each step is a sufficiently accurate approximation. (See figures 2.15 and 2.16)

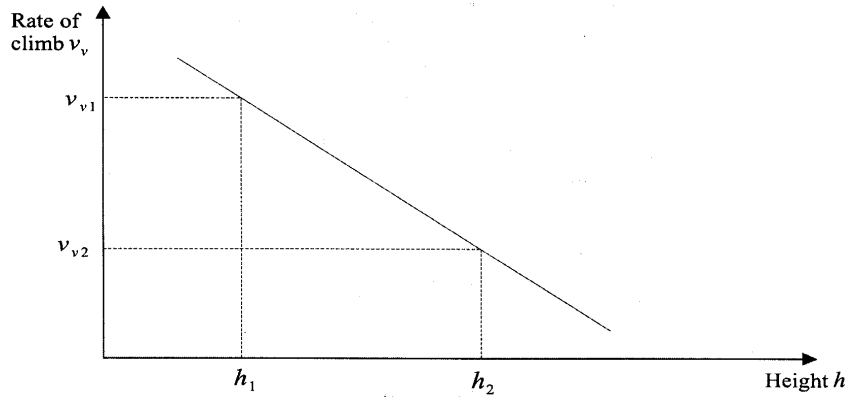


**Figure 2.16** Rate of climb (Straubinger, 2000a)

By determining the slope and using the form  $y = mx + b$  for ROC a function is obtained, which is easier to handle in the integral:

The slope is defined as: 
$$m = \frac{v_{v,i} - v_{v,i+1}}{h_{i+1} - h_i} \tag{2.7-19}$$

Applied on ROC: 
$$v_v = m(h - h_i) + v_{v,i} \tag{2.7-20}$$

Substitution and solving: 
$$t = \int_{h_i}^{h_{i+1}} \frac{1}{m(h - h_i) + v_{v,i}} = \frac{1}{m} \ln \left( \frac{v_{v,i+1}}{v_{v,i}} \right) \tag{2.7-21}$$

Since the weight, and thus ROC, at the end of each climb step are unknown, the calculation has to be based on further estimates. Several methods exist and the one used in this work may be described in detail as follows. A simple scheme is given in figure 2.17.

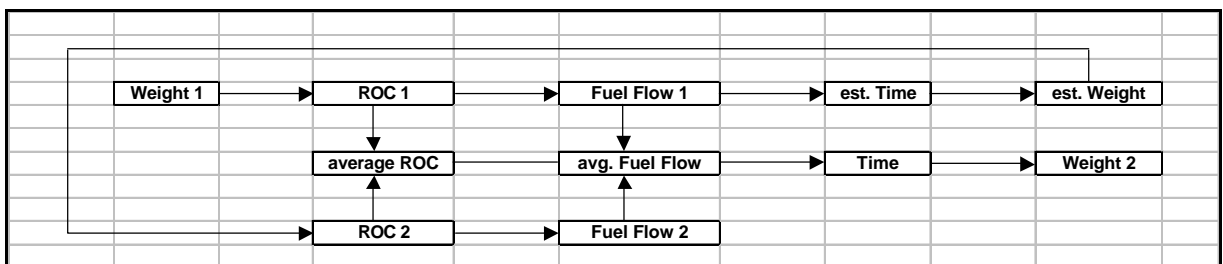


**Figure 2.17** Simple scheme for a weight determination method

Considering an interval limited by the heights 1 and 2, the start weight and altitude  $h_1$  are used to determine ROC and the fuel flow. Using these, first estimate for the time, and hence for the weight is made. Subsequently, the latter is applied on altitude  $h_2$  for determination of a second ROC as well as a second fuel flow. Afterwards, both are used to calculate an average value in each case, which gives results for time and fuel required to climb from an altitude  $h_1$  to an altitude  $h_2$ . Hence, the weight at the end of this climb step may be obtained, which is equivalent to the start weight of the next one. After determining the times for all increments, their total sum represents the final result for the time needed to climb from sea level up to cruise altitude.

### 2.7.5 Descent Calculations

The descent is calculated in the same manner as the climb. The only difference is that the climb angle  $\tilde{\alpha}$  is negative. By taking this into account, the expression developed for the climb gradient and ROC are valid again, whereas the vertical component of speed is now called *Rate of Descent* (ROD). This is by definition positive when the ratio of change in height to change in time is negative; therefore, equation [2.7-11] may be rewritten by considering the sign convention (Young, 1999):

$$ROD = -\frac{dh}{dt} = -v \sin \mathbf{g} = -\frac{T - D}{1 + f_{acc}} \frac{L}{W} v \quad (2.7-22)$$

### 2.7.6 Glide angle

The simultaneous failure of all engines on a transport jet is a rare occurrence. Nevertheless, such an aircraft performing a descent can reach states similar to a glide, since the idle thrust used for this is sometimes even less than zero, which means that additional drag is produced. For efficiency and eventual emergency reasons it may be desired to cover the greatest possible distance in descent performance, which is obviously achieved at the lowest glide angle.

If an approximation of steady descent, which requires a constant TAS during a change of height, is assumed and the thrust considered to be zero, the following correlation for small angles can be found by using equations [2.7-4] and [2.5-9]:

$$\mathbf{g} \approx \frac{D}{L} = \frac{1}{E} \quad (2.7-23)$$



This means that flying at maximum  $L/D$  for the unpowered flight leads to a minimum glide angle. It is of interest that this statement is apparently not influenced by the weight. In the interest of thoroughness it may be cited, that for unpowered flight the term *Rate of Sink* (ROS) is preferred to rate of descent.

Since the idle thrust is small the minimum glide angle at a given altitude is indeed approximately the same for all weights, as is clear from figure 2.18. However, it is shown that speed and ROC necessary to maintain the lowest angle increase with the aircraft mass.

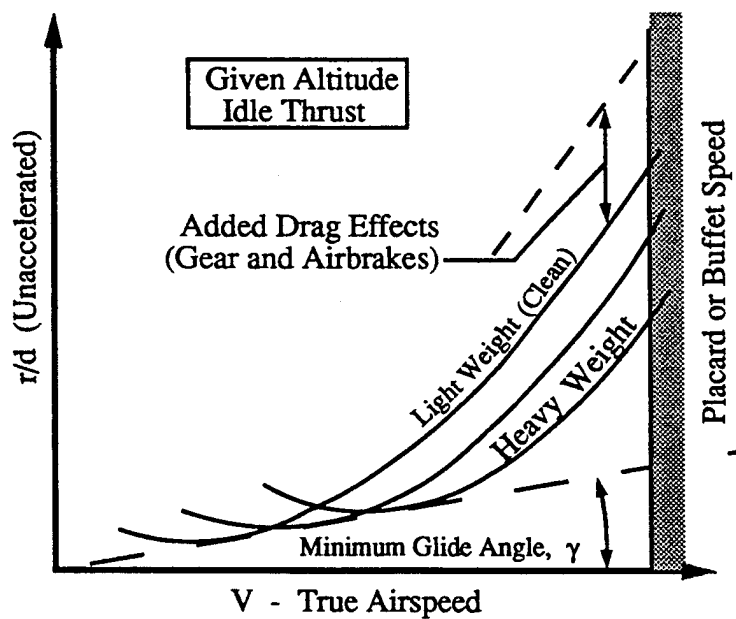


Figure 2.18 Minimum glide angle consideration (Boeing, 1989)

### 3 Hybrid Laminar Flow Control (HLFC)

Hybrid Laminar Flow Control (HLFC) is an active drag-reducing device. This means it must be provided energy and the pilot is able to turn it on or off in making a decision on whether it would work or not on a specific occasion.

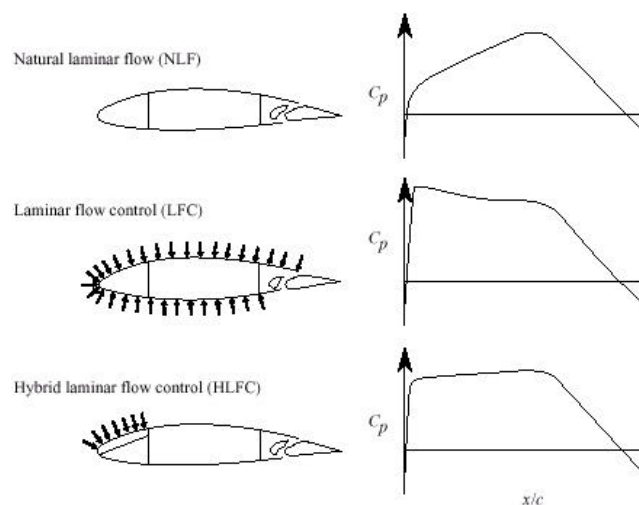
This is unlike a passive device, which operates through its shape. Examples for this could be either the sharkskin or the use of a Krueger flap as an insect shield. A third type exists, called reactive, which steps into the process rather haphazardly due to the existence of certain occurrences. This is, for instance, the set-up of a feather fan at the trailing edge of an eagle's wing in performing a flight at low speeds.

HLFC is a combination of both, Natural Laminar Flow (NLF) and Laminar Flow Control (LFC), which do not relaminarize a turbulent flow state. The latter defines as follows

*LFC is an active boundary-layer flow control (usually suction) technique employed to maintain the laminar state chord Reynolds numbers beyond that which is normally characterized as being transitional or turbulent in the absence of control.*

**(Joslin, 1998)**

If the airfoil is given a special shape, which favours the occurrence of a laminar boundary layer due to an appropriate pressure distribution, this is called NLF. Since the laminar boundary layer is disturbed here by cross-flow vortices, as the flow over a swept wing is three-dimensional, a single application of NLF is not meaningful. This is unlike the use of a LFC system, however, the combination of both to HLFC unifies all available advantages (See figure 3.1). **(Joslin, 1998), (DLR, 2001a)**



(a) NLF, LFC, and HLFC concepts for wing.

**Figure 3.1** Comparison of laminar flow techniques **(Joslin, 1998)**

### 3.1 Structure and Function of HLFC

The delay of transition is achieved by the application of boundary layer suction over the first 10 - 20% of chord, which depends on the location of the front spar. (See figure 3.2). For this reason, the surface of the corresponding area is perforated. Because of an estimated size of about 0.05 mm and a spacing between them of about 0.025 mm, millions to billions holes will be required for an entire application to an airplane, which obviously is going to be a significant manufacturing task. Special techniques like laser or electron-beam drilling are used to achieve this. (Young/Fielding, 2001), (Joslin 1998)

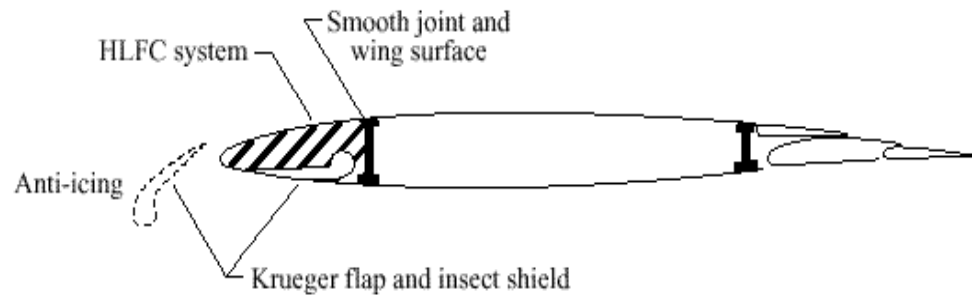


**Figure 3.2** Location of HLFC applied on a wing (Joslin, 1998)

A study made by Boeing concluded that an application of HLFC systems to a fuselage is not recommendable (Joslin, 1998). However, such a system is useful for the wings, the empennage and the nacelles, respectively. Correctly profiled bodies could achieve a laminar flow extend back to 50% chord (Young/Fielding, 2000). Due to the drag reducing function it offers the possibility of saving a considerable amount of fuel.

On the other hand the application during the flight mission is limited to the end term of climb, the cruise and the beginning of descent. Reasons for this will be discussed in the next chapter. As is apparent from figure 3.1, the system will cause an increase in OEW and furthermore effect a higher SFC, since some power is needed to use the suction pumps. For this reason studies are required to explore the efficiency, dependent on the factors above. It is evident that the benefits of using a HLFC system are increasing with the cruise time and therefore the range of an airplane.

### 3.2 Reasons for HLFC system failures

It cannot be assumed that HLFC provides the same reliability as other conventional aircraft systems. A number of possible failure causing impacts have been indicated and are shown in table 3.1.

While it is expected that the mechanical system failure rates will be comparable with other aircraft systems, the environmental “failure modes” will have a greater impact than usual. This is due to the sensibility of the perforated surface, which is necessary for a HLFC system. A dent due to hailstone or bird impact could cause transition and result in a turbulent wedge aft of this impact site. It will be a design task to develop an appropriate structure to reduce the probability of these failures to an acceptably low level. (Young/Fielding, 2001)

A further possible failure is the holes being blocked by dust, insects and ice. As the likelihood of encountering insects decreases with higher altitudes it is proposed to limit the application of HLFC systems to the end term of climb, the cruise and the initial descent, whereat the density of dust is also lower. Furthermore the frequency of rain at these heights is not that great and can be largely discounted. (Young/Fielding, 2001)

In performing a climb at lower altitudes, conventional solutions like the Krueger flap or the use of anti-icing systems, based on glycol or hot air, to clean the holes, would be a sufficient protection. Potential difficulties in dust storms or after volcanic eruptions could be solved by inactivation or flow reversion in these situations. (Young/Fielding, 2001)

**Table 3.1** Events which impact fuel usage on HLFC aircraft, based on Young/Fielding (2000)

Description	Mission Phase	Consequence	Mitigation	Factors
System failure	- Take off - Climb - Cruise - Initial descent	Partial or complete loss for the remainder of the mission	- System design - Maintenance	- System reliability - Design issue
Damage to laminar flow surface (e.g. hail impact; birds)	- Take off - Climb - Cruise - Initial descent	Partial or complete loss for the remainder of the mission	- Route planning - Pilot avoidance - Surface design	- Weather - Design issue
Insect contamination	- Take off - Initial climb	Partial or complete loss for the remainder of the mission	Cleaning by: - On-board system - Rain/Ice	- Weather - Season - Location - Design issue
Airborne particles	- Take off - Climb - Cruise - Initial descent	Partial or complete loss for the remainder of the mission	Cleaning by: - On-board system - Rain/Ice	- Volcanic - Weather - Operational issue
Ice, rain and snow	- Top of climb - Cruise - Initial descent	Complete loss of laminar flow for finite time	- Route planning - Pilot avoidance	- Weather - Operational issue
Ice crystals	- End of climb - Cruise - Initial descent	Partial or complete loss of laminar flow for finite time	- Pilot avoidance	- Weather - Season

Finally, the problem of encountering cirrus clouds remains during the cruise performance. The ice crystals in clouds between 25000 ft and 40000 ft are big enough to cause transition. This poses a unique problem for HLFC aircraft, as they are not an issue for current turbulent designs.

This topic is further explored by a study made by Young<sup>a</sup> and Fielding<sup>b</sup>. Using data of Boeing about the distribution of cloud occurrence this resulted in an average cloud encounter of about 25% during long-range flights. Considering this in the fuel planning, still a block fuel saving of more than 8% could be estimated. (Young/Fielding, 2001)

### 3.3 HLFC research undertaken

Since 1941 laminar flow control is a topic of aerodynamic research on airplanes (See figure 3.3). Over the years several attempts bore expanded improvements, however, the high costs of such experiments handicapped the efforts quite often. Additionally, the shape and the engines were not yet optimized at this stage, wherefore research concerning these areas was more profitable.

Since 1970, the laminar flow control research has flourished suddenly due to the shortage of kerosene, which went along with the oil crises. The rising fuel prices forced the manufacturers to develop more efficient models. A result of this time was NLF, which is achieved by a special shape of the airfoil that favours laminar flow. The application of LFC was still too risky, since its application was expensive and nobody could predict the actual advantages.

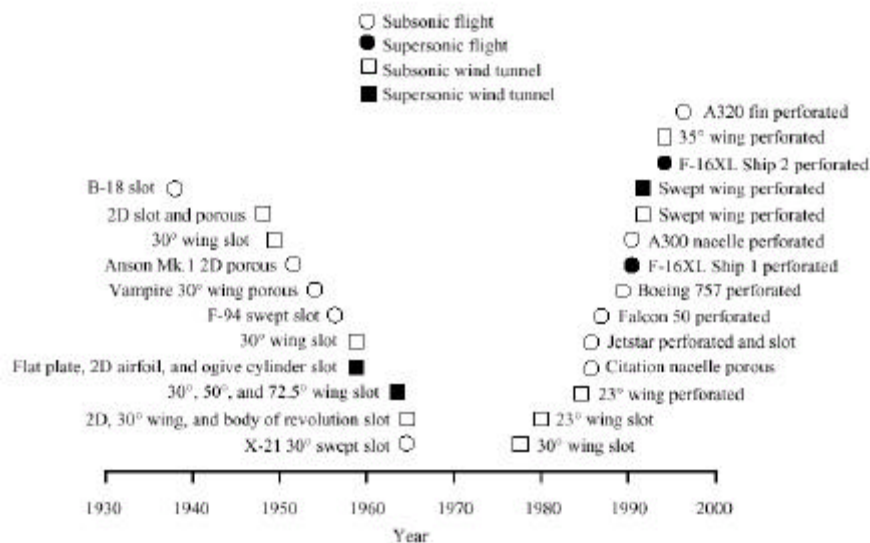


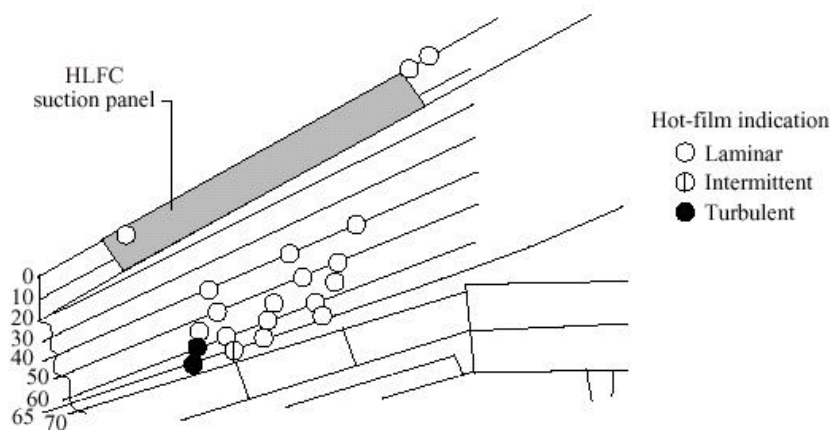
Figure 3.3 Overview of laminar flow control projects (Joslin, 1998)

Nowadays, the hard competition between the airlines requires optimized aerodynamic characteristics. Therefore, and for the reason that NLF succumbs some practical problems, applying it on swept wings, the combination of both, NLF and LFC, the so-called HLFC is considered to be the most compromising solution. In order to keep the market position the manufacturers are under pressure again to put this into practice.

Fortunately, the situation has changed meanwhile. Wind tunnels and computer models are available now. These reduce the costs, and thus the risks, of such research, which made immense progress in the last few years.

Only a few milestones shall be cited here. Boeing installed a HLFC suction panel on the wing of its 757 versions. This yielded first practically obtained information for aircraft of this size. A partial laminar flow extension up to 65% (**Joslin, 1998**) of chord could be measured (See figure 3.4). This data provided the basis for the studies of Young and Fielding, and thus, also for the studies this report is dealing with.

Also, Airbus carried out important projects. A HLFC nacelle test article has flown on an Airbus A300/B2. It could be investigated that here the laminar flow extent is independent of altitude with suction. In 1993, a vertical fin model of an Airbus A320 was examined in the wind tunnel with great success. A laminar flow extent back to about 40% could be achieved by perforation of 20% chord, despite of a swept angle of 35%. Since 1997 this is applied in operational tests. (**Joslin, 1998**)



(a) Laminar flow extent;  $M = 0.82$ ;  $h = 38\,600$  ft;  $C_L = 0.48$ .

**Figure 3.4** Laminar flow extend obtained on Boeing 757 HLFC flight test (**Joslin, 1998**) (Original from Maddalon 1990, 1991; Collier 1993)

Nowadays, new developed techniques enable the manufactures to put HLFC systems into practice, even on the gigantic surfaces of aircraft. In summary, it can be expected that HLFC systems will be encountered on the aircraft in the next future.

### 3.4 Other Drag Reducing Devices

HLFC is not the only attempt undertaken in order to reduce the drag of an aircraft. Other research is being carried out as new knowledge from the bionic science and advanced techniques concerning the properties of materials are available which are practically not yet used.

One example is the so-called sharkskin layer. The German zoologist Reif discovered that the skin of fast swimming sharks has a certain structure, containing microscopic small grooves along the direction of flow (See figure 3.5). The exploration of an enlarged model came to a significant drag reduction of about 10%. The grooves prevent the formation of normally developing cross flows, which have an impairing, and thus a braking impact. An Airbus A340, equipped with a layer of the same structure as a shark, had a lower skin-friction drag of about 8% during flight tests. This means that on long range missions 2.4 tons kerosene could be saved, which is equivalent to about 3% fuel. **(Bechert, 2001)**

For engineering reasons, application is limited to about 75% of the aircraft surface. The first aircraft, which is already using this technique, is equipped with a lamination of 30% and burns demonstrably 1% less kerosene. Applying an optimal lamination, the aircraft could take on-board 15 passengers more on account of the resulting fuel saving. **(G-O, 2001)**

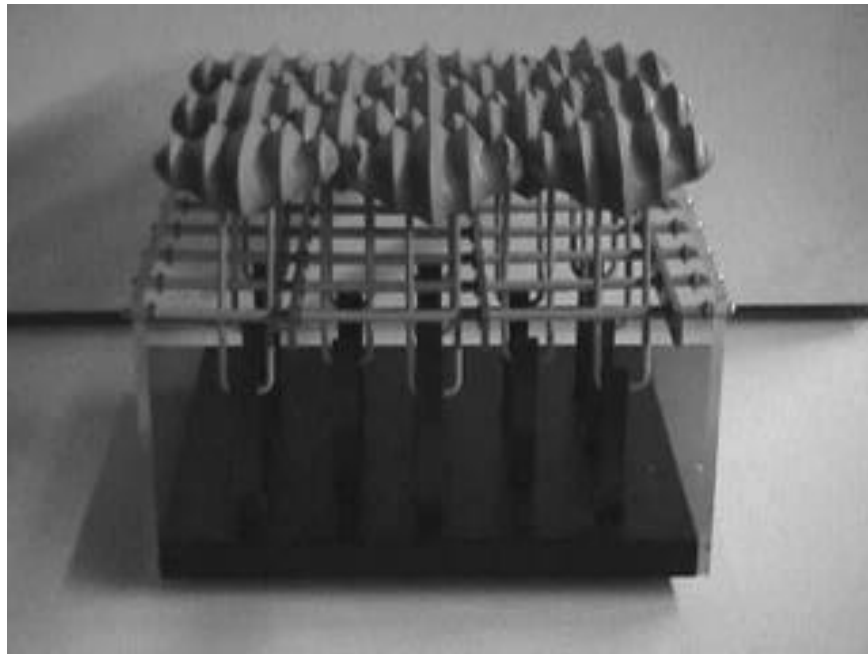


**Figure 3.5** Enlarged model of the sharkskin **(Bechert, 2001)**

---

<sup>a</sup> Lecturer at the Department of Mechanical and Aeronautical engineering, University of Limerick, Ireland

<sup>b</sup> College of Aeronautics, Cranfield University, Cranfield, Bedfordshire MK430AL, UK

Another example of bionic science, based on the observation of flying birds, is the cognition that most of the birds soaring over land show characteristically slotted wing-tips shown in figure 3.6.

Due to the difference of pressure between upper and lower wing surface, trailing vortices occur at the wing tips, which leads to a significant drag, the so-called induced drag. By spreading their feathers at this place the bird achieves an apportionment in several smaller vortices with much less kinetic energy, and the induced drag is considerably reduced. This resulted in the Multi-Winglet idea. (TU - Berlin, 2001)

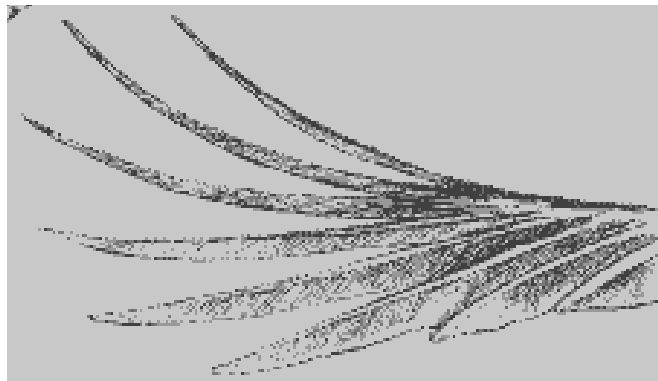


**Figure 3.6** Slotted wing tips of a bird (TU - Berlin, 2001)

Since this model contains some problems concerning its structural integrity, it was further expanded. By exploring and understanding the principles of this effect, the Multi-Wing-Loop has been developed which is very likely to be applied on future aircraft models (See figure 3.7). (TU - Berlin, 2001)

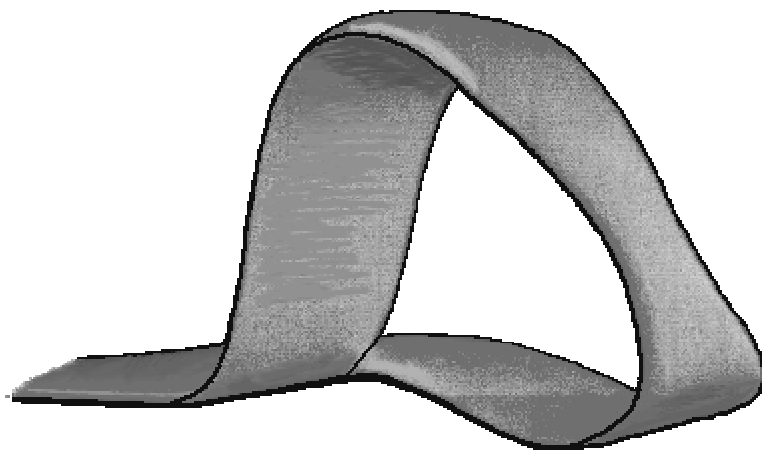


**Figure 3.7** Multi-Wing-Loop (TU - Berlin, 2001)



A further concept is the adaptive wing, which could revolutionize the aircraft construction, as it offers the possibility of designing an aircraft for several flight configurations. Like its name reveals, this wing is able to adapt its shape to a certain flight performance. Two different ways are considered to put this into practice; pneumatic muscles responding on their inner pressure or metallic muscles, made of so-called memory wires, responding on temperature. A model of the latter can be seen in figure 3.8. (TU - Berlin, 1999)

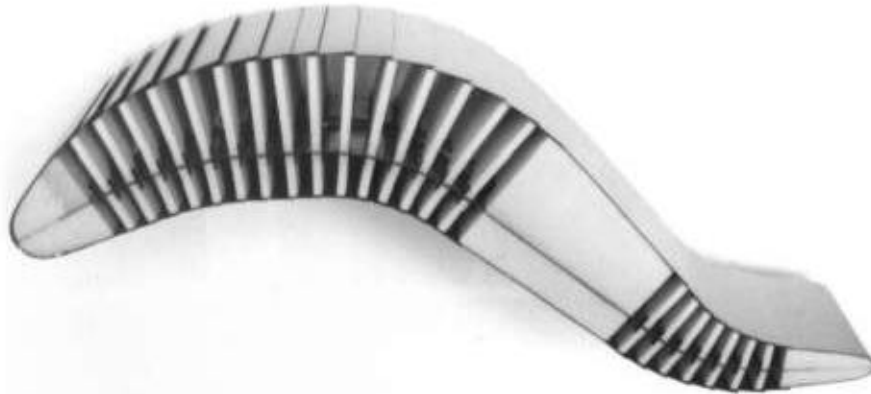


**Figure 3.8** Model of an adaptive wing based on memory wires (TU - Berlin, 1999)

## 4 Performance Calculation Software

The provided program was developed by Young. It is part of a research project in cooperation with the Cranfield University, Cranfield, UK.

This software has been developed to enable the calculation of the fuel consumption for a generic twin-engine aircraft and to explore the influence of using a HLFC system. It is based on a flight test data set for a typical airplane of medium-range class, which was provided by **Boeing** in the PEM.

### 4.1 Structure of Young's Program

The program consists of a Lotus 1-2-3 file, which includes 10 pages with various functions, as is shown in table 4.1.

Sheet A is the master sheet. It controls the calculations and nearly all-necessary variable parameters can be keyed in here. Furthermore it contains 4 buttons, which are connected to several macros. These conduct different calculations by keeping certain parameters constant while allowing others to change. This is achieved by several backsolve functions, whose working method will be explained in chapter 4.2.3. In addition, it supplies all computed results and provides the integrated range and the integrated time for any single part of the flight mission.

In the spreadsheets B to C, the essential calculation tables for cruise, climb and descent in each case of the main and alternate mission can be found. Spreadsheet D is used to work out the hold.

Since the program is based on data obtained from in-flight tests, the file contains several tables containing these. The data was provided in the Performance Engineers Manual (PEM) for a generic twin-engine jet transport aircraft of short range class and was transferred into the spreadsheets E to H. Table 4.1 shows, which data the particular pages contain.

The International Standard Atmosphere is given in spreadsheet I in the form of a tabulator, which includes the values of the major atmospheric properties such as pressure, temperature and density in several units and their ratios with regards to sea level conditions.

While the main answers are displayed on page A, the results of several runs are tabulated for later analysis on page J called Output. Here one can find, the input values as well as the results of the calculated burned fuel for any part of the mission, their sum to trip, block and total fuel, and the trip time.

**Table 4.1** The contents of the particular pages

Spreadsheet	Contents
<b>A</b>	Master spreadsheet including input and output information
<b>B</b>	Table A: - cruise range calculation for mission Table B: - cruise range calculation for alternate
<b>C</b>	Table A: - climb analysis for mission cruise Table B: - climb analysis for mission alternative Table C: - descent analysis for mission cruise Table D: - descent analysis for mission alternative
<b>D</b>	Table A: - hold fuel calculation
<b>E</b>	High speed drag polar for Boeing 7G7/DL-5191
<b>F</b>	Tables A - L: - corrected fuel flow data from sea level up to 42000 ft
<b>G</b>	Table A: - maximum climb thrust data Table B: - minimum idle in-flight thrust data Table C: - minimum idle fuel flow data
<b>H</b>	Table A: - brake release to 1500 ft (several data) Table B: - data for recommended holding speed at 1500 ft
<b>I</b>	International Standard Atmosphere tables
<b>J (Output)</b>	Output summary of results

## 4.2 Function of Young's Program

This chapter will explain how the program has to be used and will show what happens after one runs a macro by hitting one of the buttons. First of all, the input parameters have to be defined. This can be done in the control box in spreadsheet A for the general information. (See figure 4.1)

<b>CONTROL BOX and INPUT DATA</b>		<b>Clear</b>
<b>Input Data (Specify BRWeight or Range)</b>		<b>Solve for</b>
BR Weight	250230 lb	<b>Range</b>
Cruise Range	2900 nm	<b>Weight</b>
Payload	56600 lb	<b>Fuel</b>
OEW Baseline A/C	128700 lb	
<b>Control Parameters (Guess start values)</b>		
TOC to TOD for cruise	2620 nm	
TOC to TOD for alternate	107 nm	
<b>Other Data</b>		
Alternate cruise	200 nm	
Hold (Final reserve)	30.0 min	
Cruise height	35000 ft	
Climb 250/290 Mach 0.80		
Contingency Fuel	3.00% of trip fuel	
Additional Fuel	0 lb	

**Figure 4.1** The control and input box

It is to remark that the climb schedule here is for information only. An actual change is to be done in the climb and descent calculation tables of spreadsheet C. In the same manner the cruise height is to be handled, which can be modified in the cruise calculation tables whereby one must pay attention to the fact, that the end height of climb, as well as the start height of descent accord to the corresponding schedules.

In order to study an installed HLFC system another input box exists. Here the advantageous and adverse influences of such a system can be keyed in. The subdivision into sectors offers the possibility either to limit the use of the system, or to simulate a system failure for parts of the cruise. (See figure 4.2)

<b>Baseline</b>	0,00425	1,86%	2270
<b>HLFC</b>	<b>Drag</b>	<b>Q</b>	<b>OEW</b>
<b>Cruise Sector:</b>	<b>Change</b>	<b>Increase</b>	<b>Increase</b>
All sectors or: specify by cruise location	0,00450	1,86%	2270
0	0,00450	1,86%	
1	0,00450	1,86%	
2	0,00450	1,86%	
3	0,00450	1,86%	
4	0,00450	1,86%	
5	0,00450	1,86%	
6	0,00450	1,86%	
7	0,00450	1,86%	
8	0,00450	1,86%	
9	0,00000	0,00%	
10	0,00000	0,00%	
11	0,00000	0,00%	
12	0,00000	0,00%	
13	0,00450	1,86%	
14	0,00450	1,86%	
15	0,00450	1,86%	
16	0,00450	1,86%	
17	0,00450	1,86%	
18	0,00450	1,86%	
19	0,00450	1,86%	
20	0,00450	1,86%	
Climb (>20 000 ft)	0,00000	0,00%	

**Figure 4.2** Input Box for HLFC data

In the following chapters the function of several calculation tables and the buttons connected to macros will be described.

### 4.2.1 The Cruise Calculation Table

In table A in spreadsheet B the necessary calculations concerning the cruise are carried out. The main input values are taken from spreadsheet A, called master sheet from hereon. These are the weights at TOC and TOD, as well as the already flown distance till TOC and the necessary time for this. Some other inputs can be made inside the chart at violet shaded cells, which are explained at appropriate places.

First of all, the difference between start and end weight is determined and divided into 20 numbered steps. This, and the following input columns offer the opportunity to allow changes during the cruise for altitude, velocity and atmospheric conditions. Note that these changes are instantaneous considered, which leads to approximations.

Depending on the altitude, the ratios for temperature and pressure, as well as speed of sound are taken from the ISA table in spreadsheet I. After determining  $W/\dot{a}$ , the lift coefficient is calculated by taking the wing area,  $S$ , out of the input box in the master sheet and using the sea level density and speed of sound from spreadsheet I:

$$c_L = \frac{W / \dot{a}}{\frac{1}{2} \rho_0 a_0^2 M^2 S} \quad (4.2-1)$$

For this value of  $c_L$ , a lower and upper limit with only two significant numbers around the actual result is determined to be able to look up a value for  $c_D$ , in each case from the drag polar table in spreadsheet E. The real  $c_{D,Base}$  is subsequently obtained by interpolation:

$$c_{D,Base} = \frac{c_L - c_{L,LO}}{c_{L,UP} - c_{L,LO}} (c_{D,UP} - c_{D,LO}) \quad (4.2-2)$$

In this place,  $c_{D,Base}$  can be modified through the HLFC reduction factor, which takes into account the influence of a virtually installed HLFC system and is conducted by the master sheet again to get the final drag coefficient  $c_D$ . From this, the gross  $D/\dot{a}$  is determined. By dividing this by two the required net thrust per engine is calculated, since a steady level flight is assumed, at least within any interval.

If enough thrust is available, which is checked against table A in spreadsheet F, the corrected fuel flow,  $Q_{corr}$ , is obtained from the same spreadsheet in an equivalent manner as for the drag coefficient. Unlike this, some on height dependent range names are regulated to enable a clean selection of the appropriate values. This is merely due to software internal problems of Lotus 1-2-3. (Young, 2001b)

Afterwards, the total temperature and the total pressure ratios are calculated to determine the fuel flow. In this the total temperature ratio taken to 0.6363 is considered, which, together with the fuel flow calculations is described in detail in chapter 2.6.

The total fuel flow is double the fuel flow obtained, since this software deals with a twin-engine aircraft. It can be modified by the additional fuel consumption of eventual-acting HLFC systems through a correction factor given from the master sheet. The final result, divided by the calculated true airspeed gives SAR for any step.

By taking the values of weight and SAR from two adjacent steps,  $n$ , an average SAR and a change in weight can be obtained, which leads to range and time increments for each interval, as is shown below:

$$r_{n-1;n} = \frac{SAR_{n-1} + SAR_n}{2} (W_n - W_{n-1}) \quad (4.2-3)$$

$$t_{n-1;n} = \frac{r_{n-1;n}}{v_n} \quad (4.2-4)$$

The sums of these increments lead to the final answer for the entire range of performing the cruise and the time needed for this. The results are put back into an output table, where the necessary fuel is obtained and from there, the results together with the fuel used are put into the master sheet.

The alternate cruise and the hold, respectively, are calculated in the same manner, whereby no HLFC correction is needed, as it cannot be used for these parts of the flight mission. Since the hold is conducted at the maximum possible endurance speed, the recommended Mach number is obtained from Table B of spreadsheet H and is dependent on the weight. Furthermore, in the hold table, the determination of range is not required and the time is computed directly:

$$t_{n-1;n} = \frac{2(W_n - W_{n-1})}{Q_{\text{total};n-1} + Q_{\text{total};n}} \quad (4.2-5)$$

## 4.2.2 The Climb Calculation Table

The climb is computed in table A of spreadsheet C. The calculations are carried out according to the method described in chapter 2.7.4 from 1500 ft up to the first stage of cruise level. This, as well as the single vertical intervals can be keyed in by the user into the violet shaded cells. In addition, input cells for non-standard conditions and the climb schedule are provided, and likewise coloured.

The master sheet gives the start weight for the first altitude. All other start weights result from passing through the calculations of the climb step before. In each case, it is applied on the start height first, to obtain  $W/\bar{a}$  and hence the lift coefficient after determining the according atmospheric properties and the Mach number.

Subsequently,  $c_L$  is used to look up and interpolate the drag coefficient for a rounded reference Mach number in the same manner as in the cruise calculation, which can be modified by the HLFC factor again at climb intervals above 20000 ft, and is needed to calculate the  $L/D$  ratio.

Now the Mach number is rounded up and down to values of two significant numbers to be able to look up the maximum climb thrust from table A of spreadsheet G. The actual Mach number is used to interpolate the thrust over delta ratio per engine, which bears subsequently the thrust required.

Afterwards, the calculations for the ROC are carried out. Originally, the term  $\ddot{O}$  is calculated using the Mach number for climb steps performed at CAS. Herewith, the acceleration factor can be worked out and, accordingly,  $\sin\tilde{\alpha}$  as all necessary parameters are now known. After determining TAS, the ROC can be finally calculated, which is multiplied by a factor to change the unit from knots to feet per minute. All this is described in detail in chapters 2.7.1 and 2.7.2.

After defining some range names for software internal reasons again, the corrected fuel flow is interpolated by looking up the appropriate values for the up and down rounded thrust values in terms of 3000 lb steps and, subsequently, using the original one. For instance, an obtained thrust of 25675 lb would lead to the limits 24000 lb and 27000 lb. For these values, the corrected fuel flow can be looked up in spreadsheet F, and by using 25675 lb, an interpolation can be carried out to determine the to 25675 lb thrust appropriate  $Q_{\text{corr}}$ . The total ratios of temperature and pressure as well as an exponent of 0.6363 for the former are used to calculate the actual fuel flow, which can be corrected by an HLFC factor given by the master sheet. Its double is the answer for the total fuel flow of the entire airplane.

Eventually, a first estimate concerning the time needed and the fuel burned is made for this climb step by using the difference between start and end height. This enables an approximate end weight to be determined:

$$\text{estimated time:} \quad t_1 = \frac{h_{end} - h_{start}}{ROC_1} \quad (4.2-6)$$

$$\text{estimated fuel:} \quad W_{F,1} = Q_{total} \frac{t_1}{60} \quad (4.2-7)$$

$$\text{and hence:} \quad W_{est} = W_1 - W_{F,1} \quad (4.2-8)$$

This estimated end weight is now applied to the end height and the calculations are passed through in the same manner as described above. Once the second values for ROC and the total fuel flow are obtained, they are each used to calculate an average, by integrating of their first results. The application of these average values ends up in the final solutions of time needed and fuel required for each interval. The hence obtained end weight result is used as the start weight of the next climb step in each case.

By also determining a mean TAS and an average for the sine of the climb angle per interval leads to the horizontal speed and eventually the flown distance. Summing these up, as well as the values for time needed and fuel used from all intervals result in the desired answers. These are given back to a little output table, and following that to the master sheet A.

It may be stated here that the necessary data concerning the start and the subsequent climb from sea level up to 1500 ft are available in table A of spreadsheet H. This is obtained directly from the master sheet. Results for this, including time, fuel and distance, depend on the actual BRW.

The climb for the alternate mission after a missed approach is computed in the same way, where no use of HLFC systems is assumed and thus the appropriate factors do not appear.

The calculations for descent performance contain some variances. Data for the idle in-flight thrust and the corresponding idle fuel flow are available in either table B or table C of spreadsheet G depending on the rounded reference Mach number and the instantaneous height. The use of HLFC systems is not assumed either; hence no correction regarding this is required.



### 4.2.3 The Macros

All calculations described above are carried out immediately after entering the input parameters. Now the active part of the program shall be illustrated by explaining the functions of the macros assigned to the buttons.

By using the RANGE button, the macro SUBMAIN1 is activated. It enables the macro trace to control the course and determine where eventual bugs occur. Two variables are defined, one to count the executed calculations and the other to obtain the steps of iteration. The latter appears with a text message in the macro work area and check box in spreadsheet A. Subsequently, the tankered fuel is set to zero, which implies that the entire fuel is to use to determine the range.

It follows the call of subroutine SUBWEIGHT, which ensures that the iteration is not carried out more than 50 times, because after this, no convergence can be expected. Afterwards, the subroutine SUBSOLVE is called.

SUBSOLVE contains a backsolve function for the cruise, the alternate cruise and the hold in each case. Such a function finds... *values for one or more cells that make the result of a formula equal to a value you specify... The formula for which you want to get a specific result must depend directly or indirectly on these cells.* (**Lotus 1-2-3**) Thus, it has to include three parameters, the formula-cell, the target-value and the adjustable-range. The first is the cell containing the value, which should be equal to target value by changing the amount of the third one. Varying the adjustable cell must implicate a change of the first parameter.

This means, for example, for the cruise, that the end weight is altered as long until the from the cruise calculation table resulting range accords exactly to the cruise range in the control box of the master sheet. Since this occurs in the first iteration for the guessed value, it should not be assigned invalid information. The alternate cruise and the hold are backsolved in the same way, whereas the latter is verified against the regulated time. Once a solution is found, the program continues with the next order.

It may be remarked, that sometimes no solution is determinable by the backsolve function. It has determined that a change of one of the guessed range values and a subsequent rerun supplies remedy. Since the mouse function is set out of control after a failed backsolve it is necessary to press the F5 button on the keyboard and then RETURN to enable it again, which is probably due to the Lotus 1-2-3 internal make up.

After returning to SUBWEIGHT, the cruise range is modified by multiplying it with the ratio of the given and the calculated BRW and the entire range in the control box is replaced by this calculated value. The alternate cruise range is corrected by the difference of required and calculated entire alternate range. Eventually, it is proved, that the error between the given and the calculated BRW, as well as that for the alternate mission, the covered range does not exceed a certain percentage. Dependent on the result of this check the program continues either with a jump back to the beginning of SUBWEIGHT in order to carry out the same procedure applying the new values or with a return to SUBMAIN1 after changing the message, which indicates that the calculation is finished now.

It follows a call of SUBPRINT, which prints the desired results into the first available free column of the output sheet by designating this column with the actual number of executed calculations. After this, it returns to the SUBMAIN1, where the macro trace function is enabled and the macro is ended.

The subroutines SUBMAIN2 and SUBMAIN3 work in the same manner as SUBMAIN1. The only difference is that either SUBRANGE, in case of using the WEIGHT button, or SUBFUEL is called. The subroutine SUBFUEL is assigned to the FUEL button.

In SUBRANGE, after returning from SUBSOLVE, the cruise range in the control box of the master sheet is corrected by the difference between required and calculated range. Subsequently, it is proved if the calculated range corresponds to the from the user desired within a certain error. Depending on the result of this check, the program either goes back to the beginning of this subroutine or it continues by replacing the BRW in the control box through the value determined by the backsolve function. With this a first estimate is made that is supposed to be quite close to the final result, which leads to a shorter computing time. A further call of SUBSOLVE has primary the reason to find appropriate solutions for the alternate cruise range and the hold. After correcting the alternate cruise range in the control box, the results are checked again in the same way as in SUBWEIGHT, which is described above. If it is necessary, a jump to the beginning of this subroutine is executed. Otherwise the for the desired range calculated BRW is checked against the maximum possible value. Whenever this is exceeded, the user will find a corresponding message in the box of checks inside the master sheet and he will know that the range he wanted cannot be covered by using this data set.

The subroutine SUBFUEL works quite similarly to the already described SUBWEIGHT. The differences are that no input values of the control box are modified and the BRW check is left out. Instead of this, the cell containing the tankered fuel is given a value, which is the result of subtracting the *Zero Fuel Weight (ZFW)* as well as the contingency and eventual additional fuel from the calculated landing weight at the alternate aerodrome. A positive sign implies that some reserves are available, a negative one means either too much payload, too long range or that more fuel is to be taken onboard if possible.



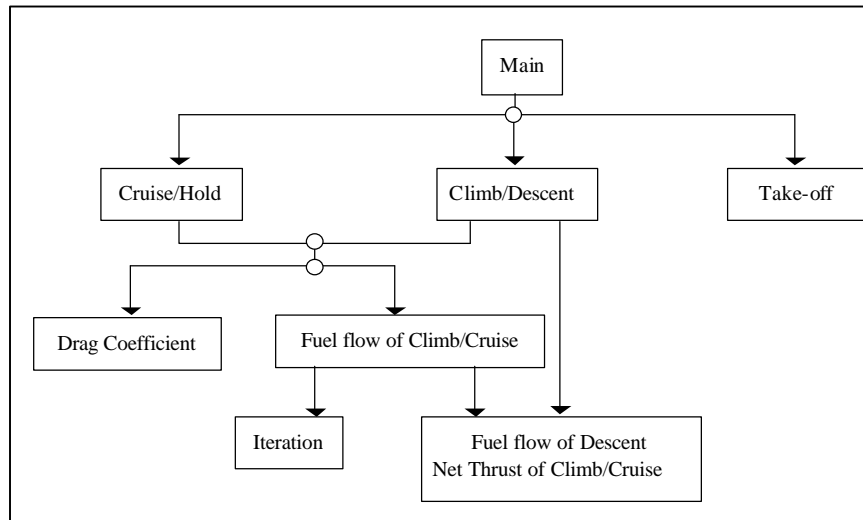


**Figure 4.3** Hierarchy of macros (Straubinger, 2000a)

A little output box right beside the input gives the main answers after one ran the macros by using the RUN button. The CHECK button enables the crosschecking of results, as here, the calculations are carried out without any iteration. The output box and the Check button can also be found in the input box.

As already stated, the way the calculations are performed depends on the given input parameters. There are three different ways available to solve proposed problems. These are shown in table 4.2. Unknown parameters should be set to zero or the corresponding cells should remain empty.

**Table 4.2** Types of input, based on (Straubinger, 2000a)

given values	calculated value
fuel, payload OR fuel, brake release weight OR only fuel (no payload) OR brake release weight, payload	range
payload, range	fuel (and hence the brake release weight)
fuel, range	payload (and hence the brake release weight)

The calculations in the subroutines work in basically the same manner as in Young's software. Appendix B gives for both programs a logical overview in flowchart form.

Since the entire calculation is based on macros, this software needs longer run times and is less flexible for modification like e.g. HLFC impacts. However, one of the aims of this report was to investigate this influence. For that reason Young's software is chosen for successive explorations.

#### 4.4 Comparison of Results from both Programs

Since Straubinger had no knowledge of the already established program, he developed his model in a completely different way. For that reason, it represents a perfect tool to check the reliability of Young's software.

Comparing the results of both programs carries out the check. This is done by running them using identical input data and limits for an aircraft, so that it performs the same flight mission under equivalent conditions. The model used may be defined as shown in figure 4.4 in the form of the input box from Straubinger's software, as in here also the climb schedule could be defined.

		MAJOR MISSION			DIVERSION		
CLIMB	schedule	250	290	0,8	250	290	0,52
		stepsize	2000 ft		stepsize	2000 ft	
		at	35000 ft		at	20000 ft	
CRUISE		mach :	0,8		mach :	0,52	
		stepsize	2000 lb		range	200 nm	
					stepsize	2000 lb	
DESCENT	schedule	0,78	290	250	0,52	290	250
		stepsize	2000 ft		stepsize	2000 ft	
Oper. empty w.	(l)	128700			LIMITS	max take-off weight (lb)	255000
						max payload (l)	56600
						max fuel weight (l)	77422
		INPUT	OUTPUT				
Fuel on board	(lb)	0		run	ERRORS	contingency fuel (%)	0,1
Payload	(l)	56600		check		range	(
Brake release w.	(lb)	0					
Range	(r)	2900					
Contingency fuel	(%)	3,00				needed time for calculation :	19:38:34

**Figure 4.4** Input box of Straubinger's program containing the input parameters, based on Straubinger (2000b)

The range, which can be found in figure 4.4 is the maximum assumed value. By reducing this down to 50 nm the appropriate BRW was obtained by several runs of both programs, where the payload was fixed. This study can be found in the file COMPAR01.WK4. The results are presented in a table, which includes the error between both answers in order to compare them. As is clear from table 4.3, the computed results show slight differences, which could be expected, since both programs allow a marginal error. The maximum error is shaded and amounts to 0.085%. This is a very close result and shows that both programs come to the same answer, although they use different methods.

**Table 4.3** Comparison of results from the programs of **Straubinger (2000b)** and **Young (2000)**

<b>Range</b>	<b>BRW (Straubinger) [lb]</b>	<b>BRW (Young) [lb]</b>	<b>Error [%]</b>
0	196817	196918	0,051
200	200338	200469	0,065
500	205763	205880	0,057
1000	215047	215194	0,068
1500	224742	224898	0,069
2000	234927	235077	0,064
2100	237027	237172	0,061
2200	239151	239312	0,067
2300	241296	241452	0,065
2400	243464	243639	0,072
2500	245657	245829	0,070
2600	247883	248072	0,076
2700	250134	250325	0,076
2800	252421	252637	0,085
2900	254773	254960	0,073

## 5. Modification for a long-range class Aircraft

Besides checking the software against results from other sources a further aim of this work has been to modify it by replacing the data with that of a long-range aircraft. This was done in order to enable an extension of the studies. The second model would offer the exploration of a wider spectrum of range and the influence of the different design parameters, since they are quite different for both classes as is shown in table 5.1.

**Table 5.1** Comparison of input data of both versions

<b>Version</b>	<b>Original Version</b> based on Boeing 757 class aircraft	<b>Modified Version</b> based on A330-200 class aircraft
<b>BRW</b>	255,000 lb	513,884 lb
<b>OEW</b>	128,700 lb	259,600 lb
<b>MPL</b>	56,600 lb	67,900 lb
<b>Fuel capacity</b>	77,422 lb	245,411 lb
<b>Range</b>	2,900 nm	6,650 nm
<b>Wing Area, S</b>	1,952 ft <sup>2</sup>	3,916.5 ft <sup>2</sup>

The information shown in table 5.1 was gathered in several references. While the Boeing class aircraft data is given in Young's software (**Young, 2000**), the values of the A330-200 class aircraft refer to **Airbus (2000)** and **Airbus (2001)**. Furthermore, the OEW is taken from the **Operating manual**, since Airbus merely provided an average value. The Wing Area, *S*, is calculated based on the available flight test data.

After entering the new data, it was required to make sure that the software runs reliably. In addition, the results computed by the program had to be compared with other data to be able to judge them. Therefore a flight crew operating manual used by airlines was provided. Another available reference, which could be used, was an advertising briefing from Airbus.

This chapter will explain how the provided data was dealt with and will show how the answers compare with published references.

### 5.1 Flight Test Data

Performance data of a typical twin engine aircraft of long range A 330-class, given in the form of a Lotus 1-2-3 spreadsheet, was available at the University of Limerick. Besides other information these tables contained data of integrated range, integrated time, total fuel flow and thrust dependent on the momentary gross weight of the aircraft, as well as the appropriate lift and drag coefficients.

Altitudes from 29000 up to 42000 feet in 1000 feet steps and, in each case, Mach numbers from 0.78 to 0.82 in steps of hundredths were covered, which are typical for a cruise performance. This information was now used to work out similar data tables to those of Young's program. Afterwards, the task was to replace the original tables, to ensure the programs function succumbing this modification and to check the results against published information.

### 5.1.1 Corrected Fuel flow tables

Based on the available flight test data, tables were constructed, which included round values of thrust per engine and their corresponding interpolated corrected fuel flow, which was obtained, according to chapter 2.6.2 by applying the mathematical analysis used exponent, which equals to 0.5, since no further engine information was available. This interpolation has been carried out in order to achieve a similar basis for all tabulations, which is necessary to build up proper working "look up" tables. An example is given as follows:

**Table 5.2** Corrected fuel flow data for rounded thrust values

Mach number	0.82	0.81	0.80	0.79	0.78
per engine FN/Delta [lb]	Corrected fuel flow per engine at FL350 [lb/hr]				
51000	21291	21399	21517	21618	21721
50000	20882	20984	21087	21193	21300
49000	20461	20559	20657	20768	20879
48000	20038	20131	20225	20334	20441
47000	19614	19703	19793	19898	20003
46000	19190	19274	19359	19461	19562
45000	18769	18844	18925	19023	19122
44000	18361	18442	18518	18607	18695
43000	17953	18041	18128	18204	18298
42000	17545	17639	17739	17801	17913

After plotting the results for each Mach number, they all ended up in nearly straight lines. This can be seen in figure 5.1.

Therefore and by comparison with developed flowcharts, based on the Boeing data the assumption was made, that data above and below the given thrust could be obtained simply by extrapolating the curves. Figure 5.1 shows furthermore, that the offset between adjacent curves of the different Mach numbers is also similar. For that reason, curves for lower speeds are generated by extrapolation again. The determination of graphs for higher velocities was not necessary, since the designed cruise Mach number of most transport jets of the considered class is not greater than 0.82.



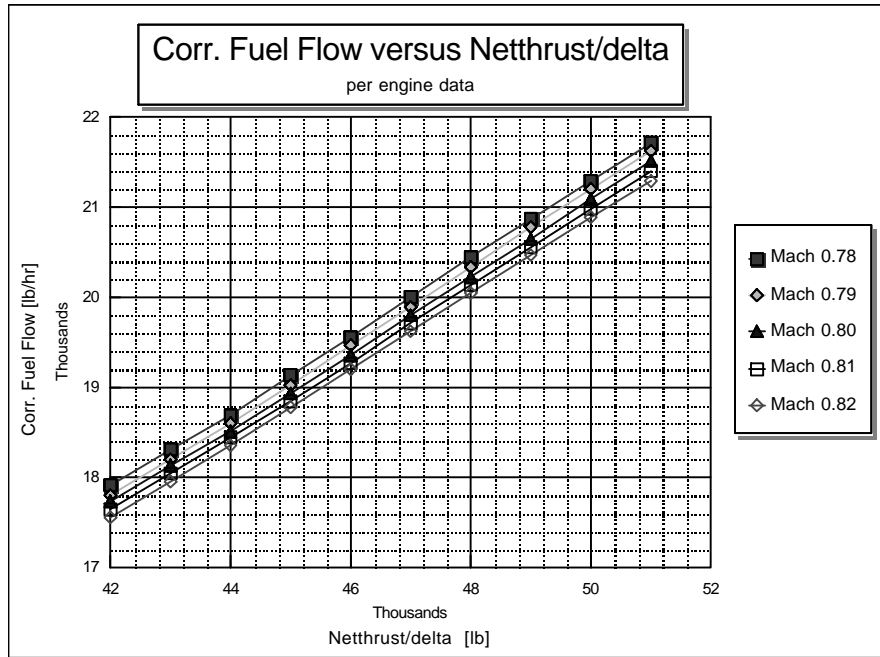


**Figure 5.1** Corrected fuel flow curves for several Mach numbers at 35000 ft

The practical application has shown, that the use of the lowest and highest available values to carry out both kinds of extrapolation led to the most useful answers. This resulted in a table containing Mach number and thrust per engine dependent data of corrected fuel flow for every given altitude. For the reason of completeness, they all were entered into spreadsheet F of the program, even though not all of them are used, because the offset of flight levels amounts to 2000 ft.

In the tables the original data is marked yellow, the values obtained through extrapolation along the curves are shaded violet and the cells, which contain the extrapolated results for new graphs, have got a green colour.

Another hypotheses have been used in order to get the climb calculation necessary tables for lower altitudes. The contemplation of the Boeing data has shown, that their curves intersect at low thrust. This intersection point peregrinates towards the higher thrust with decreasing height. Such a point is also to be found by plotting the data of the long-range class aircraft at heights from 30000 and 29000 feet. This can be seen in figures 5.2 and 5.3.

To achieve a similar result, tables based on the Boeing data have been made, which include the ratios of values from the 29000 feet table referring to the corresponding data for the same Mach number and the same thrust at lower heights. These ratios were used as divisors for the 29000 feet long-range data chart of the long-range class aircraft, each assigned to the appropriate altitude, Mach number and the doubled thrust, to generate the required tables.

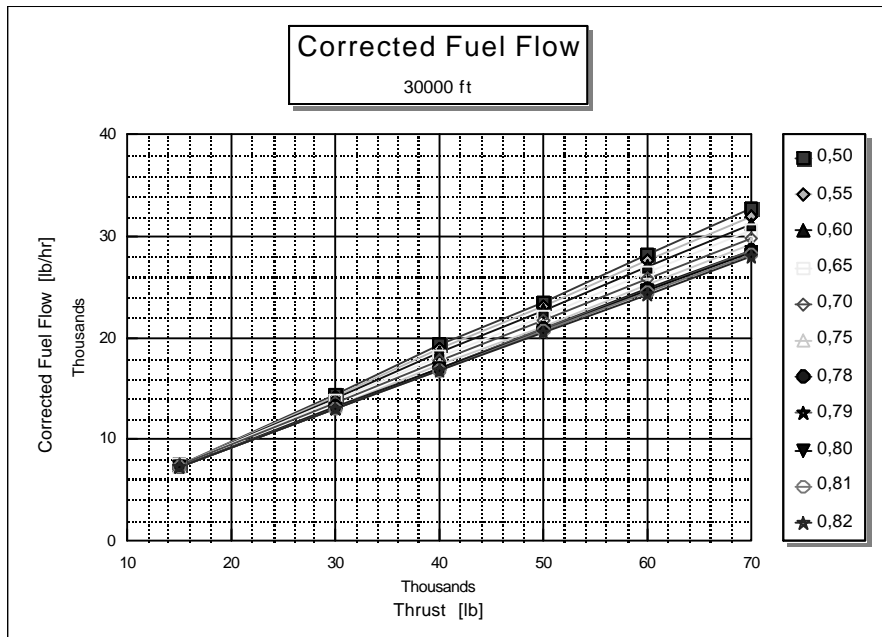


**Figure 5.2** Intersection point at 30000 ft

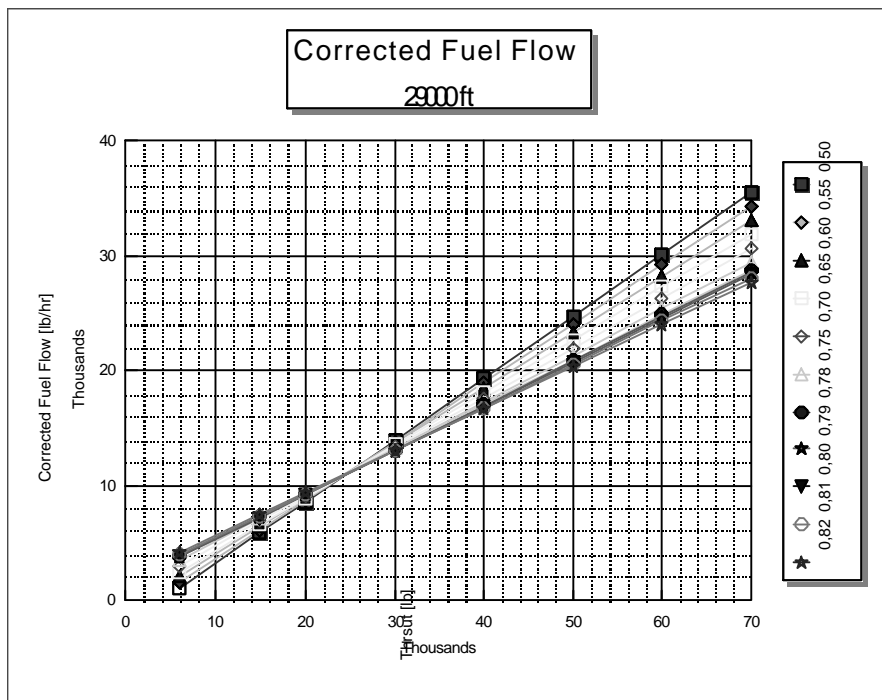


**Figure 5.3** Intersection point at 29000 ft

The thrust has been doubled, as a similar design point and duplex weight was assumed for the long-range aircraft. The results of this method have also been coloured yellow in the lower altitude tables, which were obtained in this way. All the other necessary data was obtained by interpolation and extrapolation again. This method was not as successful as expected, but the results were found to be acceptable in absence of any other available information, since an actual move of the intersection point would require too many guesses.

### 5.1.2 The Drag Polar

The lift and drag coefficient data supplied an approximate idea about the aerodynamic properties. In order to obtain the drag coefficients corresponding to lift coefficient values of two significant numbers, interpolations had to be made for each Mach number. By using the two lowest provided values, data for the zero-lift drag coefficient has been determined. This gave the results, which can be seen in the following table:

**Table 5.3** High-speed drag polar data

$c_L$	M 0.78	M 0.79	M 0.80	M 0.81	M 0.82
<b>0,00</b>	0,01452	0,01549	0,01536	0,01531	0,01538
<b>0,40</b>	0,02008	0,02022	0,02037	0,02057	0,02085
<b>0,45</b>	0,02165	0,02177	0,02191	0,02212	0,02243
<b>0,50</b>	0,02342	0,02355	0,02366	0,02390	0,02418
<b>0,55</b>	0,02547	0,02561	0,02573	0,02590	0,02637
<b>0,60</b>	0,02809	0,02830	0,02856		

A comparison with the Boeing drag polar data showed that the zero-lift coefficient should steadily increase with the Mach number. However, in order to use the original data no further changing assumption had been made, as the extrapolated values complied with this trend at their limits.

Since only some of the typical cruise performance data was available, it was attempted to ascertain, in what way the parabolic approximation could be applied to determine further information. For that reason, the results were plotted versus the squared  $C_L$ . In addition the curve of the squared deviation was drawn into the same diagram. For the factor  $k_1$  the assumption had been made, that the Oswald's efficiency factor equals to 0.85 (**Scholz, 1999**), which is normally the case, and the aspect ratio amounts to 9.26 (**Jenkinson, 2001**). The latter assumption was made, in order to come as close as possible to (for comparing reasons) provided data in the form of an Operating Manual for an A330, which is later specified in detail.

As is apparent from figure 5.4, this did not lead to a satisfying result. Therefore, another factor,  $k_3$  had been introduced in the following manner:

$$c_D = c_{D,0} + k_1 c_L^2 \quad \text{with} \quad k_1 = \frac{1}{k_3 \rho A e} \quad (5.1-1)$$

Furthermore, figure 5.4 shows that the parabolic approximation was not sufficient for lift coefficients higher than 0.5 as the curves could no longer be considered as being a straight line in this region.

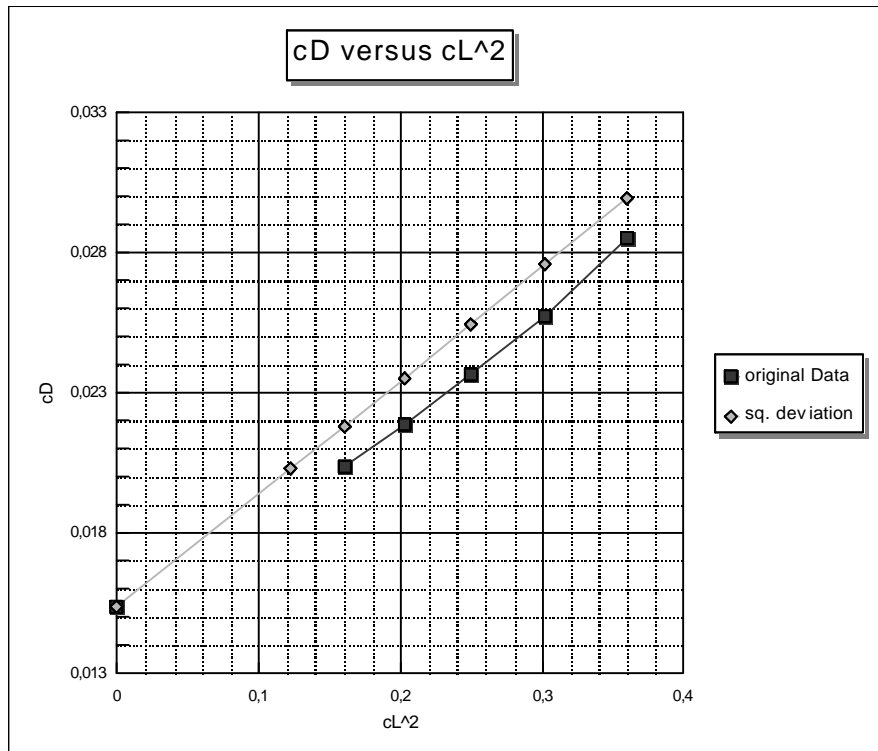


**Figure 5.4** Comparison of available drag polar data with parabolic deviation

Therefore, the expression 2.5-10 has been used, which considers the effect of Mach number as is discussed in chapter 2.5.4. Since still no adequate results could be gathered, the decision was made to raise the exponent for  $c_L$  in the last term of the equation, as this is a further respected method. (Young, 2001b) An exponent equal to 6 finally led to sufficient accuracy:

$$c_D = c_{D,0} + k_1 c_L^2 + k_2 c_L^6 \quad (5.1-2)$$

Subsequently, for each given Mach number the parabolic equation was used to find the part of the drag polar below the available data and expression 5.1-2 for the proportion above them. This is shown by the example for a Mach number of 0.80 in figure 5.5.

The practical application has shown that the factors  $k_3$  and  $k_2$  had to be new determined for every Mach number, which led to the conclusion that the factor  $k_3$  is not only influenced by the aspect ratio, but also by a slight change of the Oswald's efficiency factor with velocity at higher speeds. A trend has been obtained from the factors for the given Mach numbers, which was applied to estimate further drag polars for Mach numbers between 0.70 and 0.87. A similar method is used for the increase of the zero-lift drag coefficient at higher speeds.

For the drag polars of lower speeds the sufficiency of the parabolic approximation has been assumed, whilst for Mach numbers greater than 0.65, equation 5.1-2 is used.

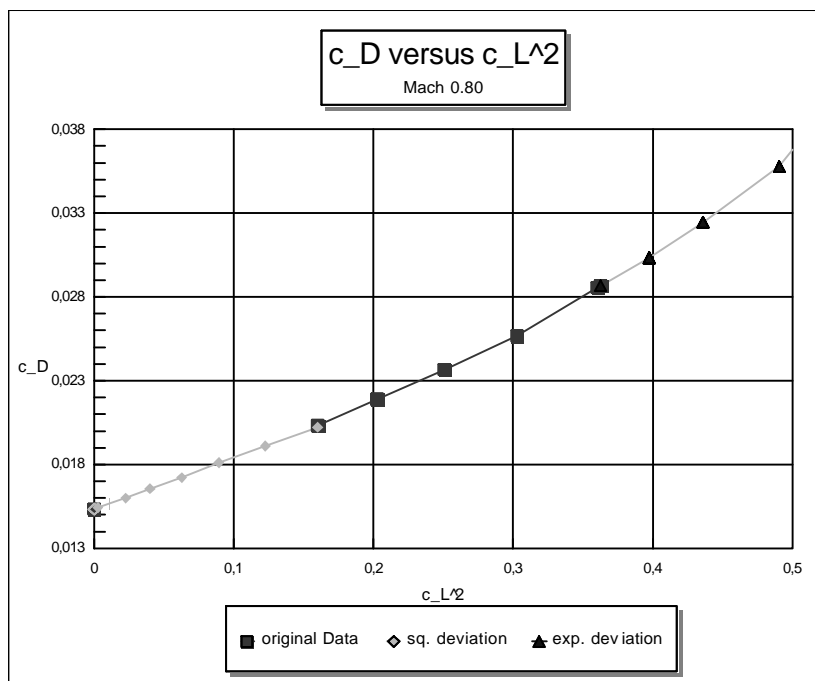


**Figure 5.5** Extrapolation of drag polar data

The factor  $k_2$  was assumed to be constant at higher velocities, since the trend from the given data had an opposite direction as it should according to theoretical knowledge and practical experiences. The necessary values to determine all drag coefficients are shown in the following table, where the factor  $k_3$  is represented as a product with the Oswald's efficiency factor:

**Table 5.4** The applied factors for the different Mach numbers

Mach number	c <sub>D</sub> zero	k <sub>3</sub> *e	k <sub>2</sub>	
			above the yellow box	below
0.30 - 0.65	0,01452	1,000	0,0000	
0,70	0,01452	1,000	0,0032	
0,71	0,01452	1,000	0,0057	
0,72	0,01452	1,000	0,0082	
0,73	0,01452	1,000	0,0107	
0,74	0,01452	1,000	0,0132	
0,75	0,01452	1,000	0,0157	
0,76	0,01452	1,000	0,0182	
0,77	0,01452	1,000	0,0207	
0,78	0,01452	0,989	0	0,0232
0,79	0,01549	1,180	0	0,0482
0,80	0,01536	1,120	0	0,0457
0,81	0,01531	1,060	0	0,0381
0,82	0,01538	1,015	0	0,0331
0,83	0,01560	0,980	0,0331	
0,84	0,01580	0,940	0,0331	
0,85	0,01600	0,900	0,0331	
0,86	0,01620	0,860	0,0331	
0,87	0,01640	0,820	0,0331	

The results are summarized in a table, which was entered in spreadsheet E of the program and is attached in appendix A. In this spreadsheet, the plots of this data versus the simple and the squared lift coefficient can also be found. The comparison with the appropriate data from Boeing has shown that a similar shape of the curves is achieved.

### 5.1.3 The maximum Climb and in-flight idle Thrust

Subsequently, the tables for the engine dependent maximum climb thrust and the in-flight idle thrust had to be modified. As the data provided are those of a typical cruise performance, no information for this was available. Therefore, the estimates are based on power plant data of an assumed A330 engine and the maximum climb thrust table in spreadsheet G of the program, based on the PEM from **Boeing**.

According to fundamental theoretical knowledge, the following correlation between thrust and height exists:

$$\frac{T}{T_{SL}} \propto S^n \quad (\text{Young, 1999}) \quad (5.1-3)$$

Since values of maximum take-off thrust are published for most engines and the density ratio is determinable, two unknown terms remain, the actual thrust and n. By assuming similar characteristics of both the Boeing and the Airbus engine some  $T/\bar{\rho}$  data was available in Young's program. In order to use only the given data, all interpolated values were deleted from a previously made copy of the corresponding table into a new spreadsheet, named THRMACH4.wk4. The remaining data are shown in table 5.5.

**Table 5.5** Thrust over delta data of Boeing 757 class aircraft (PEM) (**Boeing**)

height ft	0	5000	10000	15000	20000	25000	31000	35000	36089	37000	39000	42000
<b>Mach 0,20</b>	25233	27687										
<b>Mach 0,30</b>	23071	25358	27717	30229	32358							
<b>Mach 0,40</b>	21243	23420	25816	28327	30685	32399						
<b>Mach 0,45</b>	20313	22609	25001	27530								
<b>Mach 0,50</b>	19671	21877	24258	26768	29290	31285	33434	34421	34529	34426	34203	33778
<b>Mach 0,55</b>			23558	26105	28694	30824						
<b>Mach 0,60</b>	18477	20604	22948	25481	28161	30473	33182	34425	34564	34456	34222	33743
<b>Mach 0,65</b>					27675	30114	33131					
<b>Mach 0,70</b>		19577	21811	24404	27170	29814	33153	34833	35021	34909	34664	34295
<b>Mach 0,75</b>						29383	33267	35258	35455	35339	35085	34702
<b>Mach 0,80</b>				23459	26228	28947	33318	35590	35933	35812	35549	35152
<b>Mach 0,85</b>							33227	35888	36240	36110	35828	35400
<b>Mach 0,90</b>					25537	28343	33036	36339	36743	36602	36296	35819

A second table was set up, wherein the values appear multiplied by their according height dependent density ratios. Afterwards, the CAS for every thrust term was calculated. Since the climb schedule was fixed as 250/300/0.8, interpolations were carried out to obtain the appropriate thrust data for every height. Furthermore, the standing position thrust at sea level was determined in the same manner. After rearranging the table for software internal reasons of the Lotus 1-2-3 package, the thrust for several heights could be plotted versus CAS, as is shown in figure 5.6.

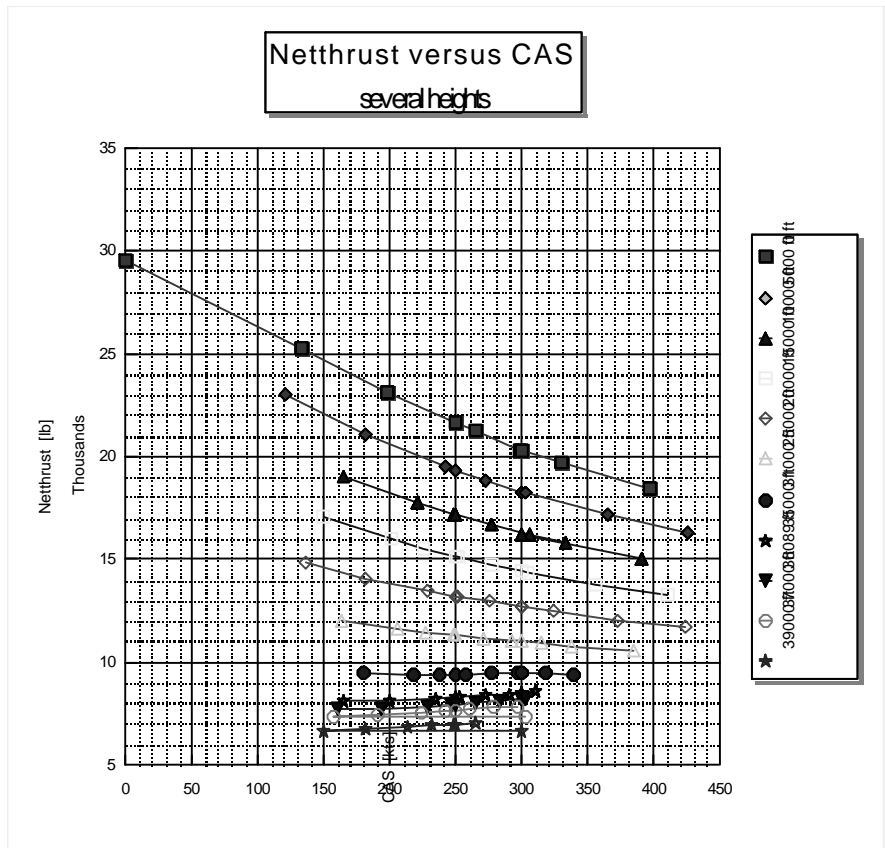


**Figure 5.6** Net thrust for several heights

In order to obtain finally the exponent  $n$ , the data of the needed velocities have been taken out into a new table for each of both. The ratio of every value to the sea level thrust was determined, which enabled the computation of an exponent  $n$  in each case by using logarithmic functions. According to theory, the result should have resulted in the same amount for all exponents, which was not the case. However, a steady increase with height could be noticed. Eventually, the average of all exponents up to the tropopause was used for further calculations.

The values for a velocity of 300 kts are given in table 5.6. In there the thrust was later calculated by using the average exponent and checked against the given thrust. A relative error of less than 2% for the heights of interest was found to be acceptable.

**Table 5.6** Calculation table of the exponent n

TABLE 2 for CAS = 300 kts						
Height	Sigma	Thrust (given) [lb]	T/T_sl	n	Thrust (calc) [lb]	rel. error
0	1,0000	20268	1,000			
5000	0,8617	18266	0,901	0,698	18160	0,58%
10000	0,7385	16238	0,801	0,731	16206	0,20%
15000	0,6292	14430	0,712	0,733	14402	0,20%
20000	0,5328	12712	0,627	0,741	12739	-0,21%
25000	0,4481	11010	0,543	0,760	11212	-1,83%
31000	0,3605	9449	0,466	0,748	9550	-1,07%
35000	0,3099	8494	0,419	0,742	8541	-0,55%
36089	0,2971	8191	0,404	0,746	8279	-1,08%
37000	0,2844	7845	0,387	0,755	8016	-2,18%
Average						
t. Trop	all heights					
0,7376	0,6272					

Subsequently, it was assumed that the considered aeroplane was equipped with a CF6-80 E1 A4 engine, which represents a typical powerplant of an Airbus A330-200. The maximum take-off thrust of this engine amounts to 66900 lb (**Janes, 1992**). It was assumed that about 93% of this power is used in performing a climb, which led to a standing position thrust of 62217 lb. From this, by using the ratios of the Boeing data to their standing position thrust the sea level thrust for both 250 kts and 300 kts could be obtained and, therefore, by taking the appropriate exponent the thrust values for the other altitudes.

By dividing these thrust data by the corresponding values of Boeing for the same altitude and the same CAS a number in each case was obtained, which makes a statement about the relation between both engines. The average of these numbers amounted to 2.11 for 250 kts and 2.13 for 300 kts. Therefore, a factor of 2.12 has been used finally to modify the maximum climb thrust table in the program.

Since this obtained factor is engine specific, it was also used for the idle in-flight thrust table of spreadsheet G and the table for brake release and climb to 1500 ft of spreadsheet H. The table for the idle fuel flow got the same modification. These modified tables can be found in appendix A.



## 5.2 Data of the Operating Manual A330

Further data was provided in the form of an *Operating Manual* for an Airbus A330. The manufacturer supplies these handbooks in order to enable the customers to carry out quick calculations for checkups and safety reasons.

They include in performance obtained data of integrated range and integrated time dependent on the instantaneous gross weight of the aircraft while performing several cruise missions at different heights. The difference between two gross weights represents the fuel consumption, while the difference between the corresponding distances and times, respectively, represents the cruise distance covered and the cruise time for this fuel consumption. In addition, diverse tables can be found containing correction terms to take into account climb, descent, non-standard atmospheric conditions and the influence of wind and eventual airport elevations, respectively. Most of these terms depend on the weight at any given moment. Further necessary corrections like hold, taxi and step climb are assumed to be constant at amounts based on experiences.

The manual is to be used in the following way. Firstly, the flight mission must be defined. This includes the BRW, the range, the airport location and the actual en-route atmospheric conditions. The range has to be adjusted for either head or tail wind by the corresponding correction value.

Knowing the BRW and the corrected range, the time needed can be determined from the cruise tables. Eventual step climbs can be considered in two different ways. The change of height can be performed either after a certain distance or at a specified gross weight. In both cases, the table of the first height is used to determine unknown value using the known one, since both are dependent on each other. With this obtained value the “look up” has to be continued in the tables concerning the end height of the step climb. In order to keep the overall view the middle and end results can be entered in a tabulation (See figure C.3), provided in the Operating Manual.

Eventually, this turns out in the end weight overhead destination, whilst the BRW is set to weight overhead departure. Since these results are not very useful, corrections have to be made by adding or subtracting several values concerning climb and descent, as well as the actual difference of air temperature from ISA conditions. These values consider, for instance, that in performing a climb more fuel is burned than in cruise performance, on which the cruise tables used before are based.

These corrections give finally the landing weight at destination, which supplies the answer for the trip fuel by subtracting it from the BRW. Now the contingency fuel can be determined, as it equals 5% of the trip fuel.

Afterwards the alternate fuel can be found in the alternate table, which is based on a referring landing weight at alternate and has to be corrected for the obtained landing weight at this place by a further factor from this table. The fuel needed for the hold amounts to a constant.

Now, the *Zero Fuel Weight (ZFW)* can be calculated by subtracting the fuel required for alternate and hold, as well as the contingency fuel from the landing weight at destination. Its difference to the given OEW represents the maximum allowable payload, and its difference to the BRW is equal to the required fuel. Adding the fuel necessary for taxi gives the block fuel, here the amount of fuel, which has to be taken on-board.

Eventually, the time needed to fly the required distance, which was a further result after using the cruise tables, is adjusted for climb and descent corrections, and thus the flight time is obtained.

All the calculations described above can be inscribed into a second table (See figure C.5), also provided in the Operating Manual. Here, every row containing a result is numbered. Under the appropriate number the single steps are more thoroughly described.

### **5.2.1 Example of Operating Manual for Long Range Speed**

To be able to use the tables properly some examples are given in the **Operating Manual**. One of them together with all the necessary pages can be found in the appendix C. It is based on LR-speed at specific heights, which means that the speed is decreasing continuously with the decrease in weight, caused by burning fuel. This is unlike the function of the program, which generally computes its results based on fixed Mach numbers during the cruise, at least within one interval. Therefore differences between both results were predictable.

Based on the input parameters given in the example and the obtained payload, the modified program version was run using the FUEL button. This should lead to a tankered fuel close to zero, however, an amount of 1702 lb was not used, where 200lb of that are attributed to the different assumptions for start up and taxi. Of course, this phenomenon was explored, which led to the fact that the trip fuel succumbed to a slight error of less than 1% only. Admittedly, the constant values differed considerably. This could be due to two reasons. On the one hand the constants are certainly effected by a safety factor in order to avoid too tight fuel planning of the airlines. On the other hand the determination of the data table for the software was characterized by several difficulties, and therefore especially the values at lower altitudes have no pretension on correctness.

The results of the program are attached to appendix C in the form of an output spreadsheet, including the main answers from the example of the Operating Manual in an extra column.

Please note, that there is obviously a little discrepancy in the example, given in appendix C, concerning the landing weight at destination used for the correction of the alternate fuel. An amount of 330100 lb is used, however, a value of 229900 was calculated before.

Subsequently, a check against the cruise tables was carried out as the major interest concerned the cruise performance for a later exploration of HLFC impact. Determining the range for every BRW listed in table 5.7 and calculating the difference to the range possible with the highest BRW used did this. All other parameters remained as in the given example described above. Thus, the integrated range of the program was obtained, which was comparable to this of the Operating Manual.

**Table 5.7** Integrated range of the program and of the **Operating Manual**

<b>Weight [lb]</b>	<b>program DIST [nm]</b>	<b>Operating Manual DIST [nm]</b>	<b>abs. Error [nm]</b>	<b>rel. Error [%]</b>
<b>498000</b>	0,00	0,00	0,00	0,00
<b>496000</b>	66,22	60,00	6,22	-10,37
<b>494000</b>	132,77	126,00	6,77	-5,38
<b>492000</b>	199,66	193,00	6,66	-3,45
<b>490000</b>	266,88	260,00	6,88	-2,65
<b>488000</b>	334,44	328,00	6,44	-1,96
<b>486000</b>	402,34	396,00	6,34	-1,60
<b>484000</b>	470,60	464,00	6,60	-1,42
<b>482000</b>	539,20	532,00	7,20	-1,35
<b>480000</b>	608,15	601,00	7,15	-1,19
<b>478000</b>	677,39	670,00	7,39	-1,10
<b>476000</b>	746,89	739,00	7,89	-1,07
<b>474000</b>	816,67	809,00	7,67	-0,95
<b>472000</b>	886,70	879,00	7,70	-0,88
<b>470000</b>	957,01	949,00	8,01	-0,84
<b>468000</b>	1027,58	1020,00	7,58	-0,74
<b>466000</b>	1098,43	1090,00	8,43	-0,77
<b>464000</b>	1169,56	1161,00	8,56	-0,74
<b>462000</b>	1240,97	1233,00	7,97	-0,65
<b>460000</b>	1312,65	1304,00	8,65	-0,66
<b>458000</b>	1384,62	1376,00	8,62	-0,63
<b>456000</b>	1456,87	1448,00	8,87	-0,61

Table 5.7 makes clear that, although the absolute error is rising, the relative error drops by increasing the distance. Since the attention of this work concerns to a long-range aircraft, this result predicts an achievable error of less than 0,6 % for the cruise performance of this A330 class aircraft.

### 5.2.2 Example for a fixed Mach number

To achieve the greatest similarity to the conditions of the program a further example has been established, based on a fixed Mach number of 0.80 performed at an optimal flight level.

Although, it was not necessary to make up the flight planning in two steps, it is carried out in this way to clarify the step climb to another flight level, which is apparent on account of the change of TAS at a weight of 454500 lb. Corrections for headwind and non standard atmospheric conditions are not done to keep the example as simple as possible. This should avoid needless errors occurring. Therefore, the input values may be defined as is shown in the following table.

**Table 5.8** Input parameters of the fixed Mach number example

<b>Mach number</b>	0.80 opt. FL
<b>Initial Flight level:</b>	FL350
<b>Ground Distance:</b>	5000nm
<b>Wind ('-' head/'+' tail)</b>	0 kt
<b>Air distance</b>	5000 nm
<b>BRW</b>	480,000 lb
<b>OEW</b>	259,600 lb
<b>ZFW</b>	330,100 lb
<b>Payload</b>	50,500 lb
<b>Alternate</b>	250 nm
<b>Hold</b>	30 min
<b>Contingency</b>	5%
<b>Atmospheric conditions</b>	Standard ISA
<b>Airport elevation</b>	0 ft
<b>Step climb</b>	One: at 454,500 lb

This example is worked out in detail and attached in appendix D together with other necessary pages from the Operating Manual. Required pages already used in the original example described in the previous chapter can be found in appendix C.

After determining the results, these were checked against computed answers from the program using the same input parameters. The comparison is listed in table D.3 and attached to appendix D. It can be seen that the tankered fuel could be reduced to an amount of about 500 lb, which corresponds to 300 lb less fuel used by considering the different assumptions for start up and taxi. The error concerning the trip fuel amounts to 0,3% only. This is very acceptable and leads to the decision to base further studies on the input parameters of this example.

### 5.3 Comparison to an Airbus Briefing

Another available published information was an Airbus Briefing of A330 aircraft (Airbus, 2000), designed for advertising reasons. Here, a payload range diagram could be found, which provides a general view about the possible aircrafts features. The heavier A330-200 version is chosen, since previous comparisons are based on this model.

The original diagram is shown in figure 5.7. It got an unfamiliar shape, which indicates that even at zero payload, more fuel can be taken on-board than the aircraft is able to carry. This offers the opportunity to make further improvements without changing the whole structure of this version, if the OEW can be reduced by newly developed techniques and materials.

#### **A330-200 payload range**

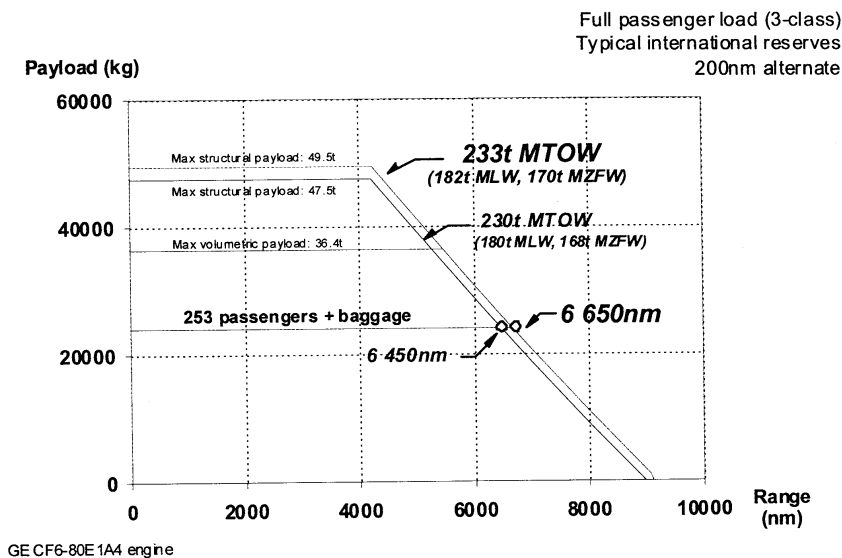


**Figure 5.7** Payload range diagram of A330-200 (Airbus, 2000)

All necessary points to enable the plot of such diagrams have been determined from figure 5.7. Afterwards, the ranges for the appropriate weights were calculated in the software using the RANGE button in each case. The results came close to the reference of the Airbus Briefing and are shown in the following table.

**Table 5.9** Comparison of payload range data

Payload	Weight [t]	Range [nm] (calc)	Range [nm] (Briefing)	rel. Error [nm]	abs. Error [%]
Max. structural	49500	3988	4231	-5,70	-243
Max. volumetric	36400	5210	5421	-3,89	-211
253 passengers + baggage	24035	6464	6650	-2,80	-186
non	0	9115	9105	0,11	10

## 6. The Sensitivity Study

Once the program has been modified and its accuracy was ensured, it could be used to carry out studies. On account of the high flexibility of the software, a bright spectrum is provided to do this. Of high concern is, if general statements about consequences of a virtually installed HLFC system could be derived. Therefore it was necessary to explore the particular influences at first and to prove afterwards, if the impacts of all modifications together would lead to similar results. The main focus of attention was the change of block fuel on this occasion, since this is what the customer has to pay for. For all these reasons the following studies were chosen.

### 6.1 Study 1 - Impact on Block fuel

The study is based on the example for the fixed Mach number according to the Operating Manual. Thus, the input parameters are already known and listed in table 5.8. It should now be examined, in what way the block fuel will change by using the WEIGHT button due to a single modification of either drag, OEW or fuel consumption, respectively, independent of each other in each case.

Therefore, a possible change of each of these parameters was guessed. In order to see whether their particular influence on block fuel is linear, the assumed values were subdivided and assigned to 5 cases, as is shown in table 6.1.

**Table 6.1** Cases of study 1

<b>Study 1</b>			
<b>case</b>	<b>OEW (increase)</b>	<b>Q (increase)</b>	<b>c<sub>D</sub> (reduction)</b>
<b>1</b>	1 %	1 %	-3 %
<b>2</b>	2 %	2 %	-6 %
<b>3</b>	3 %	3 %	-9 %
<b>4</b>	4 %	4 %	-12 %
<b>5</b>	5 %	5 %	-15 %

By changing one parameter whilst the others are left at zero the desired results could be obtained (See table 6.2). Subsequently, the changes of each case are applied together and the results are compared to the sum of the particular answers.

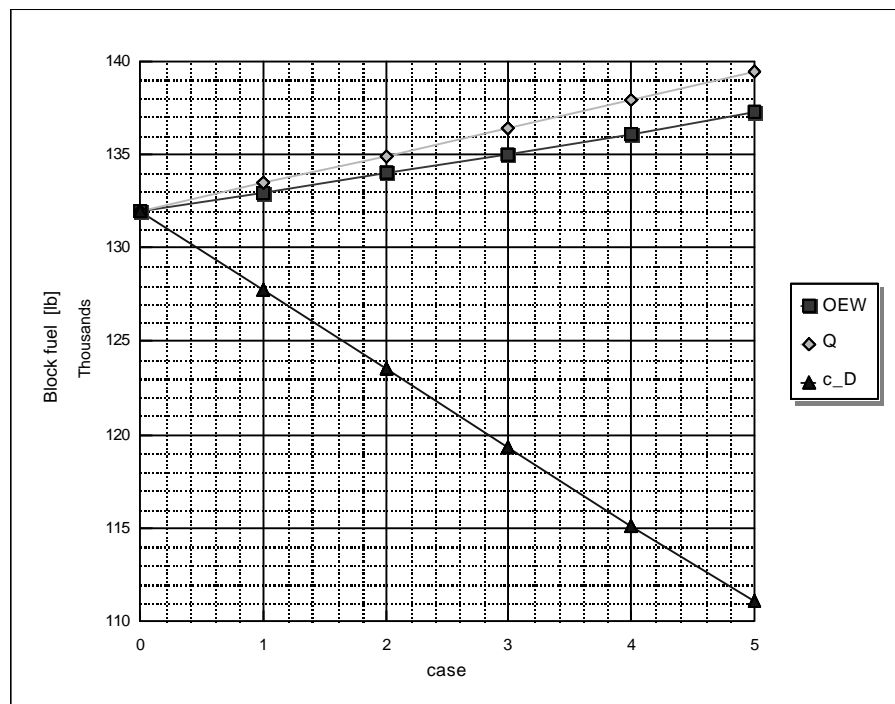
It should be noted that the baseline was obtained by running the weight button without any modifications. This led to a slightly lower BRW for reasons, which are discussed in chapter 5.1.

## 6.2 Results of study 1

The method described above gave the following results for the particular impacts on the block fuel, which are shown in the following table and illustrated in figure 6.1:

**Table 6.2** Results for block fuel (study 1)

Block fuel for the particular impacts [lb]						
case	Baseline (=0)	1	2	3	5	4
OEW	132007	132961	133977	134964	136043	137268
Q	132007	133456	134915	136379	137902	139372
$c_D$	132007	127712	123525	119332	115139	111065



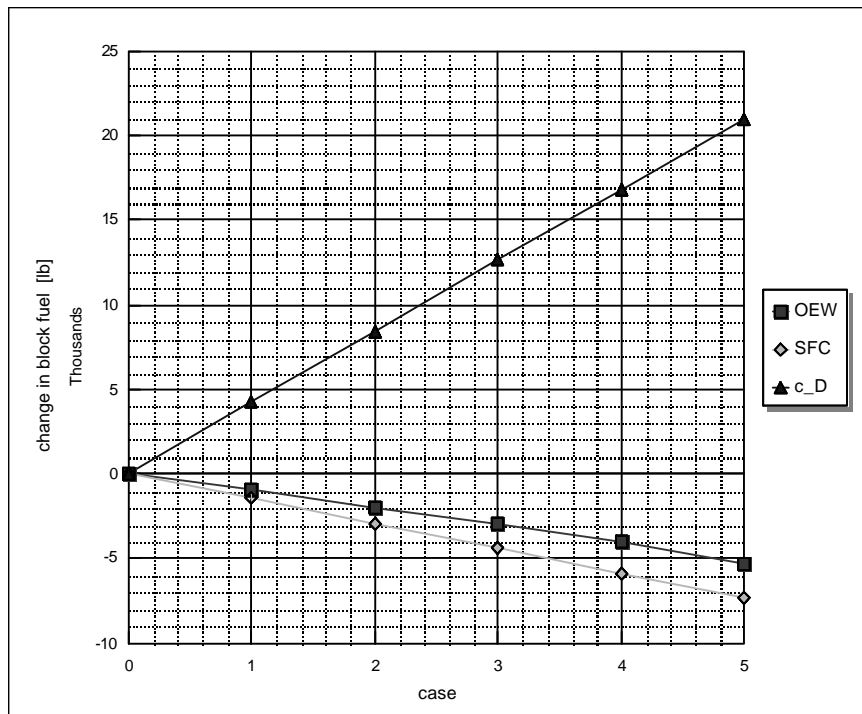
**Figure 6.1** Block fuel affected by the particular impacts (study 1)

Figure 6.1 shows an expected result. While the higher OEW and the higher fuel consumption cause an increase of block fuel, the reduced drag lowers the amount of fuel needed. It is apparent that the influence of fuel consumption is higher than that of OEW. In addition this diagram shows, that the impact of drag is similar to that of the fuel consumption for the same percentage (i.e. 3%). Fortunately, in practice, a higher percent of drag reduction can be achieved with a smaller percentage of the other impacts.

In order to achieve more predicative results, the change in block fuel was subsequently determined by subtracting the baseline block fuel from every value of the above table, as the thus obtained amounts are lower and the change of block fuel could be read directly from plotted results. (See figure 6.2)

**Table 6.3** Change in block fuel (study 1)

Change in Block fuel for the particular impacts [lb]						
case	Baseline (=0)	1	2	3	5	4
OEW	0	954	1970	2957	4036	5261
Q	0	1449	2908	4372	5895	7365
$c_D$	0	-4295	-8482	-12675	-16868	-20942
sum	0	-1892	-3605	-5348	-6939	-8317



**Figure 6.2** Block fuel savings due to the particular impacts (study 1)

Figure 6.2 shows that the impacts of a raised OEW and SFC are not linear, but increase with a higher percentage. The curve for the drag reduction is nearly a straight line within these limits.

It is to notice, that the signs of the appropriate values, which represent the change in block fuel are reversed for this diagram (See table 6.3). This is done in order to illustrate the block fuel savings, which are rather of interest, especially for the customers.



Then, a test row of all modifications simultaneously was obtained for each case. The results were subtracted again by the baseline to determine the block fuel savings by subsequent reversion of the signs. These were compared to the formerly obtained entire fuel reduction caused by all particular impacts. The resulting values are shown in table 6.4 and the comparison is illustrated in figure 6.3.

**Table 6.4** Block fuel savings (study 1)

Block fuel and Block fuel savings [lb]					
case	1	2	3	5	4
Complete installation - Block fuel	130054	128027	125875	123587	121251
Block fuel savings for compl. install.	1953	3981	6132	8421	10757
Block fuel for the sum of part. imp.	130115	128402	126660	125069	123690
Sum of savings for particular impacts	1892	3605	5348	6939	8317
Error for block fuel	3,25%	10,41%	14,67%	21,36%	29,33%

It can be seen that the full practical application leads to more optimistic results than the summed up savings of the particular impacts. The error between both answers, which is increasing quickly, is calculated in table 6.4. Only in the cases 1 and 2 the difference remains within acceptable limits. Figure 6.3 shows that both influences are not linear and each curve follows an opposite trend. While the slope concerning the particular impacts drops, the rise of block fuel savings regarded to the complete installation increases with higher percentage.

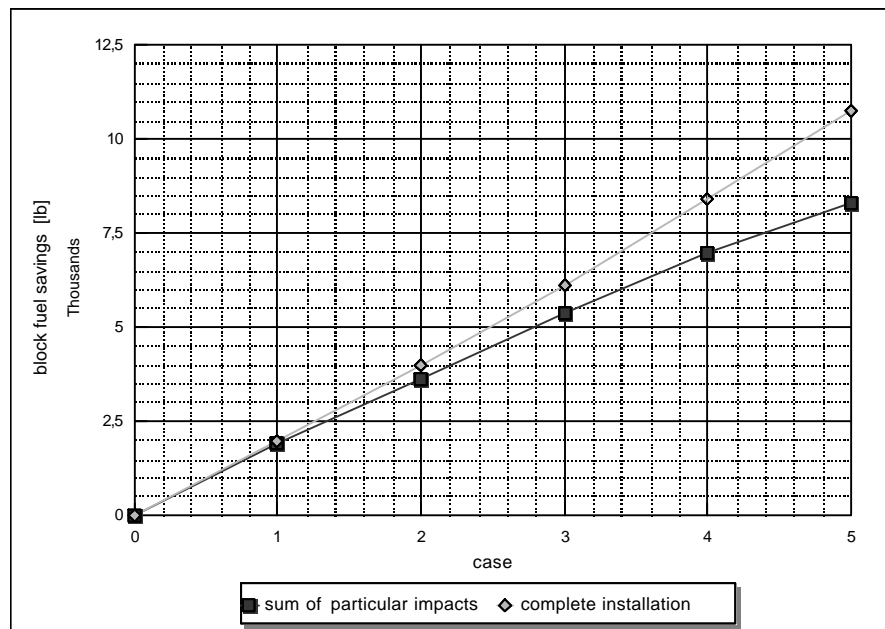


**Figure 6.3** Comparison of block fuel savings (study 1)

The results of this study would not enable conclusive predictions. A further information had to be integrated into the explorations, data about how much drag reduction can be achieved at the expense of how much more weight and higher fuel consumption. Therefore, another survey, based on values of previous explorations, was carried out

### 6.3 Study 2 - Modification based on practical Information

In 1993, explorations have been made by Boeing concerning the application of HLFC system on a Boeing 757-200 (Joslin, 1998). Based on this research and some newer knowledge, Young and Fielding used a reduced drag by 0.00425 compared to the turbulent baseline aircraft, an increased OEW by 1032 kg and an increased SFC by 1,86 %, as they had selected an aircraft of this particular class for their own survey (Young/Fielding, 2001). The conclusion of these values induced a change in the single cases of study 1 in the following way:

**Table 6.5** Cases of study 2

Study 2			
case	OEW (increase)	Q (increase)	$c_D$ (reduction)
1	1 %	1 %	-5 %
2	2 %	2 %	-10 %
3	3 %	3 %	-15 %
4	4 %	4 %	-20 %
5	5 %	5 %	-25 %

These cases were examined using the same method as in study 1, which produced the results shown in the following chapter.

### 6.4 Results of Study 2

To begin with, the results for the particular influences on the block fuel are shown again in table 6.6.

**Table 6.6** Results for block fuel (study 2)

Study 2 - Block fuel for the particular impacts [lb]						
case	Baseline (=0)	1	2	3	5	4
OEW	132007	132961	133977	134964	136043	137268
Q	132007	133456	134915	136379	137902	139372
$c_D$	132007	124918	117898	111058	102270	92251

This led to block fuel savings as is illustrated in figure 6.4. The results for this were obtained by subtracting the baseline OEW from each value of table 6.6 and, subsequently, reversing the sign in each case.

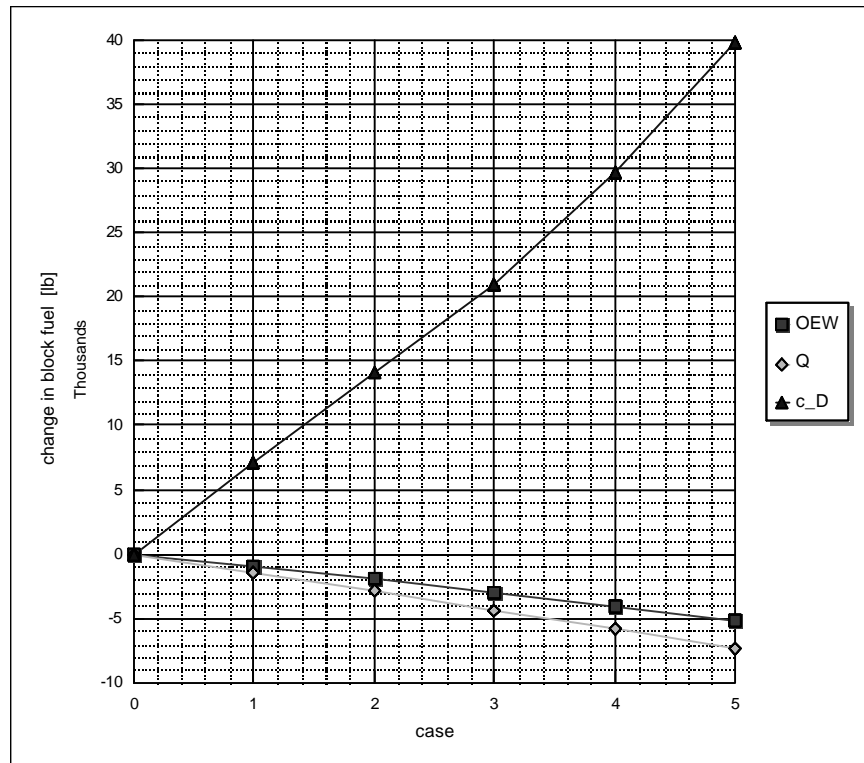


**Figure 6.4** Block fuel savings due to the particular impacts (study 2)

As expected, the results of table 6.6 and figure 6.4 show that the influence of the drag is raised in comparison to the answers of study 1. This is due to the fact, that in study 2, a higher drag reduction was used while the other impacts remained equivalent. It can also be seen that a sudden rise of this impact occurs in case 4.

As a possible drag reduction of more than 15 % is not expected, the results were simply proved by another run, which led to the same answers (Young, 2001c). Therefore, no further analysis concerning this took place.

Now, the results of all modifications simultaneously for each case were obtained in order to simulate a complete installation of the HLFC. Again, the baseline OEW was subtracted from all values. This enabled the determination of the appropriate block fuel savings by reversion of the signs, which are shown in table 6.7. Eventually, the savings in block fuel were compared to those, which resulted from summing up the particular influences. (See figure 6.5)

In addition, the error between both appropriate values of block fuel savings is calculated in each case. This is also shown in the table below.

**Table 6.7** Block fuel savings (study 2)

<b>Block fuel and Block fuel savings [lb]</b>					
<b>case</b>	<b>1</b>	<b>2</b>	<b>3</b>	<b>5</b>	<b>4</b>
<b>Complete installation - Block fuel</b>	127198	122164	117001	111719	101019
<b>Block fuel savings for compl. inst.</b>	4809	9843	15006	20288	30988
<b>Block fuel for the sum of part. imp.</b>	127321	122776	118387	112201	104877
<b>Sum of savings for particular impacts</b>	4686	9231	13620	19806	27130
<b>Error for block fuel savings</b>	2,63%	6,63%	10,17%	2,43%	14,22%

This time, the comparison of the block fuel savings due to either the full installation or the sum of the particular impacts only resulted in slight differences between both, up to case 4. Below that point, the biggest error amounts to 10.17% as can be seen in table 6.7. This is very acceptable as for making predictions no exact results are necessary, but merely approximate trends expressed in percentage form.

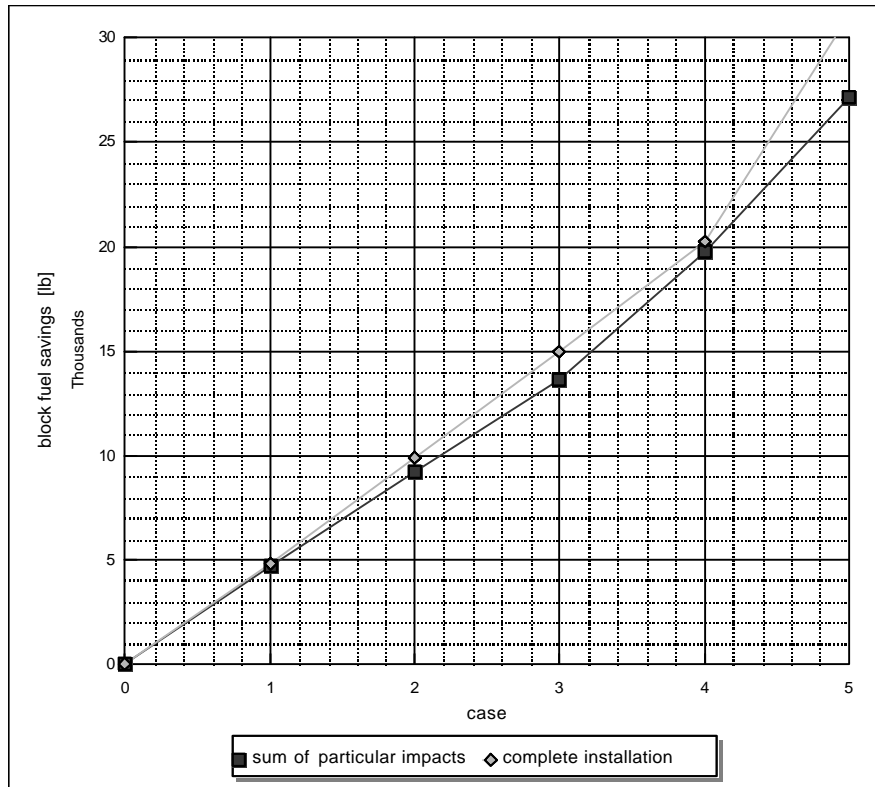


**Figure 6.5** Comparison of block fuel savings (study 2)

Furthermore in case 4 the two curves can be replaced by a straight line from the origin to a point of approximately 19000 lb block fuel savings. That could mean that all cases, which were not independent of each other until now, as the different results of both studies showed, could be uncoupled again within these limits. The following example aims to prove this.

## 6.5 Study 3 - General Statement

This final study is done to prove the assumption made in the previous chapter. The similarity of the in both ways obtained results in study 2 offers the opportunity to cross-read values for assumed percentages of the particular impacts from figure 6.4 as is shown in figure 6.6.

It may be estimated that a new technique will cause an increase in OEW of about 4%, but will only need 2 % more fuel in order to achieve 15 % less drag. A run of the program gives a necessary block fuel of 117547 lb, which equals to 14460 lb less fuel needed compared to the baseline. The sum of to the here defined percentages corresponding values from study 2 results in 119227 lb, which is equivalent to 12780 lb (See figure 6.6). This arises in an error of 11.6%, which is just acceptable for such a prediction, since exacter software results are always some more optimistic.

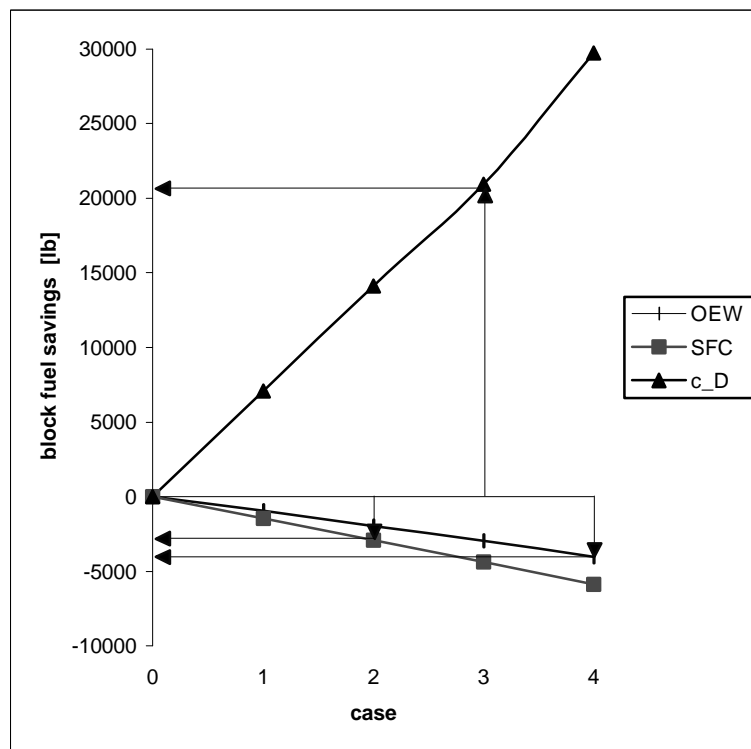


**Figure 6.6** Cross-reading of block fuel savings

In practice the changes will probably not be that high and mostly only slight modifications of one parameter will occur. Therefore, the error will amount to less than 10 %, which is sufficient enough in order to establish predictions and trends, respectively. Considering the saving results of entire block fuel, leads even to smaller differences.

Thus, this diagram provides a simple tool to make approximate estimates of what way the change of the components of HLFC systems will influence the block fuel.

## 7. Discussion

HLFC systems offer the potential of significant fuel savings due to drag reduction. Respectable sources estimate a possible amount of up to 20 % (**DLR, 2001b**), which would also considerably reduce aircraft emissions.

Since it is an active device, this occurs, unfortunately, at the expense of a higher OEW and an increased SFC. This is due to the necessity of suction pumps and required tube-system to drive them, which have a certain weight and consume some fuel while working.

A further disadvantage is that the reliability will not achieve that of conventional aircraft systems due to the high sensibility to environmental impacts. This is caused by the structure, consisting of by billions of small holes perforated parts, and the function, presupposing a very smooth surface, of such systems. However, incidents which could cause a failure are indicated and research is undertaken to improve this technique. Anyhow, it might be necessary to increase the on the International Reserves flight profile based contingency fuel in order to accommodate eventual system failures with an acceptable low rate of en-route deviations, as these failures mostly result in the complete loss of laminar flow for the entire remainder mission. An amount of 10% (**Young/Fielding, 2000**) is a today's estimate to realize this without any risks.

Additionally, potential customers will consider the higher maintenance costs the price they have to pay for purchase and installation, since they are dependent on their own efficiency. The possible block fuel savings must counterbalance all these points above in order to make HLFC systems attractive to the airlines.

Most of the failure modes can be avoided by using the system only at higher altitudes. This would concern the end term of climb, the cruise and the initial descent, which makes clear that the advantages rise with longer range. Therefore, an installation on short-range aircraft might be inefficient.

Studies, considering the disadvantages, have shown that already today more than 8% fuel saving can be achieved, even by taking into account a failure mode of 25% during cruise time due to the encountering cirrus clouds containing ice crystals, and orientating the fuel planning corresponding to this. (**Young/Fielding, 2001**)

The technique will be further improved over the next few years, since intensive research is being undertaken in this area. The increasing fuel prices due to the shortage of the worldwide oil reserves will support this attempts and therefore HLFC systems will very probably be encountered on prospective aircraft.

Since flight tests are very expensive, the attempt is undertaken to base current research on computer models. For example, software has been established in the form of Lotus 1-2-3 spreadsheets to simulate the whole flight mission of a generic twin engine jet transport aircraft of a Boeing 757 class by **Young** based on data provided by **Boeing** in the PEM. It computes the fuel and time required for a specific mission. Alternatively, the mission range can be calculated for a specified fuel weight.

**Straubinger** made up a similar program, based on the same data set, without any knowledge of structure and function of Young's software. A comparison of the computed results showed that both programs came up to very close results of less than 1% difference in calculating the BRW for several ranges. The reliability of Young's software is also given by checks against information of published sources, which also led to acceptable results (**Young/Fielding, 2001**).

The usefulness of Young's program is grounded in the possibility to study the impact of a virtually installed HLFC system. The necessary modifications such as higher OEW, increased SFC and reduced drag can be entered quickly into the conducting master sheet. Since this parameters can be keyed in independent of each other, this software can also be used for other drag reducing techniques like, for instance, the shark skin layer, if the necessary information is available.

On account of its high flexibility, studies considering partial failure modes are possible, since the HLFC input is subdivided into several intervals. Using this function, a study was made by Young and Fielding to explore the influence of en-route cloud encounters, which led to the result described above.

One of the tasks was to examine whether the software could be modified by replacing the data set by that of an aircraft representing a long-range class. For this, flight test data of a typical twin-engine aircraft in this class was provided by the University of Limerick. The available information consisted of Integrated Range and Thrust data, and information about the lift and drag coefficients. All values were given for Mach numbers from 0.78 to 0.82 and heights from 29000 ft to 41000 ft dependent on the instantaneous gross weight of the aircraft.

Since this is typical cruise performance information, it did not supply the whole picture of the aerodynamic and operating properties of the aircraft, but provided the required clue. Based on this and on comparison to the Boeing data, new data tables for the software were attempted by applying numerical techniques, basic aeronautical knowledge and additional information out of published sources. On this occasion, the decision was made to found necessary assumptions on an Airbus A330-200, since some published references for this version were available, to which later computed results could be compared with.

The obtainment of the non-existing data caused some difficulties as many guesses had to be made. Also, some of the applied methods did not work how they promised. Therefore, especially the values concerning lower altitudes and thus the climb and descent performance have no pretension of accuracy. It is necessary to prove this data before using the modified software, if these portions play an important role for eventual other studies. For the work, this report is dealing with, this was not the case, as HLFC is mainly applied in cruise performance and the long ranges considered here would not allow for a large error compared to the entire mission.

After replacing the tables and ensuring that these were fully compatible to the software, the validation of computed results had to be proved. They could be compared to published information in the form of a provided Operating Manual for an Airbus A330, including a self-explanatory example. This manual represents the common tool enabling flight crews to carry out their fuel planning quickly for any given flight mission and is described in detail in chapter 5.1.

A simulation of the example using the modified software came to the astonishing close result of only 1.2% less burned fuel. It could be indicated that this error was assembled by 0.9% less trip fuel needed and an error, which arose due to large differences to constants of the example, considering the partial results for the climb, the descent, the alternate and the hold.

Since the performed cruise of the example did not fully accord to the software, which generally works without changing the Mach number during the cruise, another example was established based on a fixed Mach number of 0.8, and according to the Operating Manual. This was done in order to achieve a lower error concerning the trip fuel. A subsequent simulation in the program resulted in a lower fuel consumption of about 300 lb as 200 lb of the displayed 499 lb tankered fuel attributed to the different assumptions of fuel required for start up and taxi. Obviously, the computed climb, descent, alternate and hold values came closer to the constants used by the Operating Manual at higher BRW. The difference between the trip fuel determined in both ways amounted to 0.3% only, which led to the decision to use the input parameters of this example for further studies as the computed results came closest to values of practice.

A further comparison was done using the payload range diagram of an Airbus A330-200 (**Airbus, 2000**), which could be found in an advertising Airbus Briefing. Also here, a satisfactory level of consistency could be attained.

Since sufficient accuracy could be ascertained, the modified software was used to perform sensitivity studies to investigate possible impacts of HLFC on the fuel usage for the previously specified mission. This was done by entering possible changes for each single impact, which is either a raised OEW, an increased SFC or a reduction of drag.



As the major interest of airlines customers concerns the block fuel, that one's changes due to the particular influences were examined using several amounts in each case. As expected, the rise of OEW and fuel consumption led to a higher amount of block fuel required, while the lower drag counterbalanced these adverse impacts, taking into account that in practice a significant higher percent drag reduction can be achieved with a smaller percentage of the other impacts. In order to obtain more predicative statements, the appropriate block fuel savings were determined as their values are represented by a lower amount.

Additionally, it should be proved whether general statements could be derived. For that reason the sum of the previously described results representing the particular impacts was compared to results obtained by simulating the full installation, which means a run of the program influenced by all impacts simultaneously. Since this did not lead to the desired answer, a second study was performed, where it was not simply guessed, which amounts of the single impact belong to each other.

This time they were based on a Boeing study concerning an HLFC application on a Boeing 757 (**Joslin, 1998**), which had been already used by **Young** and **Fielding**. Comparing the full installation to the addition of the appropriate results due to the particular impacts resulted in an illustration, which made apparent, that the two developed curves for block fuel savings (See figure 6.5) could be replaced by an average straight line up to 20% drag reduction.

A third study was carried out, in which independent changes of the single percentage influences were allowed again. The from results of block fuel savings obtained from study 2 are used to make predictions by cross-reading the appropriate values from figure 6.4 and summing them up (See figure 6.6). Subsequently, this is crosschecked against the result due to the same modifications simultaneously using the software, which led to acceptable errors of about 12%.

Thus, figure 6.4 provides a simple tool to en-couple the parameters again and to make approximate predictions concerning the influence on the fuel savings effected by possible changes of an impacts percentage amount quickly and without using the software. This could be useful, for instance, if a new technique could offer lower fuel consumption of the suction pumps or the decision has to be made, which material should be used considering its weight.

Further studies are necessary to examine the influence of range and BRW to this, since all studies above are based on the same input parameters. It might be necessary to obtain several curves for several classes of aircraft and missions, in order to achieve actual general statements.

## 8. Conclusion

HLFC is a very promising technique to reduce the fuel consumption of medium and long-range class aircrafts progressively. The restriction to limit the application of HLFC to cruising altitudes makes its use for short ranges not recommended.

This work shows that computer models work sufficient accurate to enable predictions and trends about, how profitable new techniques will be. Even, relative reliable estimates about a possible expectable amount can be established, which, however, are approximations. Results gained in that way have to be substantiated by flight tests and subsequent application over a longer period, to make them certain. Although, these models do not provide a full substitute for practical flight tests, they reduce them, accelerate the research, and thus lower the costs considerably.

A computer performance model based on flight test data of a Boeing 757 class aircraft has been developed to study the sensitivity on fuel burn due to HLFC technology, but can also be used to explore the impacts of other drag reducing devices on account of its high flexibility. Computed answers of this model and of its version modified by replacing the data set by that of an Airbus A330 class aircraft, have been proved, which led acceptable results compared to published sources.

Using the modified program version and input parameters, which gave closest information of practice, the impact due to changes of Drag, SFC and Weight on the fuel burn was explored. While the single impacts due to a rised OEW, and increased SFC, respectively, led to a higher block fuel in each case, the drag reduction resulted in considerable block fuel savings. In the practical data based study 2, for example, 2957 lb more fuel was burned due to 3% increased OEW, and 4372 lb due to 3% higher SFC. The drag reduction of 15% led to a by 20949 lb lower block fuel. The sum of all these impacts amounted to a fuel saving of 13620 lb, which equals to 10.3%. The simulation of the full HLFC installation (all impacts simultaneously) using the same input parameters resulted in 15006 lb, and thus 11.4% less needed fuel.

For the reason, that the particular consideration of increased OEW and SFC in each case succumbs to the adverse effect of additional weight caused by the additionally fuel required due to their own impacts, the results for a complete HLFC installation will always be more optimistic compared to the sum of all particular influences.

Therefore, the obtained diagrams illustrating the single block fuel savings due to the particular impacts can be used to make predictions accepting a little error, since they promise nothing what cannot be kept, as long as the effect described above can be counterbalanced by the drag reduction at full HLFC installation.

## 8. References

- Airbus 2000** AIRBUS INDUSTRIE G.I.E: *A330-Briefing*. AI/CM 310.0015/98, printed in France, June 2000
- Airbus 2001** AIRBUS INDUSTRIES: *A330-200 Specifications*. URL: <http://www.airbus.com/>, 12-May-2001
- ATA** AIR TRANSPORT ASSOCIATION: “*Specification 100, Manufacturer’s Technical Data*”. from **Scholz 1999**, Anhang A
- Boeing** THE BOEING COMPANY: “Performance Engineers Manual 7G7”, Seattle: The Boeing Company, undated
- Boeing 1989** THE BOEING COMPANY: *Jet Transport Performance Methods*. Seattle: The Boeing Company, 1989 - (D6-1420)
- Boeing 1996** THE BOEING COMPANY: *Performance Engineer General Course Notes*. Volume No. 1 and 2. Seattle: The Boeing Company, 1996
- Bechert 2001** BECHERT, Dietrich: *Folie nach dem Prinzip der Haifischhaut*. URL: <http://www.uni-saarland.de/fak8/bi13wn/gtbb/umsetzung/fischhaut.html>, 08-May-2001
- DLR 2001a** ERNST, Andreas: *Aerodynamischer Entwurf, Laminarhaltung*. URL: [http://infoserv.kp.dlr.de:8000/EA/Abt\\_AE/laminar](http://infoserv.kp.dlr.de:8000/EA/Abt_AE/laminar)
- DLR 2001b** DLR: *Laminarflügel für Verkehrsflugzeuge - weniger Verbrauch durch verbesserte Aerodynamik*. URL: [http://www.kp.dlr.de/pressestelle/HI283\\_96.HTM](http://www.kp.dlr.de/pressestelle/HI283_96.HTM), 11-May-2001 - Nr. 28.3/96 – Ri
- DVA 2001** DVA: *Nurfluegler*. URL: [http://wissensnavigator.europop.net/wissenschaft/neue\\_technologien/artikel\\_11.html](http://wissensnavigator.europop.net/wissenschaft/neue_technologien/artikel_11.html), 11-May-2001
- G-O 2001** G-O: *Rillen gegen Reibung*, URL: <http://www.g-o.de/index03.htm>, 10-May-2001

- Janes 1992** LAMBERT, Mark: Janes all the world's aircraft 1992-93. JanesInformation Group Limited, Coulsdon, UK, printed by Butler & Tanner Ltd., Frome and London, 1992
- JAR** JAR-OPS 1: *Joint Airworthiness Requirements OPS*. European Joint Aviation Authorities
- Joslin 1998** JOSLIN, Ronald D. J., *Overview of Laminar Flow Control*. Hampton, Virginia : Langley Research Center, October 1998 - NASA/TP-1998-208705
- Jenkinson 2001** JENKINSON, L.; SIMPKIN, P; RHODES. D.: *Civil Jet Aircraft Design*. URL: <http://www.bh.com/companions/aerodata/appendices/data-a/table-1/default.htm>, 10-May-2001
- Lotus 1-2-3** LOTUS 1-2-3, Release 4.01 for Windows: *1-2-3 Release 4 Help*. Lotus Development Corporation, 1993
- Operating Manual** AIRBUS INDUSTRIES: *Flight Crew Operating Manual A330*. SEQ 147, undated
- Schmidt 1998** SCHMIDT, Artur P.: *Nurfluegler*. Heise Verlag, 17.11.1998  
URL: <http://www.ix.de/tp/deutsch/inhalt/co/2531/1.html>, 26-01-2000
- Scholz 1999** SCHOLZ, Dieter: *Skript zur Vorlesung Flugzeugentwurf*. Hamburg, University of applied sciences Hamburg, Department of Automotive and Aerospace Engineering, Lecture Notes, Summer Semester 1999
- Scholz 2001** SCHOLZ, Dieter: *Diplomarbeiten normgerecht verfassen: Schreibtipps zur Gestaltung von Studien-, Diplom- und Doktorarbeiten*. Würzburg : Vogel, 2001 - ISBN 3-8023-1859-5
- Straubinger 2000a** STRAUBINGER, Gerold: *Development of an aircraft performance model for the prediction of trip fuel and trip time for a generic twin engine jet transport aircraft*, Hamburg, University of applied sciences Hamburg, Department of Automotive and Aerospace Engineering, Diplom thesis, 2000
- Straubinger 2000b** STRAUBINGER, Gerold: *perform.wk4*. Lotus 1-2-3 file, Hamburg, University of applied sciences Hamburg, Department of Automotive and Aerospace Engineering, Program for diplom thesis, 2000

- TU-Berlin 1999** SEELECKE, Stefan: *Adaptive Optimierung von Flugzeugprofilen mit Gedächtnislegierungen*, URL: <http://www.thermodynamik.tu-berlin.de/DFG/echtzeit/profil.html#Projektleitung>, 10-May-2001
- TU-Berlin 2001** STACHE, Michael: *Verminderung des induzierten Strömungswiderstandes nach dem Vorbild der Natur*. URL: <http://lautaro.fb10.tu-berlin.de/user/michaels/projekt.html>, 10-May-2001
- Young 1999** YOUNG, Trevor: *Flight Mechanics*. Limerick, University of Limerick, Department of Mechanical and Aeronautical Engineering, Lecture Notes, Spring Semester 1999
- Young 2000** YOUNG, Trevor: *b7g7\_i\_e.wk4*. Lotus 1-2-3 file, Limerick, University of Limerick, Department of Mechanical and Aeronautical Engineering, 2000
- Young 2001a** YOUNG, Trevor: Discussion at Meeting. Limerick, University of Limerick, Department of Mechanical and Aeronautical Engineering, 09-April-2001
- Young 2001b** YOUNG, Trevor: Discussion at Meeting. Limerick, University of Limerick, Department of Mechanical and Aeronautical Engineering, 16-April-2001
- Young 2001c** YOUNG, Trevor: Discussion at Meeting. Limerick, University of Limerick, Department of Mechanical and Aeronautical Engineering, 25-April-2001
- Young/Fielding 2000** YOUNG, Trevor M.; FIELDING, J. P.: *Flight Operational Assessment of Hybrid Laminar Flow Control (HLFC) Aircraft*. Limerick, University of Limerick, Department of Mechanical and Aeronautical Engineering, 2000
- Young/Fielding 2001** YOUNG, Trevor M.; FIELDING, J. P.: *Potential Fuel Savings due to Hybrid Laminar Flow Control under Operational Conditions*. Limerick, University of Limerick, Department of Mechanical and Aeronautical Engineering, 2001

## Acknowledgement

First of all, I want to thank my family, especially my wife, for letting me go away for such a long time in order to do this work and supporting me all the time. It was certainly the bigger task to mind our children alone in this 6 month.

Of course, special thanks to the DAAD for believing in me und providing the necessary financial background.

Thanks to Trevor Young for being such a good supervisor, for always taking some time, even when non was available and for the patience with my English. The less formal company at Irish universities was very appreciated.

Thanks to my lecturers at the University of applied sciences in Hamburg for mediating all this knowledge to me, and especially to Prof. Dr.-Ing. Scholz, MSME for the fresh wind he brought into the dusty walls of our department.

Special thanks to Paula Lahiff, Eoin Gaughran, and Louis my flatmates, as well as Marie, Paul, Tess, Mora, J.J., Dave, Laur, Sharon and Karen, which treated me like an old friend and never made me feel like a stranger. I feel deep respect to all of you!

Thanks to the Spanish students, especially to Pepe, Carlos, Natcho, Natxo, Pablo, Isabella and Virginia for giving my stay in Ireland a further unexpected colourful note. Thanks for the only proper meals of the last 6 month, for teaching me my first spanish words and having so much fun together.

# Appendix A

## Configuration tables of the modified Program

In the tables A.1 to A.14, the corrected fuel flow for lower altitudes is given. This is gathered by using factors, which represent the ratios of the shaded fuel flow values to the appropriate values at 29000 ft, obtained by using the Boeing data in Young's program. All other values are simply calculated by linear interpolations and extrapolations. This is also valid for values not listed here. All this is described in detail in chapter 5.1.1.

**Table A.1** Corrected Fuel Flow, altitude 0 ft (part 1)

$F_N/d$ (lb/eng.)	6000	12000	15000	18000	20000	24000	25000	30000	35000	36000	37000
Mach	Corrected Fuel Flow (lb/hr/engine)										
0,20		2007	3889	5771	7055	9624	10302	13693	17096	17777	18537
0,25		2318	4138	5959	7201	9686	10341	13619	16899	17555	18282
0,30		2629	4388	6146	7347	9747	10380	13544	16702	17333	18027
0,35		2941	4637	6334	7492	9808	10419	13469	16505	17112	17772
0,40	68	3252	4887	6522	7638	9870	10457	13394	16308	16890	17517
0,45	525	3564	5137	6710	7783	9931	10496	13320	16111	16669	17262
0,50	982	3875	5386	6897	7929	9993	10535	13245	15914	16447	17007
0,55	1437	4185	5634	7083	8072	10051	10570	13165	15709	16218	16745
0,60	1896	4498	5885	7273	8220	10116	10612	13095	15519	16004	16497

**Table A.2** Corrected Fuel Flow, altitude 0 ft (part 2)

$F_N/d$ (lb/eng.)	38000	39000	40000	41000	42000	43000	44000	45000	65000
Mach	Corrected Fuel Flow (lb/hr/engine)								
0,20	19298	20059	20820	21581	22342	23089	23836	24583	39522
0,25	19010	19737	20465	21192	21919	22629	23338	24047	38232
0,30	18721	19415	20109	20803	21497	22168	22840	23512	36942
0,35	18433	19093	19754	20414	21075	21708	22342	22976	35652
0,40	18144	18771	19398	20025	20652	21248	21844	22440	34362
0,45	17856	18449	19043	19636	20230	20788	21346	21905	33072
0,50	17567	18127	18687	19247	19807	20328	20849	21369	31782
0,55	17271	17797	18323	18849	19376	19858	20341	20823	30472
0,60	16990	17483	17976	18470	18963	19408	19853	20298	29201

**Table A.3** Corrected Fuel Flow, altitude 1500 ft (part 1)

$F_N/d$ (lb/eng.)	6000	12000	15000	18000	20000	24000	25000	30000	35000	36000	37000
Mach	Corrected Fuel Flow (lb/hr/engine)										
0,20		1991	3878	5765	7057	9642	10325	13739	17145	17826	18582
0,25		2307	4131	5955	7204	9702	10362	13658	16941	17598	18321
0,30		2623	4384	6146	7351	9762	10398	13577	16738	17370	18061
0,35		2938	4637	6337	7499	9823	10435	13496	16534	17141	17800
0,40	68	3254	4891	6527	7646	9883	10471	13415	16330	16913	17539
0,45	527	3570	5144	6718	7793	9943	10508	13335	16127	16685	17279
0,50	986	3885	5397	6909	7940	10003	10544	13254	15923	16457	17018
0,55	1443	4200	5649	7098	8085	10059	10577	13168	15712	16221	16750
0,60	1904	4516	5903	7290	8234	10123	10618	13092	15516	16000	16497

**Table A.4** Corrected Fuel Flow, altitude 1500 ft (part 2)

$F_N/d$ (lb/eng.)	38000	39000	40000	41000	42000	43000	44000	45000	65000
Mach	Corrected Fuel Flow (lb/hr/engine)								
0,20	19337	20093	20849	21604	22360	23084	23809	24533	39021
0,25	19045	19768	20491	21214	21938	22628	23319	24010	37824
0,30	18752	19442	20133	20824	21515	22172	22829	23486	36627
0,35	18459	19117	19776	20434	21093	21716	22339	22963	35430
0,40	18166	18792	19418	20044	20670	21260	21850	22439	34233
0,45	17873	18466	19060	19654	20248	20804	21360	21916	33037
0,50	17580	18141	18703	19264	19825	20348	20870	21393	31840
0,55	17278	17807	18336	18865	19394	19882	20370	20859	30625
0,60	16994	17490	17987	18484	18981	19436	19891	20346	29446

**Table A.5** Corrected Fuel Flow, altitude 5000 ft (part 1)

$F_N/d$ (lb/eng.)	6000	12000	15000	18000	20000	24000	25000	30000	35000	36000	37000
Mach	Corrected Fuel Flow (lb/hr/engine)										
0,20		1973	3865	5756	7080	9727	10431	13950	17398	18088	18837
0,25		2296	4124	5953	7228	9777	10454	13838	17156	17820	18538
0,30		2618	4384	6150	7375	9827	10476	13725	16914	17552	18239
0,35		2941	4644	6346	7523	9876	10499	13612	16671	17283	17940
0,40	88	3264	4903	6543	7671	9926	10522	13500	16429	17015	17641
0,45	542	3586	5163	6739	7818	9976	10544	13387	16187	16747	17342
0,50	996	3909	5422	6936	7966	10026	10567	13274	15945	16479	17043
0,55	1457	4232	5682	7132	8114	10079	10595	13174	15718	16227	16762
0,60	1922	4559	5945	7331	8267	10139	10630	13084	15506	15991	16496
0,65	2369	4878	6202	7526	8411	10181	10644	12954	15241	15698	16172
0,70	2813	5199	6461	7722	8556	10224	10658	12824	14975	15406	15848

**Table A.6** Corrected Fuel Flow, altitude 5000 ft (part 2)

$F_N/d$ (lb/eng.)	38000	39000	40000	41000	42000	43000	44000	45000	65000
Mach	Corrected Fuel Flow (lb/hr/engine)								
0,20	19585	20334	21083	21831	22580	23237	23894	24551	37688
0,25	19256	19974	20692	21410	22128	22763	23398	24033	36736
0,30	18926	19614	20301	20989	21676	22289	22903	23516	35784
0,35	18597	19254	19910	20567	21224	21815	22407	22999	34832
0,40	18267	18893	19519	20146	20772	21342	21912	22481	33880
0,45	17938	18533	19129	19724	20320	20868	21416	21964	32928
0,50	17608	18173	18738	19303	19868	20394	20920	21447	31976
0,55	17296	17831	18366	18901	19436	19938	20440	20942	30982
0,60	17001	17507	18012	18517	19022	19500	19978	20456	30017
0,65	16646	17119	17593	18067	18541	18999	19458	19917	29094
0,70	16290	16732	17175	17617	18059	18499	18938	19378	28167

**Table A.7** Corrected Fuel Flow, altitude 10000 ft (part 1)

$F_N/d$ (lb/eng.)	6000	12000	15000	18000	20000	24000	25000	30000	35000	36000	37000
Mach	Corrected Fuel Flow (lb/hr/engine)										
0,30		1973	3865	5756	7080	9727	10431	13950	17398	18088	18837
0,35		2296	4124	5953	7228	9777	10454	13838	17156	17820	18538
0,40		2618	4384	6150	7375	9827	10476	13725	16914	17552	18239
0,45		2941	4644	6346	7523	9876	10499	13612	16671	17283	17940
0,50	88	3264	4903	6543	7671	9926	10522	13500	16429	17015	17641
0,55	542	3586	5163	6739	7818	9976	10544	13387	16187	16747	17342
0,60	996	3909	5422	6936	7966	10026	10567	13274	15945	16479	17043
0,65	1457	4232	5682	7132	8114	10079	10595	13174	15718	16227	16762
0,70	1922	4559	5945	7331	8267	10139	10630	13084	15506	15991	16496



**Table A.8** Corrected Fuel Flow, altitude 10000 ft (part 2)

$F_N/d$ (lb/eng.)	38000	39000	40000	41000	42000	43000	44000	45000	65000
Mach	Corrected Fuel Flow (lb/hr/engine)								
0,30	19002	19689	20377	21064	21751	22383	23015	23647	36282
0,35	18664	19321	19978	20635	21291	21897	22503	23109	35230
0,40	18327	18953	19579	20205	20831	21412	21992	22572	34178
0,45	17989	18585	19180	19776	20371	20926	21480	22035	33125
0,50	17652	18217	18782	19346	19911	20440	20969	21498	32073
0,55	17390	17926	18462	18998	19534	20038	20542	21045	31121
0,60	17010	17515	18020	18525	19029	19505	19981	20456	29970
0,65	16656	17130	17603	18077	18550	19001	19452	19902	28917
0,70	16302	16744	17187	17629	18071	18497	18923	19348	27864

**Table A.9** Corrected Fuel Flow, altitude 15000 ft (part 1)

$F_N/d$ (lb/eng.)	6000	12000	15000	18000	20000	24000	25000	30000	35000	36000	37000
Mach	Corrected Fuel Flow (lb/hr/engine)										
0,50	1022	4032	5578	7124	8167	10254	10795	13499	16153	16684	17246
0,55	1489	4358	5840	7322	8319	10314	10830	13411	15947	16454	16988
0,60	1961	4682	6092	7503	8447	10336	10824	13262	15662	16142	16644
0,65	2427	5008	6349	7691	8582	10366	10826	13124	15394	15848	16320
0,70	2893	5335	6607	7879	8719	10397	10828	12986	15126	15553	15995

**Table A.10** Corrected Fuel Flow, altitude 15000 ft (part 2)

$F_N/d$ (lb/eng.)	38000	39000	40000	41000	42000	43000	44000	45000	65000
Mach	Corrected Fuel Flow (lb/hr/engine)								
0,50	17809	18371	18933	19496	20058	20589	21121	21652	32282
0,55	17521	18054	18588	19121	19655	20161	20667	21173	31294
0,60	17147	17650	18152	18655	19158	19636	20114	20593	30159
0,65	16791	17263	17735	18207	18679	19132	19585	20038	29097
0,70	16436	16877	17319	17760	18201	18629	19056	19484	28034

**Table A.11** Corrected Fuel Flow, altitude 20000 ft (part 1)

$F_N/d$ (lb/eng.)	6000	12000	15000	18000	20000	24000	25000	30000	35000	36000	37000
Mach	Corrected Fuel Flow (lb/hr/engine)										
0,50	1036	4127	5698	7269	8325	10437	10977	13678	16318	16846	17406
0,55	1510	4452	5953	7455	8462	10477	10992	13566	16087	16591	17122
0,60	1985	4776	6203	7630	8584	10492	10979	13414	15805	16283	16783
0,65	2458	5101	6455	7809	8710	10513	10972	13270	15533	15986	16457
0,70	2930	5427	6708	7989	8837	10534	10966	13125	15262	15690	16130

**Table A.12** Corrected Fuel Flow, altitude 20000 ft (part 2)

$F_N/d$ (lb/eng.)	38000	39000	40000	41000	42000	43000	44000	45000	47000
Mach	Corrected Fuel Flow (lb/hr/engine)								
0,50	17966	18525	19085	19645	20204	20739	21273	21807	32491
0,55	17652	18183	18714	19245	19775	20284	20792	21300	31467
0,60	17284	17784	18285	18785	19286	19767	20248	20729	30348
0,65	16927	17397	17868	18338	18808	19264	19719	20174	29277
0,70	16570	17010	17451	17891	18331	18760	19190	19619	28205

**Table A.13** Corrected Fuel Flow, altitude 25000 ft (part 1)

$F_N/d$ (lb/eng.)	6000	12000	15000	18000	20000	24000	25000	30000	35000	36000	37000
Mach	Corrected Fuel Flow (lb/hr/engine)										
0,50	1050	4221	5818	7415	8483	10619	11159	13857	16483	17008	17566
0,55	1530	4545	6067	7588	8605	10639	11153	13720	16226	16728	17256
0,60	2010	4869	6313	7757	8721	10648	11134	13566	15947	16424	16922
0,65	2488	5193	6560	7927	8838	10660	11119	13415	15673	16125	16593
0,70	2967	5518	6808	8098	8956	10671	11103	13264	15399	15826	16265

**Table A.14** Corrected Fuel Flow, altitude 25000 ft (part 2)

$F_N/d$ (lb/eng.)	38000	39000	40000	41000	42000	43000	44000	45000	65000
Mach	Corrected Fuel Flow (lb/hr/engine)								
0,50	18123	18680	19237	19794	20351	20888	21425	21962	32700
0,55	17784	18312	18840	19368	19896	20407	20917	21428	31640
0,60	17420	17919	18417	18916	19414	19898	20381	20865	30538
0,65	17062	17531	18000	18469	18938	19395	19852	20310	29456
0,70	16704	17143	17583	18022	18461	18892	19323	19754	28375

In table A.15 to A.27, data of altitudes with available information is given. The values inside the shaded area can be considered as original information, obtained in flight tests. All other values, included these not represented here, are gathered by linear extrapolations.

**Table A.15** Corrected Fuel Flow, altitude 29000 ft

$F_N/d$ (lb/eng.)	6000	35000	36000	37000	38000	39000	40000	41000	42000	70000
Mach	Corrected Fuel Flow (lb/hr/engine)									
0,50	1062	16695	17138	17674	18201	18762	19320	19876	20468	35562
0,55	1546	16406	16837	17347	17850	18380	18909	19436	19993	34340
0,60	2029	16116	16536	17020	17498	17999	18498	18996	19517	33118
0,65	2513	15827	16235	16693	17146	17617	18087	18555	19041	31896
0,70	2997	15538	15935	16366	16795	17235	17676	18115	18565	30674
0,75	3480	15249	15634	16039	16443	16854	17264	17675	18089	29452
0,78	3770	15075	15453	15843	16232	16625	17018	17411	17804	28718
0,79	3738	14991	15379	15767	16156	16544	16932	17319	17707	28572
0,80	3757	14924	15308	15692	16079	16467	16851	17235	17619	28401
0,81	3918	14881	15258	15635	16013	16391	16769	17148	17527	28112
0,82	4157	14844	15213	15582	15951	16320	16689	17058	17423	27741

**Table A.16** Corrected Fuel Flow, altitude 30000 ft

$F_N/d$ (lb/eng.)	15000	35000	36000	37000	38000	39000	40000	41000	42000	43000	70000
Mach	Corrected Fuel Flow (lb/hr/engine)										
0,50	7529	16685	17208	17729	18248	18766	19270	19783	20128	20347	32707
0,55	7492	16398	16898	17395	17891	18386	18869	19359	19712	19961	31983
0,60	7456	16112	16588	17061	17534	18005	18468	18935	19295	19574	31260
0,65	7419	15826	16277	16727	17176	17625	18067	18512	18879	19188	30537
0,70	7382	15539	15967	16393	16819	17245	17665	18088	18463	18802	29814
0,75	7346	15253	15657	16059	16462	16865	17264	17664	18047	18416	29091
0,78	7324	15081	15470	15859	16248	16637	17023	17410	17797	18184	28657
0,79	7240	15008	15396	15783	16171	16559	16947	17336	17726	18115	28602
0,80	7202	14931	15319	15707	16094	16481	16867	17252	17637	18022	28456
0,81	7247	14897	15274	15651	16029	16406	16784	17161	17559	17957	28284
0,82	7294	14852	15222	15592	15962	16332	16702	17071	17464	17875	28078

**Table A.17** Corrected Fuel Flow, altitude 31000 ft

$F_N/d$ (lb/eng.)	15000	37000	38000	39000	40000	41000	42000	43000	44000	70000
Mach	Corrected Fuel Flow (lb/hr/engine)									
<b>0,50</b>	7780	17760	18254	18780	19298	19861	20306	20624	20935	32729
<b>0,55</b>	7685	17424	17899	18400	18895	19428	19864	20197	20523	32034
<b>0,60</b>	7589	17089	17544	18021	18492	18994	19422	19769	20112	31339
<b>0,65</b>	7493	16753	17189	17641	18088	18560	18980	19342	19700	30644
<b>0,70</b>	7397	16418	16833	17261	17685	18127	18539	18915	19288	29949
<b>0,75</b>	7301	16082	16478	16881	17282	17693	18097	18487	18876	29254
<b>0,78</b>	7244	15881	16265	16653	17040	17433	17832	18231	18629	28837
<b>0,79</b>	7150	15795	16188	16575	16962	17351	17749	18147	18546	28762
<b>0,80</b>	7142	15726	16111	16496	16883	17270	17664	18061	18457	28602
<b>0,81</b>	7119	15665	16043	16421	16799	17175	17574	17979	18384	28483
<b>0,82</b>	7167	15613	15981	16349	16718	17086	17478	17889	18300	28281

**Table A.18** Corrected Fuel Flow, altitude 32000 ft

$F_N/d$ (lb/eng.)	6000	38000	39000	40000	41000	42000	43000	44000	45000	46000	70000
Mach	Corrected Fuel Flow (lb/hr/engine)										
<b>0,50</b>	7391	18753	19144	19491	19884	20320	20645	20964	21291	21594	30116
<b>0,55</b>	6719	18311	18702	19056	19449	19878	20217	20550	20890	21209	29904
<b>0,60</b>	6047	17869	18260	18621	19014	19437	19788	20136	20488	20825	29692
<b>0,65</b>	5375	17427	17819	18187	18580	18995	19360	19721	20086	20440	29480
<b>0,70</b>	4703	16985	17377	17752	18145	18554	18931	19307	19685	20056	29268
<b>0,75</b>	4031	16543	16935	17318	17710	18112	18503	18893	19283	19671	29056
<b>0,78</b>	3627	16278	16670	17057	17449	17847	18246	18644	19042	19441	28928
<b>0,79</b>	3555	16184	16592	16978	17368	17764	18160	18554	18948	19342	28814
<b>0,80</b>	3656	16132	16515	16899	17286	17681	18074	18466	18859	19251	28608
<b>0,81</b>	3562	16064	16440	16815	17191	17590	17991	18394	18791	19189	28565
<b>0,82</b>	3090	15924	16317	16709	17102	17494	17903	18312	18721	19133	28759

**Table A.19** Corrected Fuel Flow, altitude 33000 ft

$F_N/d$ (lb/eng.)	15000	39000	40000	41000	42000	43000	44000	45000	46000	47000	70000
Mach	Corrected Fuel Flow (lb/hr/engine)										
<b>0,50</b>	10966	19558	19778	20052	20359	20664	20981	21530	21989	22422	30656
<b>0,55</b>	10247	19046	19295	19591	19914	20235	20566	21094	21546	21978	30410
<b>0,60</b>	9528	18533	18812	19129	19468	19806	20152	20657	21104	21535	30165
<b>0,65</b>	8809	18021	18330	18668	19023	19377	19737	20220	20662	21091	29919
<b>0,70</b>	8090	17508	17847	18206	18578	18948	19322	19784	20219	20648	29674
<b>0,75</b>	7371	16996	17364	17745	18132	18519	18908	19347	19777	20204	29428
<b>0,78</b>	6940	16689	17075	17468	17865	18262	18659	19085	19512	19938	29281
<b>0,79</b>	6954	16607	16996	17385	17781	18176	18571	18989	19407	19825	29076
<b>0,80</b>	6713	16498	16900	17302	17697	18090	18484	18889	19325	19760	29138
<b>0,81</b>	6614	16407	16807	17206	17606	18008	18409	18811	19241	19671	29056
<b>0,82</b>	6364	16279	16689	17099	17509	17919	18327	18736	19158	19583	29085

**Table A.20** Corrected Fuel Flow, altitude 34000 ft

$F_N/d$ (lb/eng.)	15000	41000	42000	43000	44000	45000	46000	47000	48000	49000	70000
Mach	Corrected Fuel Flow (lb/hr/engine)										
<b>0,50</b>	7969	20069	20374	20692	20987	21559	22139	22684	23237	23792	33564
<b>0,55</b>	7710	19608	19929	20261	20574	21121	21676	22202	22735	23269	32879
<b>0,60</b>	7450	19147	19485	19831	20161	20682	21213	21720	22233	22746	32194
<b>0,65</b>	7191	18686	19040	19400	19748	20244	20749	21238	21730	22223	31508
<b>0,70</b>	6931	18225	18595	18970	19335	19805	20286	20756	21228	21701	30823
<b>0,75</b>	6672	17765	18150	18539	18922	19366	19822	20274	20726	21178	30138
<b>0,78</b>	6516	17488	17884	18281	18675	19103	19544	19984	20424	20864	29727
<b>0,79</b>	6506	17406	17799	18193	18588	19005	19443	19881	20320	20760	29564
<b>0,80</b>	6522	17322	17715	18107	18500	18906	19342	19775	20210	20645	29369
<b>0,81</b>	6227	17176	17600	18024	18426	18827	19257	19687	20116	20545	29389
<b>0,82</b>	6308	17120	17528	17936	18345	18752	19174	19599	20022	20446	29178

**Table A.21** Corrected Fuel Flow, altitude 35000 ft

$F_N/d$ (lb/eng.)	15000	42000	43000	44000	45000	46000	47000	48000	49000	50000	51000	70000
Mach	Corrected Fuel Flow (lb/hr/engine)											
<b>0,50</b>	7754	20488	20717	21029	21591	22169	22723	23265	23811	24225	24733	33694
<b>0,55</b>	7527	20028	20285	20612	21150	21703	22237	22761	23287	23703	24195	32992
<b>0,60</b>	7301	19568	19853	20195	20709	21238	21751	22256	22764	23181	23657	32290
<b>0,65</b>	7075	19108	19421	19778	20268	20772	21265	21752	22240	22658	23119	31587
<b>0,70</b>	6849	18648	18990	19361	19827	20307	20780	21248	21717	22136	22582	30885
<b>0,75</b>	6623	18189	18558	18945	19387	19841	20294	20744	21193	21614	22044	30183
<b>0,78</b>	6487	17913	18298	18695	19122	19562	20003	20441	20879	21300	21721	29761
<b>0,79</b>	6348	17801	18204	18607	19023	19461	19898	20334	20768	21193	21618	29678
<b>0,80</b>	6402	17739	18128	18518	18925	19359	19793	20225	20657	21087	21517	29495
<b>0,81</b>	6358	17639	18041	18442	18844	19274	19703	20131	20559	20984	21399	29338
<b>0,82</b>	6306	17545	17953	18361	18769	19190	19614	20038	20461	20882	21291	29199

**Table A.22** Corrected Fuel Flow, altitude 36000 ft

$F_N/d$ (lb/eng.)	15000	44000	45000	46000	47000	48000	49000	50000	51000	52000	53000	54000	70000
Mach	Corrected Fuel Flow (lb/hr/engine)												
<b>0,50</b>	4557	21186	21639	22205	22752	23284	23841	24244	24676	25152	26085	26921	36096
<b>0,55</b>	4829	20745	21193	21736	22264	22780	23316	23721	24149	24614	25464	26233	35015
<b>0,60</b>	5100	20303	20747	21268	21776	22275	22790	23198	23623	24076	24842	25546	33934
<b>0,65</b>	5372	19862	20301	20800	21289	21770	22264	22675	23096	23538	24221	24858	32853
<b>0,70</b>	5644	19420	19855	20331	20801	21266	21738	22153	22570	23000	23599	24171	31772
<b>0,75</b>	5916	18979	19409	19863	20314	20761	21212	21630	22043	22461	22978	23483	30691
<b>0,78</b>	6079	18714	19141	19582	20021	20458	20897	21316	21727	22138	22605	23071	30042
<b>0,79</b>	6152	18607	19043	19479	19916	20350	20785	21208	21617	22025	22464	22902	29775
<b>0,80</b>	6292	18516	18947	19377	19810	20241	20673	21099	21506	21913	22322	22731	29475
<b>0,81</b>	6385	18448	18870	19292	19720	20148	20574	21000	21406	21810	22214	22608	29263
<b>0,82</b>	6296	18361	18784	19207	19631	20054	20476	20898	21306	21708	22107	22521	29177

**Table A.23** Corrected Fuel Flow, altitude 37000 ft

$F_N/d$ (lb/eng.)	15000	45000	46000	47000	48000	49000	50000	51000	52000	53000	54000	70000
Mach	Corrected Fuel Flow (lb/hr/engine)											
<b>0,50</b>	4113	21755	22269	22778	23328	23872	24282	24716	25188	26117	27048	36457
<b>0,55</b>	4461	21294	21795	22291	22822	23346	23758	24188	24649	25496	26344	35321
<b>0,60</b>	4810	20833	21320	21804	22315	22820	23234	23660	24110	24875	25640	34185
<b>0,65</b>	5158	20371	20846	21317	21808	22295	22710	23132	23571	24253	24935	33049
<b>0,70</b>	5507	19910	20371	20830	21301	21769	22186	22604	23033	23632	24231	31913
<b>0,75</b>	5855	19449	19897	20343	20794	21243	21663	22077	22494	23011	23527	30777
<b>0,78</b>	6064	19172	19612	20051	20490	20928	21348	21760	22171	22638	23105	30095
<b>0,79</b>	7592	19069	19509	19946	20382	20817	21240	21650	22059	22501	22512	28633
<b>0,80</b>	6159	18973	19406	19840	20273	20705	21132	21538	21946	22363	22817	29651
<b>0,81</b>	6401	18867	19322	19750	20179	20606	21031	21439	21842	22247	22607	29256
<b>0,82</b>	6343	18803	19232	19661	20085	20508	20929	21338	21740	22141	22541	29186

**Table A.24** Corrected Fuel Flow, altitude 38000 ft

$F_N/d$ (lb/eng.)	15000	45000	46000	47000	48000	49000	50000	51000	52000	53000	54000	70000
Mach	Corrected Fuel Flow (lb/hr/engine)											
<b>0,50</b>	3840	21742	22290	22810	23359	23911	24318	24749	25234	26141	27113	36661
<b>0,55</b>	4238	21288	21818	22323	22853	23385	23794	24221	24693	25522	26403	35496
<b>0,60</b>	4637	20834	21345	21836	22346	22858	23270	23694	24153	24902	25693	34332
<b>0,65</b>	5035	20380	20872	21349	21839	22331	22745	23166	23612	24283	24983	33167
<b>0,70</b>	5434	19926	20400	20862	21333	21805	22221	22638	23071	23663	24274	32003
<b>0,75</b>	5832	19472	19927	20375	20826	21278	21697	22111	22531	23044	23564	30838
<b>0,78</b>	6072	19200	19643	20083	20522	20962	21382	21794	22206	22672	23138	30140
<b>0,79</b>	6173	19100	19539	19977	20414	20849	21273	21684	22094	22536	22979	29873
<b>0,80</b>	6280	18996	19438	19871	20305	20738	21166	21574	21981	22396	22811	29593
<b>0,81</b>	6152	18920	19353	19782	20211	20639	21064	21472	21877	22282	22751	29560
<b>0,82</b>	6390	18836	19265	19694	20117	20541	20962	21372	21774	22177	22570	29208

**Table A.25** Corrected Fuel Flow, altitude 39000 ft

$F_N/d$ (lb/eng.)	15000	45000	46000	47000	48000	49000	50000	51000	52000	53000	70000
Mach	Corrected Fuel Flow (lb/hr/engine)										
<b>0,50</b>	4981	21738	22303	22853	23408	23946	24360	24788	25275	26207	35702
<b>0,55</b>	5197	21291	21833	22364	22899	23419	23834	24260	24733	25582	34702
<b>0,60</b>	5413	20843	21364	21875	22390	22892	23309	23731	24191	24958	33702
<b>0,65</b>	5629	20396	20895	21386	21880	22365	22783	23203	23650	24333	32701
<b>0,70</b>	5844	19948	20425	20897	21371	21838	22257	22674	23108	23709	31701
<b>0,75</b>	6060	19501	19956	20408	20861	21311	21732	22146	22567	23085	30701
<b>0,78</b>	6190	19232	19675	20115	20556	20995	21416	21828	22242	22710	30101
<b>0,79</b>	6204	19132	19571	20009	20446	20884	21307	21720	22130	22579	29905
<b>0,80</b>	6298	19030	19467	19904	20338	20771	21199	21607	22017	22425	29639
<b>0,81</b>	6274	18942	19383	19813	20243	20672	21099	21507	21914	22320	29499
<b>0,82</b>	6363	18874	19299	19724	20148	20573	20996	21406	21808	22210	29300

**Table A.26** Corrected Fuel Flow, altitude 40000 ft

$F_N/d$ (lb/eng.)	15000	45000	46000	47000	48000	49000	50000	51000	52000	53000	70000
Mach	Corrected Fuel Flow (lb/hr/engine)										
<b>0,50</b>	4329	21618	22274	22894	23436	23979	24389	24829	25305	26228	36025
<b>0,55</b>	4660	21196	21815	22403	22927	23452	23864	24300	24764	25606	34977
<b>0,60</b>	4991	20775	21357	21913	22418	22925	23339	23770	24224	24984	33929
<b>0,65</b>	5322	20354	20898	21423	21910	22398	22814	23241	23683	24362	32880
<b>0,70</b>	5652	19932	20439	20932	21401	21871	22289	22711	23142	23740	31832
<b>0,75</b>	5983	19511	19980	20442	20893	21344	21765	22181	22601	23118	30784
<b>0,78</b>	6182	19258	19705	20148	20587	21028	21450	21864	22277	22745	30155
<b>0,79</b>	6279	19160	19602	20042	20479	20915	21342	21754	22164	22595	29895
<b>0,80</b>	6353	19060	19499	19935	20370	20805	21232	21643	22051	22449	29650
<b>0,81</b>	6347	18981	19414	19845	20274	20705	21132	21542	21948	22350	29509
<b>0,82</b>	6447	18921	19338	19755	20181	20606	21030	21440	21844	22247	29316

**Table A.27** Corrected Fuel Flow, altitude 41000 ft

$F_N/d$ (lb/eng.)	15000	45000	46000	47000	48000	49000	50000	51000	52000	53000	70000
Mach	Corrected Fuel Flow (lb/hr/engine)										
<b>0,50</b>	5197	21848	22386	22922	23481	24025	24433	24880	25342	26289	35725
<b>0,55</b>	5377	21392	21913	22432	22971	23496	23906	24347	24801	25663	34739
<b>0,60</b>	5557	20936	21440	21943	22460	22967	23380	23815	24260	25037	33752
<b>0,65</b>	5737	20480	20967	21453	21949	22437	22853	23283	23718	24411	32766
<b>0,70</b>	5917	20024	20493	20963	21439	21908	22326	22751	23177	23785	31779
<b>0,75</b>	6097	19567	20020	20473	20928	21379	21800	22219	22636	23160	30793
<b>0,78</b>	6205	19294	19736	20179	20621	21062	21484	21899	22311	22784	30201
<b>0,79</b>	6219	19185	19633	20074	20512	20949	21375	21789	22201	22642	29989
<b>0,80</b>	6280	19081	19530	19967	20403	20837	21265	21677	22086	22495	29749
<b>0,81</b>	6318	19006	19445	19877	20307	20738	21166	21575	21983	22389	29579
<b>0,82</b>	6349	18929	19358	19787	20213	20638	21062	21474	21878	22283	29412

**Table A.28** Maximum climb thrust

Mach	0.20	0.25	0.30	0.35	0.40	0.45	0.50	0.55	0.60	0.65	0.70	0.75	0.80	0.85	0.90
Height (ft)	Net thrust /delta per engine (lb)														
0	53494	51202	48911	46973	45035	43064	41703	40437	39171						
1000	54534	52207	49880	47919	45958	44037	42638	41355	40073						
1500	55055	52710	50365	48392	46420	44524	43106	41815	40524						
2000	55575	53212	50850	48866	46881	45011	43573	42274	40975						
3000	56615	54218	51820	49812	47804	45984	44509	43193	41877						
4000	57656	55223	52789	50758	48727	46958	45444	44111	42779						
5000	58696	56228	53759	51705	49650	47931	46379	45030	43680	42592	41503				
6000			54759	52713	50666	48945	47389	46012	44674	43562	42450				
7000			55759	53721	51682	49959	48398	46995	45668	44533	43398				
8000			56760	54729	52698	50974	49408	47978	46662	45503	44345				
9000			57760	55737	53714	51988	50417	48960	47656	46474	45292				
10000			58760	56745	54730	53002	51427	49943	48650	47445	46239				
11000			59825	57810	55795	54074	52491	51023	49724	48531	47339				
12000			60890	58875	56859	55147	53555	52103	50798	49618	48438				
13000			61955	59940	57924	56219	54620	53183	51872	50705	49538				
14000			63020	61004	58989	57291	55684	54263	52946	51791	50637				
15000			64085	62069	60053	58364	56748	55343	54020	52878	51736	50735	49733		
16000			64988	63021	61053	59406	57817	56440	55156	54037	52909	51908	50907		
17000			65891	63972	62053	60448	58887	57538	56292	55195	54082	53082	52081		
18000			66794	64923	63053	61490	59956	58636	57429	56354	55255	54255	53255		
19000			67696	65874	64052	62532	61025	59734	58565	57512	56428	55428	54429		
20000			68599	66826	65052	63574	62095	60831	59701	58671	57600	56602	55603	54871	54138
21000					65779	64360	62941	61734	60682	59705	58721	57740	56756	56042	55328
22000					66506	65146	63787	62638	61662	60739	59843	58878	57909	57214	56518
23000					67232	65932	64632	63541	62642	61773	60964	60016	59062	58385	57708
24000					67959	66719	65478	64444	63622	62808	62085	61154	60215	59556	58897
25000					68686	67505	66324	65347	64603	63842	63206	62292	61368	60727	60087
26000							67084	66225	65560	64908	64385	63664	62912	62346	61745
27000							67843	67102	66517	65974	65565	65037	64456	63965	63404
28000							68602	67980	67474	67040	66745	66409	66001	65584	65062
29000							69361	68858	68431	68106	67925	67781	67545	67203	66720
30000							70121	69735	69389	69172	69105	69154	69090	68822	68378
31000							70880	70613	70346	70238	70284	70526	70634	70441	70036
32000							71403	71204	71005	71032	71175	71581	71838	71852	71787
33000							71926	71795	71663	71826	72065	72637	73042	73262	73538
34000							72449	72386	72322	72620	72956	73692	74247	74672	75288
35000							72973	72977	72981	73413	73846	74747	75451	76083	77039
36089							73201	73239	73276	73760	74245	75165	76178	76829	77895
37000							72983	73015	73047	73527	74007	74919	75921	76553	77596
38000							72747	72773	72799	73273	73747	74649	75643	76254	77272
39000							72510	72531	72551	73019	73488	74380	75364	75955	76948
40000							72210	72211	72212	72720	73227	74110	75083	75653	76610
41000							71910	71892	71874	72420	72966	73839	74803	75350	76273
42000							71609	71572	71535	72120	72705	73568	74522	75048	75936

**Table A.29** Minimum idle inflight thrust

Mach	0.20	0.25	0.30	0.35	0.40	0.45	0.50	0.55	0.60	0.65	0.70	0.75	0.80	0.85	0.90
Height (ft)	Net thrust/delta per engine (lb)														
0	1679	1394	1109	873	638	413	153	-166	-485						
5000	1914	1605	1295	1059	823	585	310	-10	-329	-705	-1081				
10000			1490	1252	1013	770	492	184	-163	-545	-926				
15000			1730	1474	1219	960	674	356	2	-379	-761	-1165	-1569		
20000			2006	1735	1465	1177	888	558	193	-189	-589	-1000	-1410	-1878	-2347
25000					1702	1411	1119	776	399	0	-399	-799	-1215	-1678	-2141
31000							1755	1365	975	581	187	-187	-566	-1001	-1433
35000							3188	2734	2279	1841	1403	982	566	61	-305
36089							3689	3196	2703	2253	1802	1365	939	416	55
37000							4085	3589	3093	2627	2160	1715	1268	742	375
39000							5096	4551	4005	3503	3002	2531	2063	1516	1166
41000							5996	5405	4813	4282	3751	3251	2745	2195	1850
42000							6896	6259	5622	5062	4501	3971	3428	2875	2533

**Table A.30** Minimum idle fuel flow

Mach	0.20	0.25	0.30	0.35	0.40	0.45	0.50	0.55	0.60	0.65	0.70	0.75	0.80	0.85	0.90
Height (ft)	Minimum corrected idle fuel flow per engine (lb/hr/eng.)														
0	1847	1830	1813	1786	1760	1728	1677	1597	1518						
5000	1717	1702	1688	1668	1649	1624	1577	1521	1465	1393	1321				
10000			1545	1539	1533	1516	1486	1448	1401	1342	1283				
15000			1401	1398	1395	1384	1365	1340	1308	1268	1227	1171	1115		
20000			1306	1300	1293	1277	1261	1236	1206	1174	1143	1101	1060	1009	958
25000					1196	1185	1174	1155	1132	1102	1073	1039	999	959	920
31000							1121	1107	1092	1075	1056	1035	1011	986	956
35000							1181	1170	1160	1145	1130	1111	1092	1071	1047
36089							1196	1185	1174	1161	1147	1130	1113	1092	1068
37000							1206	1196	1185	1172	1160	1145	1126	1107	1085
39000							1230	1219	1208	1197	1185	1170	1155	1138	1117
41000							1243	1234	1224	1213	1202	1188	1174	1159	1140
42000							1257	1249	1240	1230	1219	1206	1194	1179	1162

**Table A.31** Data for brake release to 1500 ft

BR Weight (lb)	Fuel (lb)	Distance (nm)	Time (min)
320000	1251	3,50	1,58
330000	1296	3,58	1,61
340000	1341	3,65	1,65
350000	1386	3,73	1,69
360000	1431	3,80	1,72
370000	1476	3,88	1,76
380000	1521	3,95	1,79
390000	1566	4,03	1,83
400000	1611	4,10	1,86
410000	1656	4,18	1,90
420000	1701	4,25	1,93
430000	1746	4,33	1,97
440000	1791	4,40	2,00
450000	1836	4,48	2,04
460000	1882	4,55	2,08
470000	1927	4,63	2,11
480000	1972	4,70	2,15
490000	2017	4,78	2,18
500000	2062	4,85	2,22
510000	2107	4,93	2,26
520000	2152	5,00	2,29

**Table A.32** Recommended holding speed at 1500 ft

Weight/delta (lb)	Mach
260000	0,47275
280000	0,48825
300000	0,50375
320000	0,51925
340000	0,53475
360000	0,55025
380000	0,56575
400000	0,58125
420000	0,59675
440000	0,61225
460000	0,62775
480000	0,64325



**Table A.33** High-speed drag polare (part 1)

Mach	Lift coefficient								
	0	0,100	0,150	0,200	0,250	0,300	0,350	0,400	0,450
	Drag coefficient								
<b>0.30</b>	<b>0,01452</b>	0,01486	0,01529	0,01589	0,01666	0,01761	0,01873	0,02002	0,02148
<b>0.35</b>	<b>0,01452</b>	0,01486	0,01529	0,01589	0,01666	0,01761	0,01873	0,02002	0,02148
<b>0.40</b>	<b>0,01452</b>	0,01486	0,01529	0,01589	0,01666	0,01761	0,01873	0,02002	0,02148
<b>0.45</b>	<b>0,01452</b>	0,01486	0,01529	0,01589	0,01666	0,01761	0,01873	0,02002	0,02148
<b>0.50</b>	<b>0,01452</b>	0,01486	0,01529	0,01589	0,01666	0,01761	0,01873	0,02002	0,02148
<b>0.55</b>	<b>0,01452</b>	0,01486	0,01529	0,01589	0,01666	0,01761	0,01873	0,02002	0,02148
<b>0.60</b>	<b>0,01452</b>	0,01486	0,01529	0,01589	0,01666	0,01761	0,01873	0,02002	0,02148
<b>0.65</b>	<b>0,01452</b>	0,01486	0,01529	0,01589	0,01666	0,01761	0,01873	0,02002	0,02148
<b>0.70</b>	<b>0,01452</b>	0,01486	0,01529	0,01589	0,01666	0,01761	0,01873	0,02003	0,02150
<b>0.71</b>	<b>0,01452</b>	0,01486	0,01529	0,01589	0,01667	0,01761	0,01874	0,02004	0,02152
<b>0.72</b>	<b>0,01452</b>	0,01486	0,01529	0,01589	0,01667	0,01762	0,01874	0,02005	0,02154
<b>0.73</b>	<b>0,01452</b>	0,01486	0,01529	0,01589	0,01667	0,01762	0,01875	0,02006	0,02157
<b>0.74</b>	<b>0,01452</b>	0,01486	0,01529	0,01589	0,01667	0,01762	0,01875	0,02007	0,02159
<b>0.75</b>	<b>0,01452</b>	0,01486	0,01529	0,01589	0,01667	0,01762	0,01876	0,02008	0,02161
<b>0.76</b>	<b>0,01452</b>	0,01486	0,01529	0,01589	0,01667	0,01762	0,01876	0,02009	0,02163
<b>0.77</b>	<b>0,01452</b>	0,01486	0,01529	0,01589	0,01667	0,01762	0,01876	0,02010	0,02165
<b>0.78</b>	<b>0,01452</b>	0,01486	0,01530	0,01591	0,01669	0,01764	0,01877	<b>0,02008</b>	<b>0,02165</b>
<b>0.79</b>	<b>0,01549</b>	0,01578	0,01614	0,01665	0,01731	0,01811	0,01906	<b>0,02022</b>	<b>0,02177</b>
<b>0.80</b>	<b>0,01536</b>	0,01567	0,01605	0,01659	0,01728	0,01813	0,01912	<b>0,02037</b>	<b>0,02191</b>
<b>0.81</b>	<b>0,01531</b>	0,01564	0,01604	0,01661	0,01734	0,01823	0,01929	<b>0,02057</b>	<b>0,02212</b>
<b>0.82</b>	<b>0,01538</b>	0,01572	0,01614	0,01674	0,01750	0,01843	0,01953	<b>0,02085</b>	<b>0,02243</b>
<b>0.83</b>	<b>0,01560</b>	0,01595	0,01639	0,01701	0,01780	0,01878	0,01996	0,02135	0,02298
<b>0.84</b>	<b>0,01580</b>	0,01617	0,01662	0,01726	0,01809	0,01912	0,02034	0,02179	0,02348
<b>0.85</b>	<b>0,01600</b>	0,01638	0,01686	0,01753	0,01840	0,01946	0,02074	0,02225	0,02401
<b>0.86</b>	<b>0,01620</b>	0,01660	0,01710	0,01780	0,01871	0,01982	0,02116	0,02273	0,02457
<b>0.87</b>	<b>0,01640</b>	0,01682	0,01734	0,01808	0,01903	0,02020	0,02160	0,02324	0,02516

**Table A.34** High-speed drag polare (part 2)

Mach	Lift coefficient								
	0,500	0,550	0,600	0,650	0,700	0,750	0,800	0,850	0,900
	Drag coefficient								
0.30	0,02311	0,02491	0,02689	0,02904	0,03136	0,03385	0,03652	0,03935	0,04236
0.35	0,02311	0,02491	0,02689	0,02904	0,03136	0,03385	0,03652	0,03935	0,04236
0.40	0,02311	0,02491	0,02689	0,02904	0,03136	0,03385	0,03652	0,03935	0,04236
0.45	0,02311	0,02491	0,02689	0,02904	0,03136	0,03385	0,03652	0,03935	0,04236
0.50	0,02311	0,02491	0,02689	0,02904	0,03136	0,03385	0,03652	0,03935	0,04236
0.55	0,02311	0,02491	0,02689	0,02904	0,03136	0,03385	0,03652	0,03935	0,04236
0.60	0,02311	0,02491	0,02689	0,02904	0,03136	0,03385	0,03652	0,03935	0,04236
0.65	0,02311	0,02491	0,02689	0,02904	0,03136	0,03385	0,03652	0,03935	
0.70	0,02316	0,02500	0,02704	0,02928	0,03174	0,03442	0,03735		
0.71	0,02320	0,02507	0,02716	0,02947	0,03203	0,03487	0,03801		
0.72	0,02324	0,02514	0,02727	0,02966	0,03232	0,03531	0,03866		
0.73	0,02328	0,02521	0,02739	0,02985	0,03262	0,03576	0,03932		
0.74	0,02332	0,02528	0,02751	0,03003	0,03291	0,03620			
0.75	0,02335	0,02535	0,02762	0,03022	0,03321	0,03665			
0.76	0,02339	0,02542	0,02774	0,03041	0,03350	0,03709			
0.77	0,02343	0,02549	0,02786	0,03060	0,03379	0,03754			
0.78	<b>0,02342</b>	<b>0,02547</b>	<b>0,02809</b>	0,03095	0,03428	0,03820			
0.79	<b>0,02355</b>	<b>0,02561</b>	<b>0,02830</b>	0,03143	0,03543				
0.80	<b>0,02366</b>	<b>0,02573</b>	<b>0,02856</b>	0,03178	0,03578				
0.81	<b>0,02390</b>	<b>0,02590</b>	0,02877	0,03189	0,03569				
0.82	<b>0,02418</b>	<b>0,02637</b>	0,02912	0,03219	0,03587				
0.83	0,02489	0,02713	0,02977	0,03292	0,03668				
0.84	0,02546	0,02778	0,03051	0,03375	0,03761				
0.85	0,02607	0,02847	0,03129	0,03463	0,03861				
0.86	0,02671	0,02921	0,03213	0,03558	0,03968				
0.87	0,02740	0,03000	0,03304	0,03661	0,04084				

**Table A.35** High-speed drag polare (part 3)

Mach	Lift coefficient	
	0,950	1,000
	Drag coefficient	
0.30	0,04554	0,04889
0.35	0,04554	0,04889
0.40	0,04554	0,04889
0.45	0,04554	0,04889
0.50	0,04554	
0.55	0,04554	

## Appendix B - Flowcharts of the Programs

### B.1 Flowcharts of Straubinger's Program

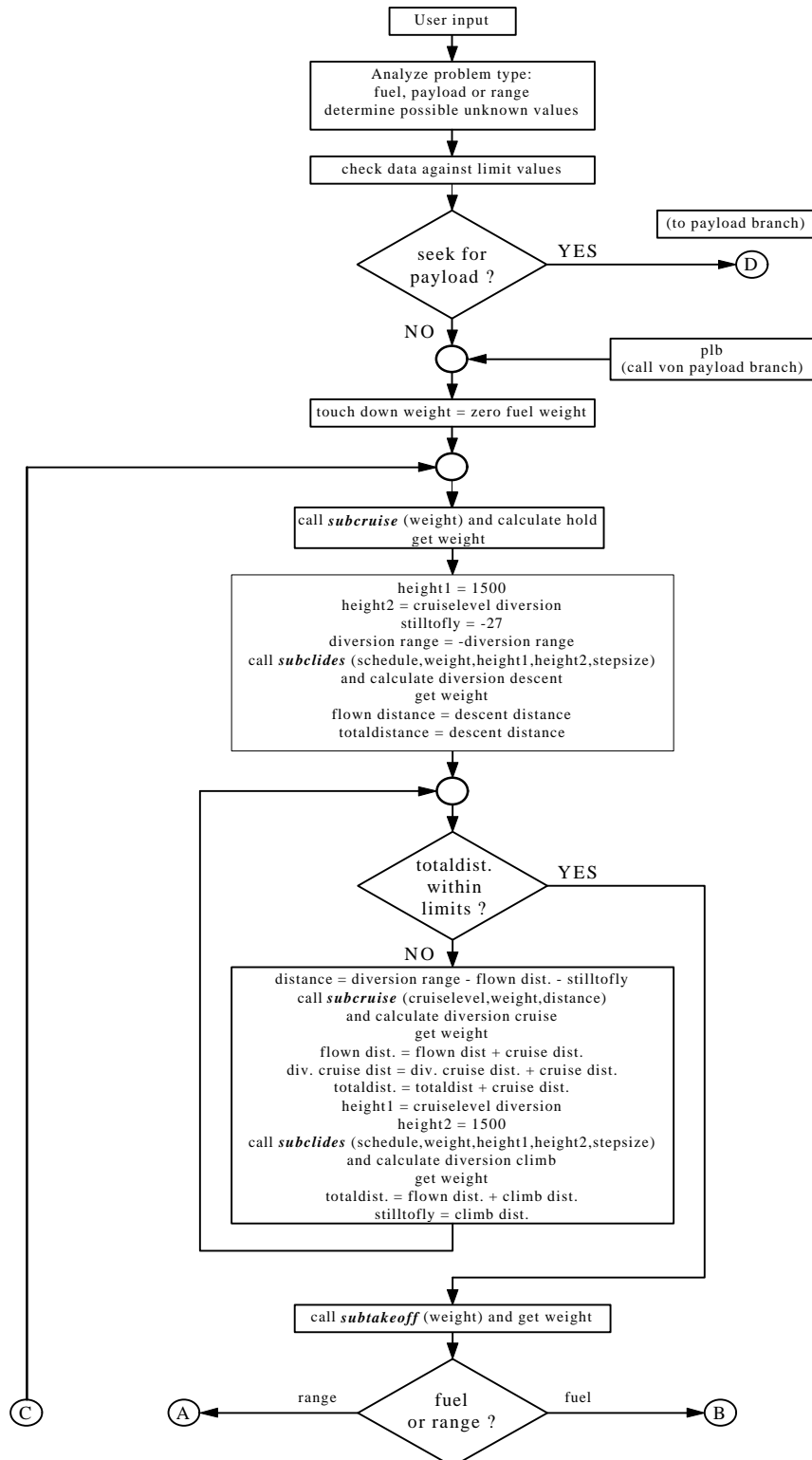


Figure B.1 Flowchart of main macro (Diversions for fuel and range calculation) (Straubinger, 2000a)

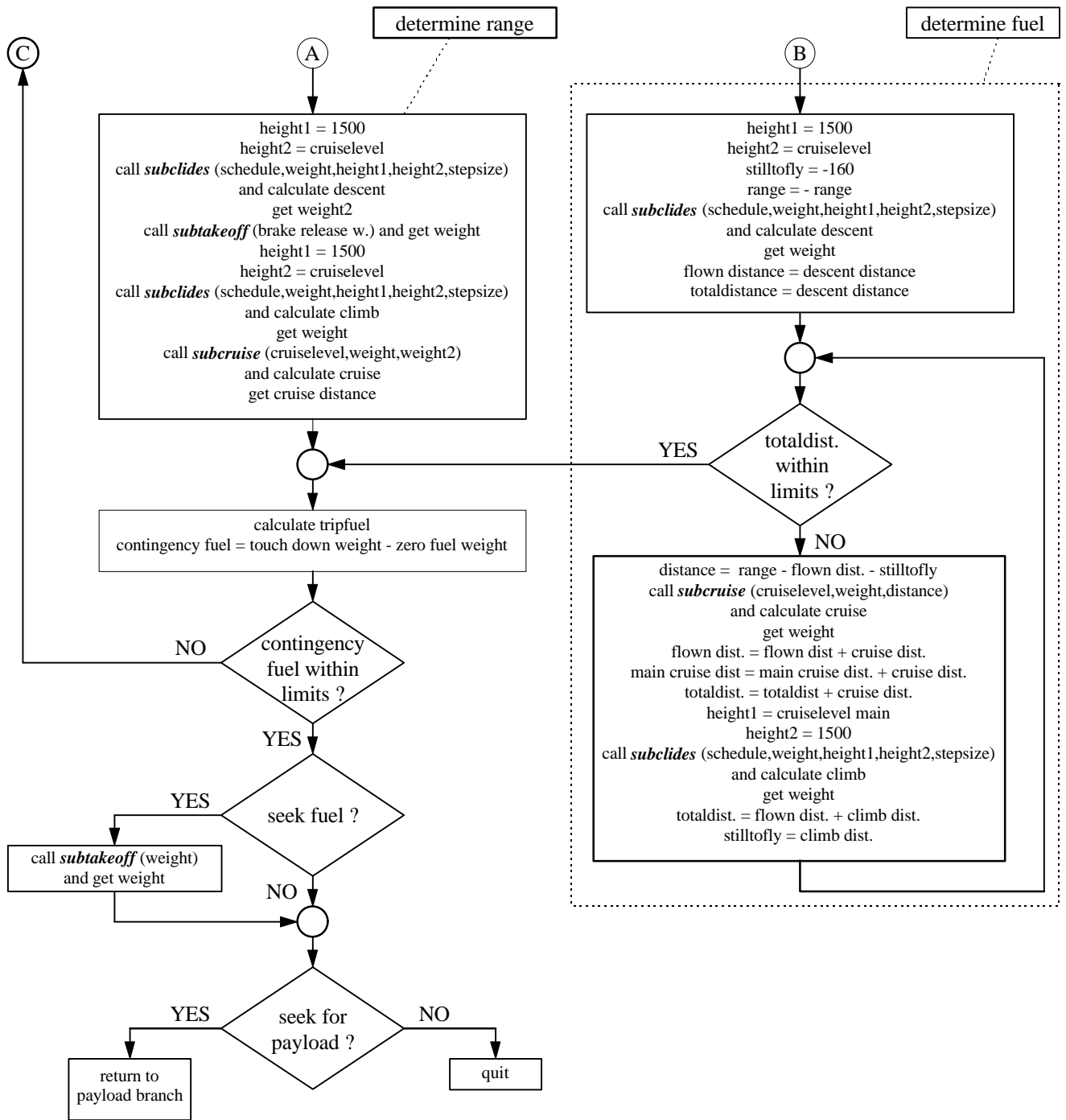


Figure B.2 Flowchart of main macro (Fuel and range calculation) (Straubinger, 2000a)

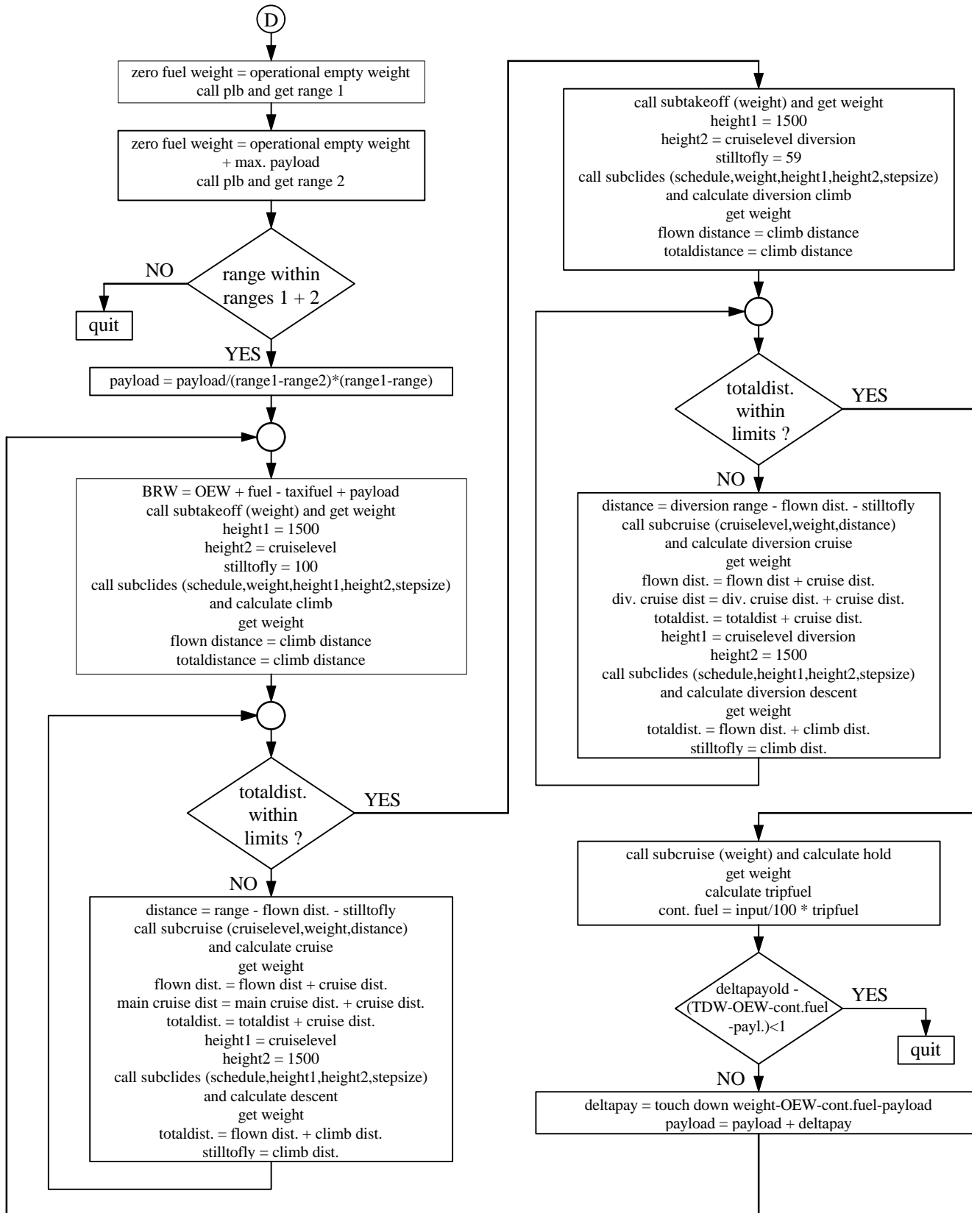


Figure B.3 Flowchart of main macro (Calculation of payload) (Straubinger, 2000a)

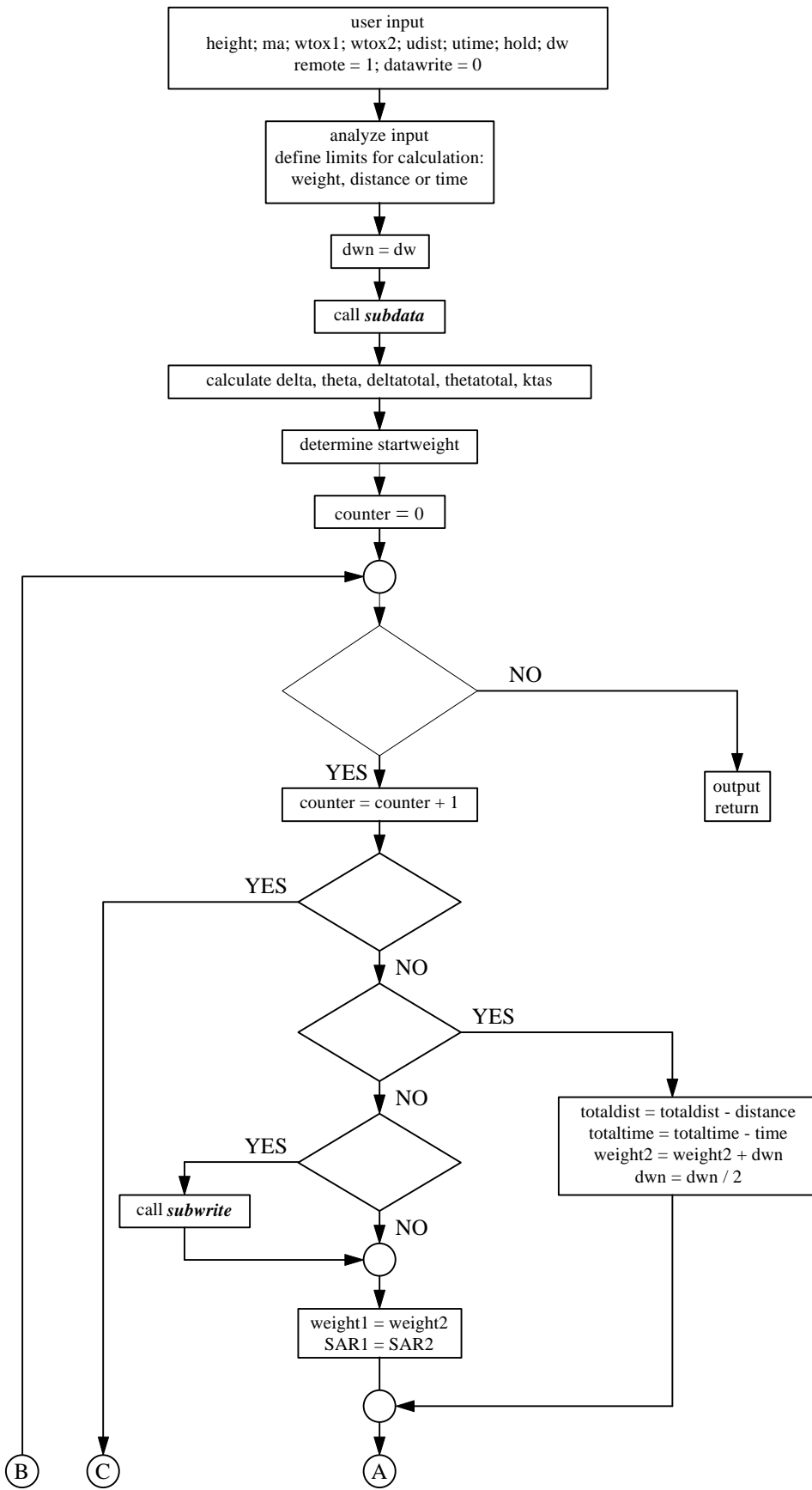
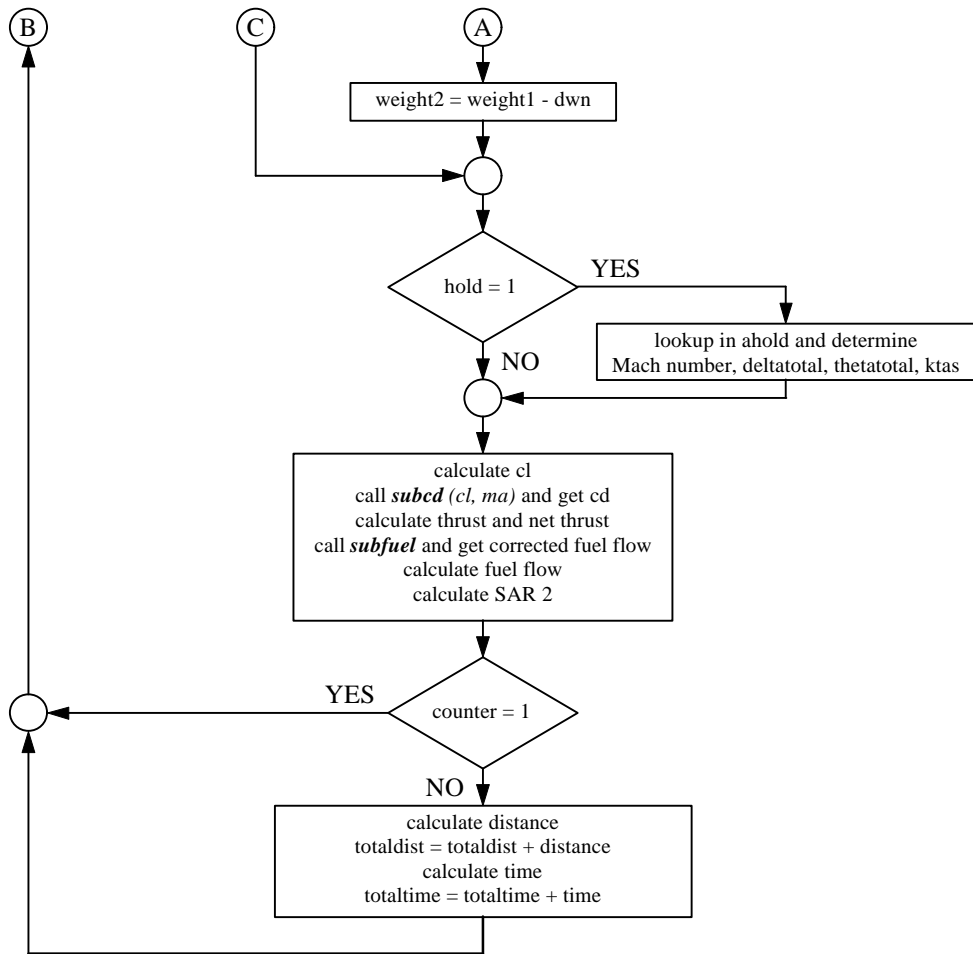


Figure B.4... Flowchart of macro for cruise calculation *subcruise* (Straubinger, 2000a)



**Figure B.5** Flowchart of macro for cruise calculation *subcruise* (Straubinger, 2000a)

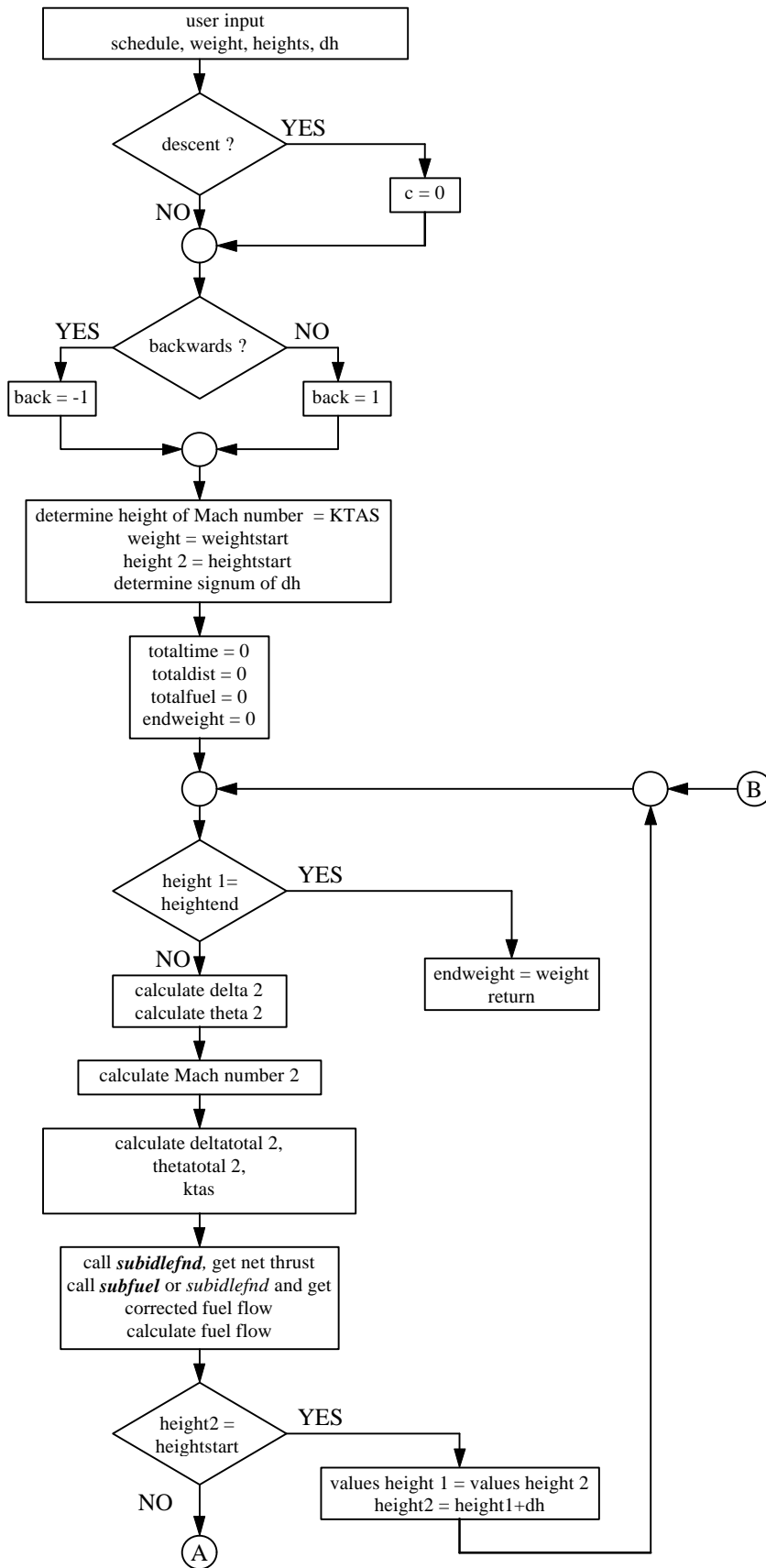
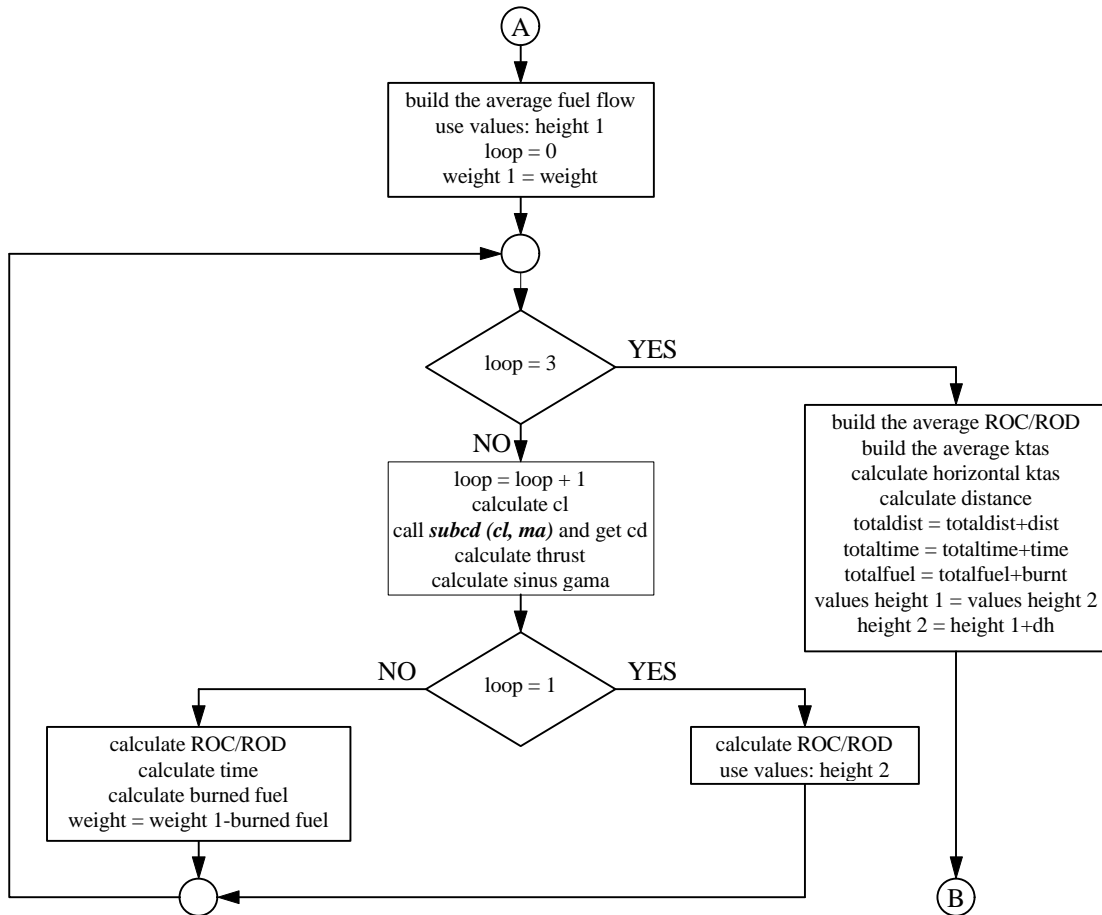
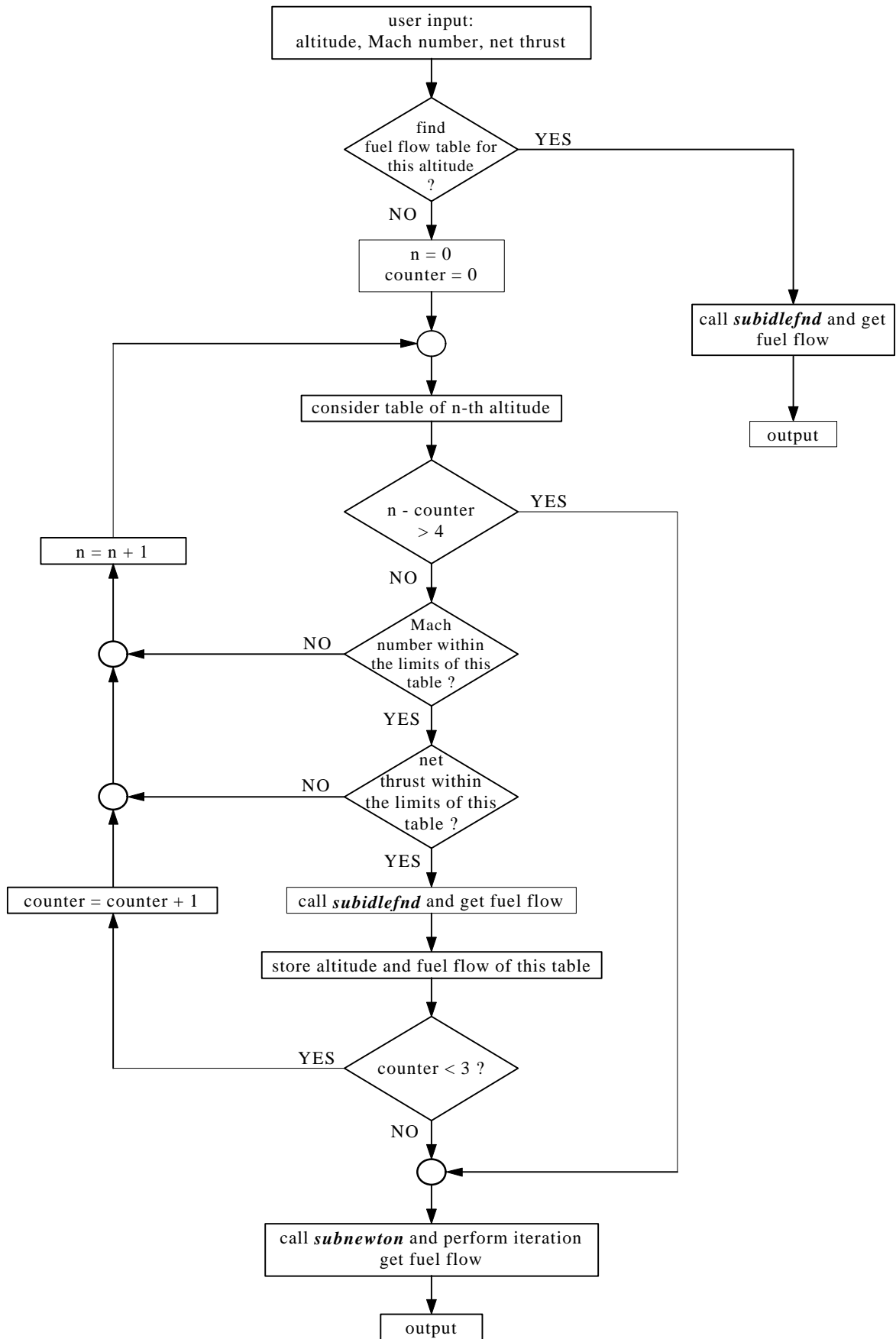


Figure B.6 Flowchart of macro for climb and descent *subclides* (Straubinger, 2000a)





**Figure B.7** Flowchart of macro for climb and descent *subclides* (Straubinger, 2000a)



**Figure B.8** Flowchart of *subfuel* (controls the interpolation of fuel flow) (Straubinger, 2000a)

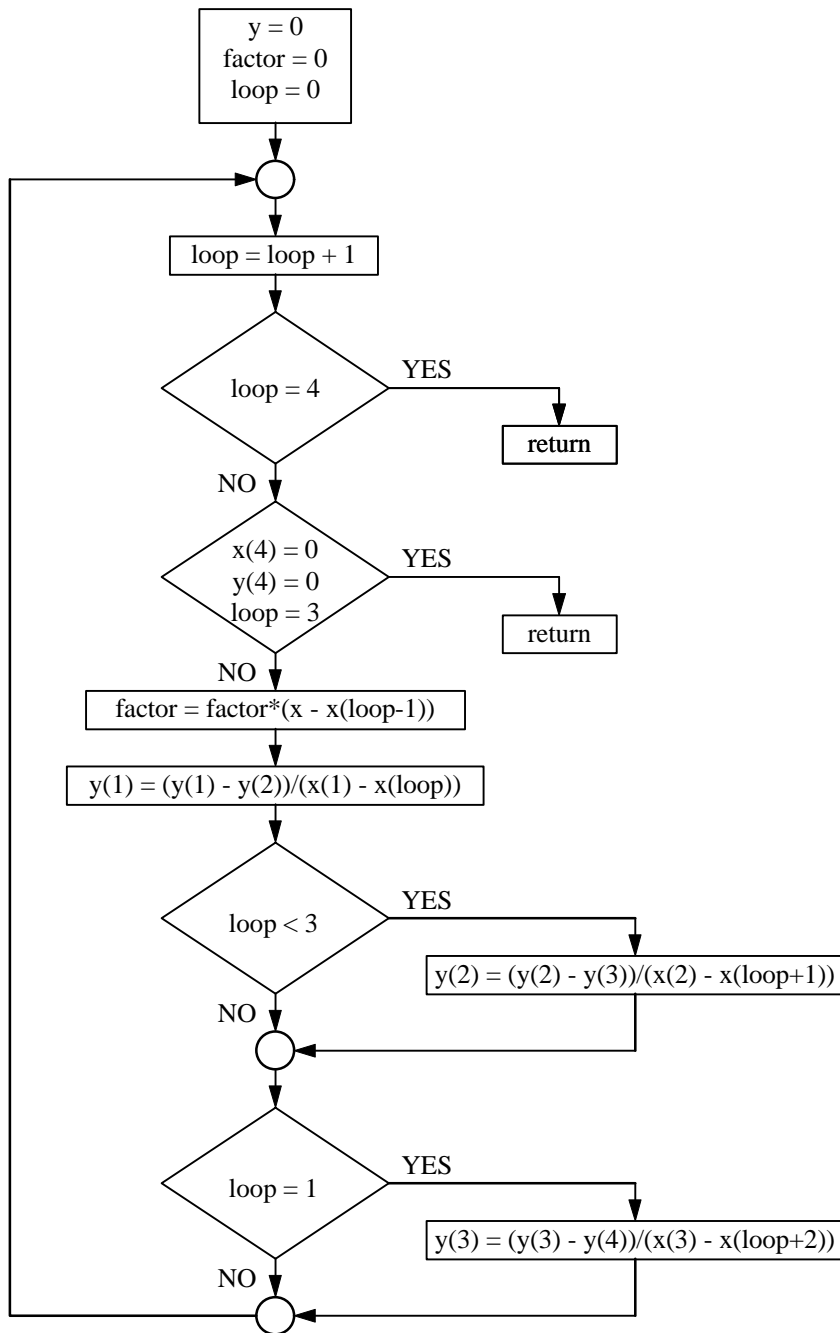


**Figure B.9** Flowchart of Newton's interpolation *subnewton* (Straubinger, 2000a)

Flowcharts for the macros *subidlefnd*, *subcd* and *subtakeoff* are not provided, since they consist of simple linear interpolations. (Straubinger, 2000a)

## B.2 Simple Flowchart of Young's Program

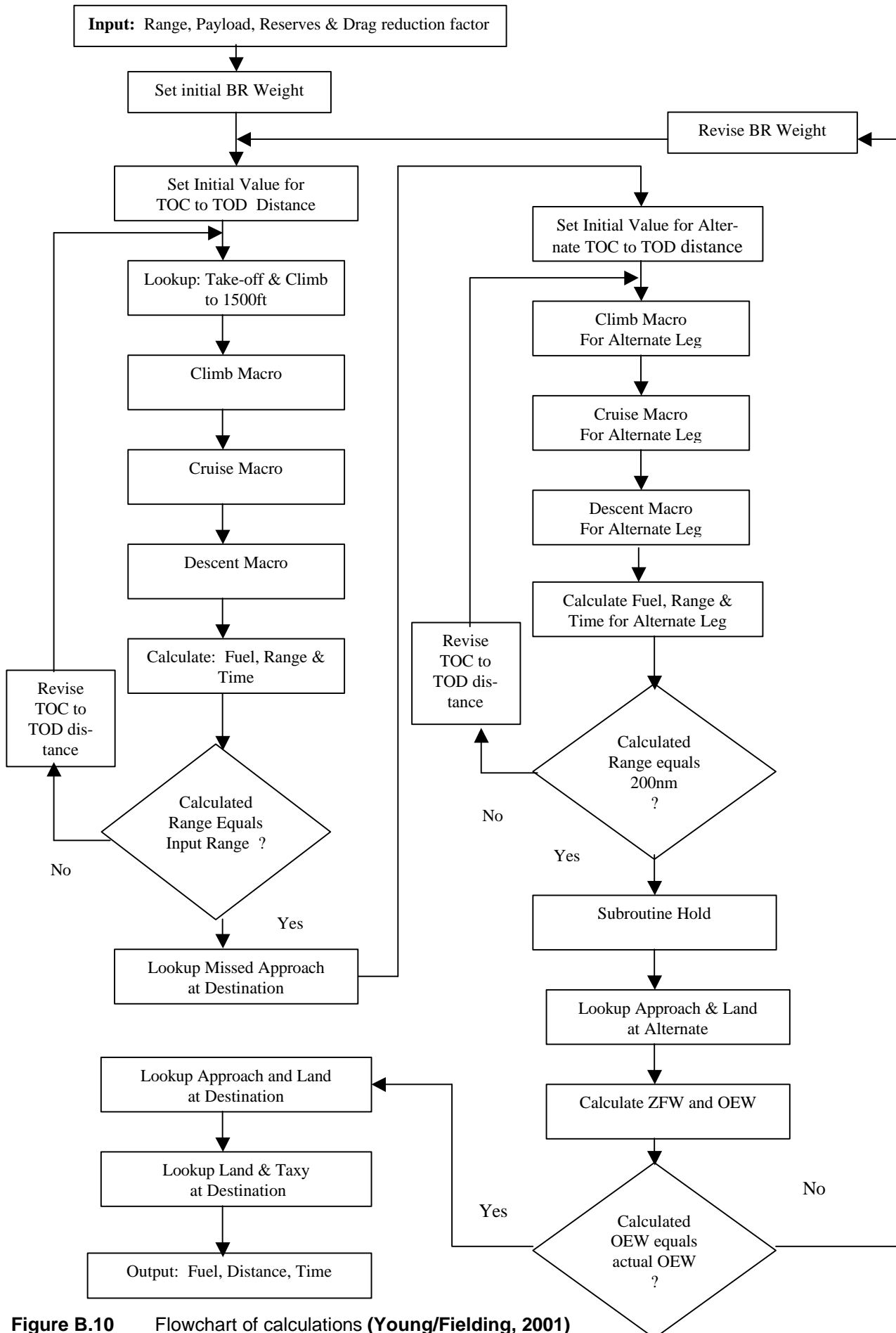


Figure B.10 Flowchart of calculations (Young/Fielding, 2001)

## Appendix C

### Original Example of Operating Manual A 330

#### C.1 Original Example for LR speed

<b>A330</b> <small>FLIGHT CREW OPERATING MANUAL</small>	<b>FLIGHT PLANNING</b>	2.05.15	P 5
	CALCULATION TABLES	SEQ 147	REV 09

#### Example

##### DATA

- T/O weight : 440 000 lb
- Ground distance to destination : 4000 NM
- Wind : - 40 kt (head wind)
- Selected initial FL : 310
- Long range speed
- Temperature : ISA + 10
- Airport elevation : 1500 ft
- Normal air conditioning

##### DETERMINATION OF CRUISE FUEL AND TIME

- A : Enter the chosen flight Mach number, flight level, ground distance to be covered and forecast windspeed in the calculation table of page 7.  
Calculate the air distance (see 2.05.60 p 6)  
here : long range speed, 40 kt head wind, 4000 NM ground distance → air distance : 4380 NM
- CRUISE TABLE FL310**
- B : Read from integrated cruise table (Long range speed, FL310) the values for time and distance for a weight of 440 000 lb (see 2.05.30 p 30)  
R → distance : 6397 NM → time : 937 min.
- C : After 250 NM a step climb to FL350 is performed.  
Calculate the new value of the distance in the integrated cruise table  
R → 6397 - 250 = 6147 NM
- R D : Enter integrated cruise table and interpolate the values for the distance of 6147 NM (begin of first step climb)  
R → weight : 432 889 lb → time : 905 min.
- R E : Calculate the values for the first cruise segment  
R Fuel : 440 000 - 432 889 = 7111 lb  
R Distance : 250 NM  
R Time : 937 - 905 = 32 min  
Remaining distance : 4380 - 250 = 4130 NM
- CRUISE TABLE FL350**
- R F : Read from integrated cruise table (Long range speed, FL350) the values for time and distance for the weight of 432 889 lb (see 2.05.30 p 36)  
R → distance : 6534 NM → time : 892 min.
- R G : The optimum aircraft weight to proceed to FL390 is 426 000 lb (2.05.20 p 1).  
Read from integrated cruise table the values for time and distance for the weight of 426 000 lb  
R → distance : 6276 NM → time : 859 min.
- R H : Calculate the values for the second cruise segment  
R Fuel : 432 889 - 426 000 = 6889 lb  
R Distance : 6534 - 6276 = 258 NM  
R Time : 892 - 859 = 33 min  
R Remaining distance : 4130 - 258 = 3872 NM

Figure C.1 Description of cruise fuel and time determination (part 1) (Operating Manual)

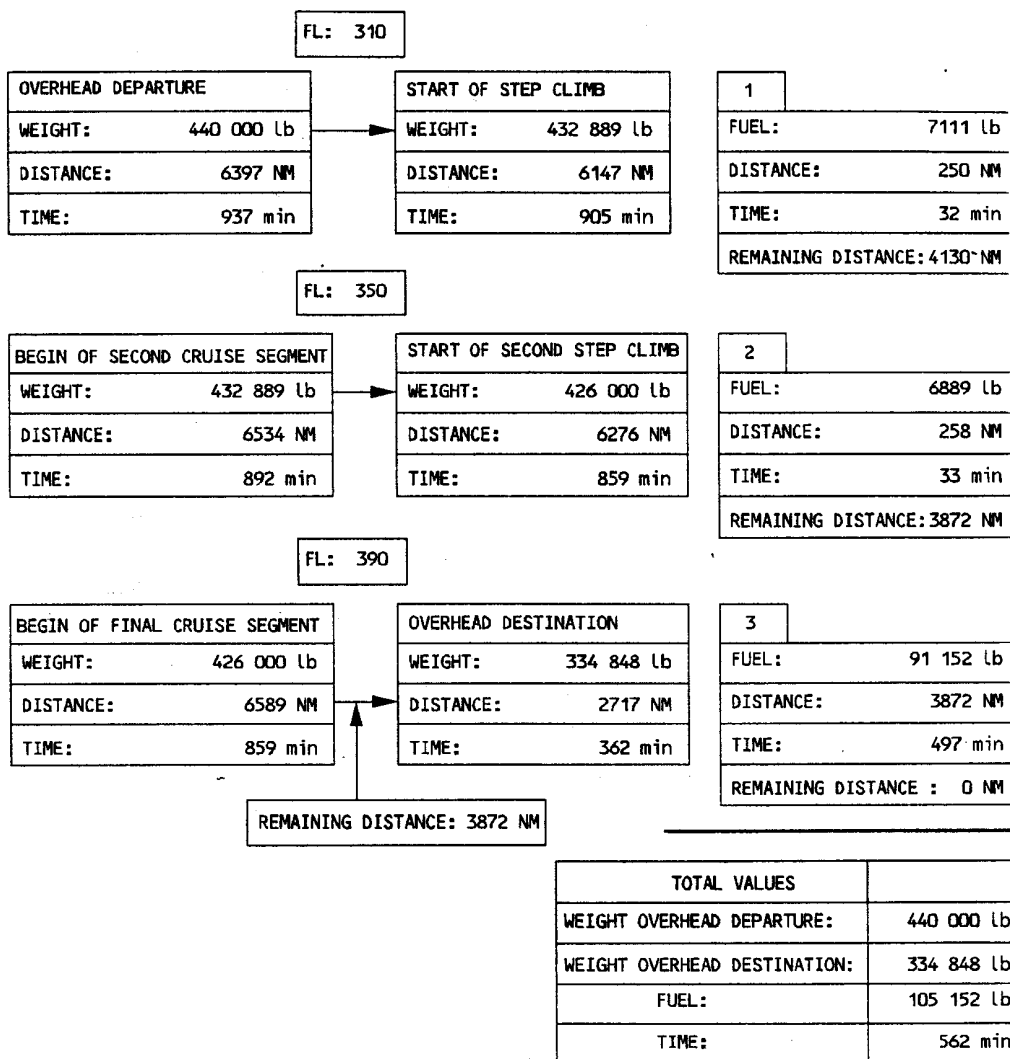
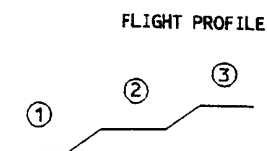
<b>A330</b> <small>FLIGHT CREW OPERATING MANUAL</small>	<b>FLIGHT PLANNING</b>	2.05.15	P 6
	CALCULATION TABLES	SEQ 147	REV 09

**CRUISE TABLE FL390**

- I : Proceed to final table ; enter distance and time values corresponding to an aircraft weight of 426 000 lb at FL390 and long range speed. (see 2.05.30 p 42)
- R → distance : 6589 NM → time : 859 min
- R J : Subtract remaining distance :  $6589 - 3872 = 2717$  NM
- K : Interpolate in integrated cruise table weight and time values corresponding to a distance of 2717 NM (see 2.05.30 p 41)
- R → weight : 334 848 lb → time : 362 min
- R L : Calculate values for last cruise segment :
- R Fuel :  $426\ 000 - 334\ 848 = 91\ 152$  lb
- R Distance :  $6589 - 2717 = 3872$  NM
- R Time :  $859 - 362 = 497$  min
- Cross-check that remaining air distance equals zero
- M : Fill in the final table with weight overhead departure (440 000 lb) and overhead destination (334 848 lb).
- R N : Calculate total values
- R Fuel :  $440\ 000 - 334\ 848 = 105\ 152$  lb
- R Time :  $32 + 33 + 497 = 562$  min = 9 h 22 min

**Figure C.2** Description of cruise fuel and time determination (part 2) **(Operating Manual)**

MACHNUMBER	LRC
INITIAL FLIGHT LEVEL:	FL310
GROUND DISTANCE:	4000 NM
WIND ('-' HEAD/'+' TAIL):	-40 KT
AIR DISTANCE:	4380 NM



6FC5-02-0515-007-A147AA

**Figure C.3** Table for cruise fuel and time determination (Operating Manual)

<b>A330</b> FLIGHT CREW OPERATING MANUAL	<b>FLIGHT PLANNING</b>	2.05.15	P 8
	CALCULATION TABLES	SEQ. 147	REV 09

- DATA** :
- TO weight : 440 000 lb
  - Ground distance to destination 4000 NM
  - Wind : – 40 kt (headwind)
  - Selected first flight level : FL310
  - Long range speed
  - Temperature : ISA + 10 along the whole flight profile
  - Airport elevation : 1500 ft
  - Normal air conditioning

**STEPS**

- 1 : Fill in Max TO weight → 440 000 lb
- 2 : Enter the integrated cruise table corresponding to chosen FL with TO weight at brake release point and calculate weight overhead destination (see 2.05.15 p7)  
Fill in → 334 848 lb
- R 3 : Apply temperature correction for given air distance  
 $4380 \text{ NM} \times 10^{\circ}\text{C} \times 0.022 \text{ lb}/^{\circ}\text{C}/\text{NM} = 964 \text{ lb}$
- 4 : Correction for air conditioning → here = 0
- 5 : Subtract climb correction for chosen FL (see 2.05.30 p47) → 5500 lb
- 6 : Add TO altitude correction  $0.9 \times 440 \times 1.5 = 594 \text{ lb}$
- 7 : Subtract value for step climb correction (see 2.05.30 p47)  $2 \times 350 = 700 \text{ lb}$
- R 8 : Calculate corrected weight overhead destination → 328 300 lb
- 9 : Enter weight overhead destination and find descent correction (including 6 min IFR) (see 2.05.30 p48) → 1600 lb
- R 10 : Calculate landing weight at destination → 329 900 lb
- R 11 : Alternate fuel e.g. 250 NM at FL310  
(see 2.05.50 p3) → 8859 lb
- R Landing weight at alternate  $330\,100 - 8859 = 321\,241 \text{ lb}$
- R Correction due to deviation from reference landing weight at alternate (see 2.05.50 p3)  $(321.3 - 310) \times 13 = 147 \text{ lb}$
- R Corrected alternate fuel  $8859 + 147 = 9006 \text{ lb}$  (~ 9000 lb)
- R 12 : Calculate alternate landing weight → 320 900 lb
- 13 : Subtract holding fuel : (Refer to 2.05.10 p2) → 5300 lb
- R 14 : Calculate weight at end of holding → 315 600 lb
- R 15 : Calculate trip fuel → 110 100 lb
- 16 : Subtract "en route" reserve (standard amount is 5 % of trip fuel → 5500 lb)
- R 17 : Calculate zero fuel weight → 310 100 lb
- 18–19 : Subtract dry operating weight to obtain maximum allowable payload
- 20–22 : Calculate block fuel
- 23–26 : Calculate flight time

**Figure C.4** Description of corrections and determination of end results (Operating Manual)



<b>A330</b> FLIGHT CREW OPERATING MANUAL	<b>FLIGHT PLANNING</b>	2.05.15	P 9
	CALCULATION TABLES	SEQ 147	REV 09

1	(1) Max TO Weight at BRAKE RELEASE	▶	4	4	0	•	0
2	WEIGHT Overhead Destination	▶	3	3	4	•	9
3	– Temperature Correction for CRUISE	–			1	•	0
4	+ Correction for Air Conditioning (+ for LO, – for HI)	+			0	•	0
5	– CLIMB correction	–			5	•	5
6	+ TO Altitude correction	+			0	•	6
7	– STEP CLIMB correction	–			0	•	7
8	= Corrected Weight Overhead Destination	=	3	2	8	•	3
9	+ DESCENT correction (including 6 min IFR)	+			1	•	6
10	(2) Landing Weight at Destination	=	3	2	9	•	9
11	– ALTERNATE Fuel	–			9	•	0
12	= ALTERNATE Landing Weight	=	3	2	0	•	9
13	– HOLDING	–			5	•	3
14	= Weight at END OF HOLDING	=	3	1	5	•	6
15	TRIP FUEL (1) – (2)		1	1	0	•	1
16	– “En Route” Reserve	–			5	•	5
17	(3) ZERO FUEL WEIGHT	=	3	1	0	•	1
18	– OPERATING WEIGHT EMPTY	–	2	5	9	•	6
19	= Max Allowable Payload	=		5	0	•	5

BLOCK FUEL CALCULATION							
20	Required Fuel (1) – (3)	▶	1	2	9	•	9
21	+ Taxi	+			0	•	7
22	= Block Fuel	=	1	3	0	•	6

FLIGHT TIME CALCULATION (H. MIN)							
23	Time from integrated Cruise Tables	▶		9	•	2	2
24	+ CLIMB Correction	+		0	•	0	6
25	+ DESCENT Correction (including 6 min IFR)	+		0	•	1	0
26	= Flight Time	=		9	•	3	8

- Note : Line 3 : temperature correction :*  
 $0.022 \text{ (lb/}^\circ\text{C/NM)} \times \Delta\text{ISA (}^\circ\text{C)} \times \text{air distance (NM)}$
- R *Line 4 : in case of low air conditioning refer to cruise table correction box.*
- R *Line 6 : TO altitude correction :*  
 $0.9 \text{ (lb/1000 lb/1000 ft)} \times \text{TOW (1000 lb)} \times \text{airport elevation (1000 ft)}$
- R *Line 10 : Check that landing weight at destination is lower than maximum landing weight.*
- R *Line 17 : Check that the zero fuel weight is lower than maximum zero fuel weight.*
- Line 22 : Check that the block fuel value is lower than maximum tank capacity*

**Figure C.5** Table of corrections and determination of end results (Operating Manual)

<b>A330</b> FLIGHT CREW OPERATING MANUAL	<b>FLIGHT PLANNING</b>		2.05.60	P 6
	GROUND DISTANCE/AIR DISTANCE		SEQ 001	REV 06

**LONG RANGE CRUISE ABOVE FL250**

GROUND DIST. (NM)	AIR DISTANCE (NM)						
	TAIL WIND		WIND COMPONENT (KT)			HEAD WIND	
	+150	+100	+ 50	0	-50	-100	-150
<b>10</b>	8	8	9	<b>10</b>	11	13	15
<b>20</b>	15	16	18	<b>20</b>	22	25	29
<b>30</b>	23	25	27	<b>30</b>	34	38	44
<b>40</b>	30	33	36	<b>40</b>	45	51	59
<b>50</b>	38	41	45	<b>50</b>	56	64	74
<b>100</b>	76	82	90	<b>100</b>	112	127	147
<b>200</b>	151	165	181	<b>200</b>	224	254	295
<b>300</b>	227	247	271	<b>300</b>	336	382	442
<b>400</b>	303	330	361	<b>400</b>	448	509	589
<b>500</b>	379	412	452	<b>500</b>	560	636	736
<b>1000</b>	757	824	903	<b>1000</b>	1120	1272	1473
<b>1500</b>	1136	1236	1355	<b>1500</b>	1680	1908	2209
<b>2000</b>	1514	1648	1807	<b>2000</b>	2240	2544	2945
<b>2500</b>	1893	2059	2258	<b>2500</b>	2799	3180	3681
<b>3000</b>	2271	2471	2710	<b>3000</b>	3359	3817	4418
<b>3500</b>	2650	2883	3162	<b>3500</b>	3919	4453	5154
<b>4000</b>	3028	3295	3613	<b>4000</b>	4479	5089	5890
<b>4500</b>	3407	3707	4065	<b>4500</b>	5039	5725	6627
<b>5000</b>	3785	4119	4517	<b>5000</b>	5599	6361	7363
<b>5500</b>	4164	4531	4968	<b>5500</b>	6159	6997	8099
<b>6000</b>	4542	4943	5420	<b>6000</b>	6719	7633	8836
<b>6500</b>	4921	5354	5872	<b>6500</b>	7279	8269	9572
<b>7000</b>	5299	5766	6324	<b>7000</b>	7839	8905	10308
<b>7500</b>	5678	6178	6775	<b>7500</b>	8398	9541	11044
<b>8000</b>	6056	6590	7227	<b>8000</b>	8958	10177	11781
<b>8500</b>	6435	7002	7679	<b>8500</b>	9518	10814	12517
<b>9000</b>	6813	7414	8130	<b>9000</b>	10078	11450	13253
<b>9500</b>	7192	7826	8582	<b>9500</b>	10638	12086	13990
<b>10000</b>	7570	8238	9034	<b>10000</b>	11198	12722	14726

FLIP22E A330-322 PW4168 3110 03701.000011 0250300 .8101 .000000 0 0300350 0 0 220200 90164 18590 FCOM-GO-02-05-60-005-001

Figure C.6 Table for corrections due to wind effects (Operating Manual)

<b>A330</b> <small>FLIGHT CREW OPERATING MANUAL</small>	<b>FLIGHT PLANNING</b>	2.05.30	P 29
	<b>INTEGRATED CRUISE</b>	SEQ 147	REV 09

<b>INTEGRATED CRUISE</b>												
MAX. CRUISE THRUST LIMITS NORMAL AIR CONDITIONING ANTI-ICING OFF				ISA CG=37.0%		DISTANCE (NM) TIME (MIN)		<b>LR FL 310</b>				
WEIGHT (1000LB)	0	.5	1.0	1.5	2.0	2.5	3.0	3.5	4.0	4.5	TAS (KT)	
<b>280</b>	0 0	23 4	46 8	69 11	92 15	115 19	138 23	160 26	183 30	206 34	366	
<b>285</b>	229 37	252 41	274 45	297 49	320 52	343 56	365 60	388 63	411 67	433 71	367	
<b>290</b>	456 74	478 78	501 82	524 85	546 89	569 93	591 96	614 100	636 104	658 107	369	
<b>295</b>	681 111	703 115	726 118	748 122	770 126	793 129	815 133	837 136	860 140	882 144	370	
<b>300</b>	904 147	926 151	949 154	971 158	993 161	1015 165	1037 169	1059 172	1081 176	1103 179	371	
<b>305</b>	1125 183	1147 186	1169 190	1191 193	1213 197	1235 200	1257 204	1279 207	1301 211	1323 214	374	
<b>310</b>	1344 218	1366 221	1388 225	1410 228	1431 232	1453 235	1475 238	1496 242	1518 245	1540 249	377	
<b>315</b>	1561 252	1583 256	1604 259	1626 262	1647 266	1669 269	1690 273	1712 276	1733 279	1755 283	379	
<b>320</b>	1776 286	1797 289	1819 293	1840 296	1861 299	1882 303	1904 306	1925 309	1946 313	1967 316	381	
<b>325</b>	1988 319	2010 323	2031 326	2052 329	2073 333	2094 336	2115 339	2136 342	2157 346	2178 349	384	
<b>330</b>	2199 352	2220 355	2241 359	2262 362	2282 365	2303 368	2324 372	2345 375	2366 378	2386 381	387	
<b>335</b>	2407 384	2428 388	2449 391	2469 394	2490 397	2510 400	2531 403	2552 406	2572 410	2593 413	391	
<b>340</b>	2613 416	2634 419	2654 422	2675 425	2695 428	2716 431	2736 434	2756 437	2777 440	2797 443	396	
<b>345</b>	2818 447	2838 450	2858 453	2878 456	2899 459	2919 462	2939 465	2959 468	2979 471	2999 473	402	
<b>350</b>	3020 476	3040 479	3060 482	3080 485	3100 488	3120 491	3140 494	3160 497	3180 500	3200 503	408	
<b>355</b>	3220 505	3240 508	3259 511	3279 514	3299 517	3319 520	3339 522	3359 525	3378 528	3398 531	421	
<b>360</b>	3418 533	3438 536	3457 539	3477 542	3497 544	3516 547	3536 550	3556 553	3575 555	3595 558	429	
<b>365</b>	3614 561	3634 564	3654 566	3673 569	3693 572	3712 574	3732 577	3751 580	3771 582	3790 585	432	
<b>370</b>	3810 588	3829 591	3848 593	3868 596	3887 599	3907 601	3926 604	3945 607	3965 609	3984 612	433	
<b>375</b>	4003 615	4023 617	4042 620	4061 623	4081 625	4100 628	4119 631	4138 633	4158 636	4177 639	435	
<b>380</b>	4196 641	4215 644	4234 647	4254 649	4273 652	4292 654	4311 657	4330 660	4349 662	4368 665	436	
<b>385</b>	4387 668	4406 670	4426 673	4445 675	4464 678	4483 681	4502 683	4521 686	4540 689	4558 691	438	
<b>390</b>	4577 694	4596 696	4615 699	4634 701	4653 704	4672 707	4691 709	4709 712	4728 714	4747 717	440	
<b>395</b>	4766 719	4785 722	4803 725	4822 727	4841 730	4860 732	4878 735	4897 737	4916 740	4934 742	440	
<b>PACK FLOW LO</b>			<b>PACK FLOW HI OR/ AND CARGO COOL ON</b>			<b>ENGINE ANTI ICE ON</b>			<b>TOTAL ANTI ICE ON</b>			
$\Delta$ FUEL = - 0.4 %			$\Delta$ FUEL = + 1 %			$\Delta$ FUEL = + 1.5 %			$\Delta$ FUEL = + 6 %			

11.1-08FOA330-223 PW4168A 22200000C5LB370 0 018590 0 0 1.0 .0 .00 03101 .990 .000 .000 0 FCOM-02-05-30-029-077

Figure C.7 Integrated cruise table for LR at FL310 (part 1) (Operating Manual)

<b>A330</b> <small>FLIGHT CREW OPERATING MANUAL</small>	<b>FLIGHT PLANNING</b>		2.05.30	P 30
	<b>INTEGRATED CRUISE</b>		SEQ 147	REV 09

<b>INTEGRATED CRUISE</b>												
MAX. CRUISE THRUST LIMITS NORMAL AIR CONDITIONING ANTI-ICING OFF				ISA CG=37.0%		DISTANCE (NM) TIME (MIN)		<b>LR FL 310</b>				
WEIGHT (1000LB)	0	.5	1.0	1.5	2.0	2.5	3.0	3.5	4.0	4.5	TAS (KT)	
<b>400</b>	4953 745	4971 747	4990 750	5009 752	5027 755	5046 757	5064 760	5083 762	5101 765	5120 767	442	
<b>405</b>	5138 770	5157 772	5175 775	5194 777	5212 780	5231 782	5249 785	5267 787	5286 790	5304 792	445	
<b>410</b>	5322 795	5341 797	5359 800	5377 802	5396 805	5414 807	5432 809	5450 812	5469 814	5487 817	447	
<b>415</b>	5505 819	5523 822	5541 824	5559 826	5578 829	5596 831	5614 834	5632 836	5650 839	5668 841	449	
<b>420</b>	5686 843	5704 846	5722 848	5740 851	5758 853	5776 855	5794 858	5812 860	5830 862	5848 865	451	
<b>425</b>	5866 867	5884 870	5902 872	5919 874	5937 877	5955 879	5973 881	5991 884	6009 886	6026 889	452	
<b>430</b>	6044 891	6062 893	6080 896	6097 898	6115 900	6133 903	6151 905	6168 907	6186 910	6203 912	454	
<b>435</b>	6221 914	6239 917	6256 919	6274 921	6292 923	6309 926	6327 928	6344 930	6362 933	6379 935	455	
<b>440</b>	6397 937	6414 940	6432 942	6449 944	6467 946	6484 949	6502 951	6519 953	6536 956	6554 958	457	
<b>445</b>	6571 960	6588 962	6606 965	6623 967	6640 969	6658 971	6675 974	6692 976	6710 978	6727 981	459	
<b>450</b>	6744 983	6761 985	6779 987	6796 989	6813 992	6830 994	6847 996	6864 998	6881 1001	6899 1003	460	
<b>455</b>	6916 1005	6933 1007	6950 1010	6967 1012	6984 1014	7001 1016	7018 1018	7035 1021	7052 1023	7069 1025	462	
<b>460</b>	7086 1027	7103 1029	7120 1032	7137 1034	7154 1036	7171 1038	7188 1040	7205 1043	7221 1045	7238 1047	463	
<b>465</b>	7255 1049	7272 1051	7289 1053	7306 1056	7323 1058	7339 1060	7356 1062	7373 1064	7390 1066	7406 1069	465	
<b>470</b>	7423 1071	7440 1073	7457 1075	7473 1077	7490 1079	7507 1081	7523 1084	7540 1086	7556 1088	7573 1090	466	
<b>475</b>	7590 1092	7606 1094	7623 1096	7639 1099	7656 1101	7673 1103	7689 1105	7706 1107	7722 1109	7739 1111	467	
<b>480</b>	7755 1113	7772 1115	7788 1118	7805 1120	7821 1122	7837 1124	7854 1126	7870 1128	7887 1130	7903 1132	469	
<b>485</b>	7919 1134	7936 1136	7952 1139	7968 1141	7985 1143	8001 1145	8017 1147	8034 1149	8050 1151	8066 1153	470	
<b>490</b>	8082 1155	8099 1157	8115 1159	8131 1161	8147 1163	8164 1165	8180 1168	8196 1170	8212 1172	8228 1174	471	
<b>495</b>	8244 1176	8260 1178	8277 1180	8293 1182	8309 1184	8325 1186	8341 1188	8357 1190	8373 1192	8389 1194	471	
<b>500</b>	8405 1196	8421 1198	8437 1200	8453 1202	8469 1204	8485 1206	8501 1208	8517 1210	8532 1212	8548 1214	472	
<b>505</b>	8564 1216	8580 1218	8596 1220	8612 1222	8628 1224	8643 1226	8659 1228	8675 1230	8691 1232	8707 1234	473	
<b>510</b>	8722 1236	8738 1238	8754 1240	8769 1242	8785 1244	8801 1246	8817 1248	8832 1250	8848 1252	8864 1254	473	
<b>515</b>	8879 1256	8895 1258	8910 1260	8926 1262	8942 1264	8957 1266	8973 1268	8988 1270	9004 1272	9019 1274	474	
PACK FLOW LO $\Delta$ FUEL = - 0.4 %			PACK FLOW HI OR/ AND CARGO COOL ON $\Delta$ FUEL = + 1 %			ENGINE ANTI ICE ON $\Delta$ FUEL = + 1.5 %			TOTAL ANTI ICE ON $\Delta$ FUEL = + 6 %			

11.1-08FOA330-223 PW4168A 2220000C5LB370 0 018590 0 0 1 1.0 .00 03101 .990 .000 .000 0 FCOM-02-05-30-030-077

Figure C.8 Integrated cruise table for LR at FL310 (part 2) (Operating Manual)

<b>A330</b> <small>FLIGHT CREW OPERATING MANUAL</small>	<b>FLIGHT PLANNING</b> INTEGRATED CRUISE	2.05.30    P 31
		SEQ 147    REV 09

INTEGRATED CRUISE												
MAX. CRUISE THRUST LIMITS NORMAL AIR CONDITIONING ANTI-ICING OFF				ISA CG=37.0%		DISTANCE (NM) TIME (MIN)		LR FL 310				TAS (KT)
WEIGHT (1000LB)	0	.5	1.0	1.5	2.0	2.5	3.0	3.5	4.0	4.5	TAS (KT)	
<b>520</b>	9140 1293	9156 1295	9171 1297	9187 1299	9202 1301	9218 1303	9233 1305	9249 1307	9264 1309	9279 1311	475	
<b>525</b>	9295 1313	9310 1315	9326 1317	9341 1319	9356 1321	9372 1322	9387 1324	9402 1326	9417 1328	9433 1330	476	
<b>530</b>	9448 1332	9463 1334	9479 1336	9494 1338	9509 1340	9524 1342	9539 1344	9555 1346	9570 1347	9585 1349	476	
<b>535</b>	9600 1351										476	
<b>540</b>												
<b>545</b>												
<b>550</b>												
PACK FLOW LO $\Delta$ FUEL = - 0.4 %			PACK FLOW HI OR/ AND CARGO COOL ON $\Delta$ FUEL = + 1 %			ENGINE ANTI ICE ON $\Delta$ FUEL = + 1.5 %		TOTAL ANTI ICE ON $\Delta$ FUEL = + 6 %				

11.1-08FOA330-223 PW4168A 22200000C5LB370 0 018590 0 0 1 1.0 .00 03101 .990 .000 .000 0 FCOM-02-05-30-031-077

Figure C.9 Integrated cruise table for LR at FL310 (part 3) (Operating Manual)

<b>A330</b> <small>FLIGHT CREW OPERATING MANUAL</small>	<b>FLIGHT PLANNING</b>		2.05.30	P 35
	<b>INTEGRATED CRUISE</b>		SEQ 147	REV 09

<b>INTEGRATED CRUISE</b>												
MAX. CRUISE THRUST LIMITS NORMAL AIR CONDITIONING ANTI-ICING OFF				ISA CG = 37.0%		DISTANCE (NM) TIME (MIN)		<b>LR FL 350</b>				TAS (KT)
WEIGHT (1000LB)	0	.5	1.0	1.5	2.0	2.5	3.0	3.5	4.0	4.5	TAS (KT)	
<b>280</b>	0 0	25 4	49 8	74 11	98 15	123 19	147 23	172 27	196 30	220 34	386	
<b>285</b>	245 38	269 41	293 45	318 49	342 52	366 56	390 60	414 63	438 67	462 71	393	
<b>290</b>	486 74	510 78	535 81	558 85	582 89	606 92	630 96	654 99	678 103	702 106	401	
<b>295</b>	725 110	749 113	773 116	797 120	820 123	844 127	867 130	891 133	915 137	938 140	415	
<b>300</b>	962 143	985 147	1009 150	1032 153	1055 157	1079 160	1102 163	1126 167	1149 170	1172 173	422	
<b>305</b>	1196 177	1219 180	1242 183	1266 186	1289 190	1312 193	1335 196	1358 200	1382 203	1405 206	424	
<b>310</b>	1428 209	1451 213	1474 216	1497 219	1520 222	1543 226	1566 229	1589 232	1612 235	1635 239	426	
<b>315</b>	1658 242	1681 245	1704 248	1727 251	1750 255	1773 258	1796 261	1819 264	1841 267	1864 271	426	
<b>320</b>	1887 274	1910 277	1932 280	1955 283	1978 287	2000 290	2023 293	2046 296	2068 299	2091 302	429	
<b>325</b>	2113 305	2136 309	2158 312	2181 315	2203 318	2226 321	2248 324	2271 327	2293 330	2315 333	431	
<b>330</b>	2338 337	2360 340	2382 343	2405 346	2427 349	2449 352	2471 355	2494 358	2516 361	2538 364	434	
<b>335</b>	2560 367	2582 370	2604 373	2626 376	2648 379	2670 382	2692 385	2714 388	2736 391	2758 394	437	
<b>340</b>	2780 397	2802 400	2824 403	2846 406	2868 409	2890 412	2911 415	2933 418	2955 421	2977 424	439	
<b>345</b>	2998 427	3020 430	3042 433	3063 436	3085 439	3107 442	3128 445	3150 448	3171 450	3193 453	442	
<b>350</b>	3214 456	3236 459	3257 462	3279 465	3300 468	3322 471	3343 474	3365 477	3386 479	3407 482	444	
<b>355</b>	3429 485	3450 488	3471 491	3493 494	3514 497	3535 500	3556 502	3577 505	3599 508	3620 511	446	
<b>360</b>	3641 514	3662 517	3683 519	3704 522	3725 525	3746 528	3767 531	3788 533	3809 536	3830 539	448	
<b>365</b>	3851 542	3872 545	3893 547	3914 550	3935 553	3956 556	3977 559	3998 561	4018 564	4039 567	449	
<b>370</b>	4060 570	4081 572	4101 575	4122 578	4143 581	4163 583	4184 586	4205 589	4225 592	4246 594	451	
<b>375</b>	4267 597	4287 600	4308 602	4328 605	4349 608	4369 611	4390 613	4410 616	4431 619	4451 621	454	
<b>380</b>	4471 624	4492 627	4512 629	4533 632	4553 635	4573 638	4594 640	4614 643	4634 646	4654 648	455	
<b>385</b>	4675 651	4695 653	4715 656	4735 659	4755 661	4775 664	4796 667	4816 669	4836 672	4856 675	457	
<b>390</b>	4876 677	4896 680	4916 682	4936 685	4956 688	4976 690	4996 693	5016 696	5036 698	5056 701	459	
<b>395</b>	5076 703	5096 706	5115 708	5135 711	5155 714	5175 716	5195 719	5214 721	5234 724	5254 726	461	
PACK FLOW LO $\Delta$ FUEL = - 0.4 %			PACK FLOW HI OR/ AND CARGO COOL ON $\Delta$ FUEL = + 1 %			ENGINE ANTI ICE ON $\Delta$ FUEL = + 1.5 %			TOTAL ANTI ICE ON $\Delta$ FUEL = + 6 %			

11.1-08FOA330-223 PW4168A 2220000C5LB370 0 018590 0 0 1 1.0 .0 .00 03501 .990 .000 .000 0 FCOM-02-05-30-035-077

Figure C.10 Integrated cruise table for LR at FL350 (part 1) (Operating Manual)

 FLIGHT CREW OPERATING MANUAL	<b>FLIGHT PLANNING</b>		2.05.30	P 36
	INTEGRATED CRUISE		SEQ 147	REV 09

INTEGRATED CRUISE												
MAX. CRUISE THRUST LIMITS NORMAL AIR CONDITIONING ANTI-ICING OFF			ISA CG=37.0%			DISTANCE (NM)		<b>LR FL 350</b>				
WEIGHT (1000LB)	0	.5	1.0	1.5	2.0	2.5	3.0	3.5	4.0	4.5	TAS (KT)	
<b>400</b>	5274 729	5293 732	5313 734	5333 737	5352 739	5372 742	5392 744	5411 747	5431 749	5450 752	462	
<b>405</b>	5470 755	5490 757	5509 760	5529 762	5548 765	5568 767	5587 770	5606 772	5626 775	5645 777	463	
<b>410</b>	5665 780	5684 782	5703 785	5723 787	5742 790	5761 792	5781 795	5800 797	5819 800	5838 802	463	
<b>415</b>	5858 805	5877 807	5896 810	5915 812	5934 815	5954 817	5973 820	5992 822	6011 824	6030 827	464	
<b>420</b>	6049 829	6068 832	6087 834	6106 837	6125 839	6144 842	6163 844	6182 846	6201 849	6219 851	465	
<b>425</b>	6238 854	6257 856	6276 859	6295 861	6314 863	6332 866	6351 868	6370 871	6389 873	6407 876	466	
<b>430</b>	6426 878	6445 880	6464 883	6482 885	6501 888	6519 890	6538 892	6557 895	6575 897	6594 899	467	
<b>435</b>	6612 902	6631 904	6649 907	6668 909	6686 911	6705 914	6723 916	6742 918	6760 921	6778 923	468	
<b>440</b>	6797 925	6815 928	6833 930	6852 933	6870 935	6888 937	6907 940	6925 942	6943 944	6961 947	468	
<b>445</b>	6980 949	6998 951	7016 954	7034 956	7052 958	7070 960	7088 963	7107 965	7125 967	7143 970	469	
<b>450</b>	7161 972	7179 974	7197 977	7215 979	7233 981	7251 984	7269 986	7287 988	7305 990	7322 993	469	
<b>455</b>	7340 995	7358 997	7376 1000	7394 1002	7412 1004	7429 1006	7447 1009	7465 1011	7483 1013	7501 1015	470	
<b>460</b>	7518 1018	7536 1020	7554 1022	7571 1025	7589 1027	7607 1029	7624 1031	7642 1034	7659 1036	7677 1038	470	
<b>465</b>	7695 1040	7712 1042	7730 1045	7747 1047	7765 1049	7782 1051	7800 1054	7817 1056	7834 1058	7852 1060	470	
<b>470</b>	7869 1063	7887 1065	7904 1067	7921 1069	7939 1071	7956 1074	7973 1076	7990 1078	8008 1080	8025 1082	470	
<b>475</b>	8042 1085	8059 1087	8077 1089	8094 1091	8111 1093	8128 1096	8145 1098	8162 1100	8179 1102	8196 1104	471	
<b>480</b>	8213 1106	8231 1109	8248 1111	8265 1113	8281 1115	8298 1117	8315 1119	8332 1122	8349 1124	8366 1126	472	
<b>485</b>	8383 1128	8400 1130	8417 1132	8433 1134	8450 1136	8467 1139	8484 1141	8500 1143	8517 1145	8534 1147	472	
<b>490</b>	8550 1149	8567 1151	8584 1153	8600 1156	8617 1158	8633 1160	8650 1162	8666 1164	8683 1166	8699 1168	473	
<b>495</b>	8716 1170	8732 1172	8749 1174	8765 1176	8781 1179	8798 1181	8814 1183	8830 1185	8847 1187	8863 1189	473	
<b>500</b>	8879 1191	8895 1193	8912 1195	8928 1197	8944 1199	8960 1201	8976 1203	8992 1205	9008 1207	9024 1209	473	
<b>505</b>	9040 1211	9056 1213	9072 1215	9088 1217	9104 1219	9120 1221	9136 1224	9152 1226	9168 1228	9184 1230	473	
<b>510</b>	9200 1232	9216 1234	9231 1236	9247 1238	9263 1240	9279 1242	9294 1244	9310 1246	9326 1248	9341 1250	473	
<b>515</b>	9357 1251										473	
PACK FLOW LO ΔFUEL = - 0.4 %			PACK FLOW HI OR/ AND CARGO COOL ON ΔFUEL = + 1 %			ENGINE ANTI ICE ON ΔFUEL = + 1.5 %			TOTAL ANTI ICE ON ΔFUEL = + 6 %			

11.1-08FOA330-223 PW4168A 2220000C5LB370 0 018590 0 0 1 1.0 .0 .00 03501 .990 .000 .000 0 FCOM-02-05-30-036-077

Figure C.11 Integrated cruise table for LR at FL350 (part 2) (Operating Manual)


<b>A330</b> <small>FLIGHT CREW OPERATING MANUAL</small>	<b>FLIGHT PLANNING</b>		2.05.30	P 41
	<b>INTEGRATED CRUISE</b>		SEQ 147	REV 09

<b>INTEGRATED CRUISE</b>												
MAX. CRUISE THRUST LIMITS NORMAL AIR CONDITIONING ANTI-ICING OFF			ISA CG=37.0%			DISTANCE (NM) TIME (MIN)		<b>LR FL 390</b>				TAS (KT)
WEIGHT (1000LB)	0	.5	1.0	1.5	2.0	2.5	3.0	3.5	4.0	4.5	TAS (KT)	
<b>280</b>	0 0	26 4	52 7	79 11	105 14	131 18	157 22	183 25	209 29	235 32	437	
<b>285</b>	261 36	287 39	313 43	339 46	364 50	390 53	416 57	442 60	468 64	493 67	440	
<b>290</b>	519 71	545 74	570 78	596 81	621 85	647 88	672 92	698 95	723 99	749 102	442	
<b>295</b>	774 105	800 109	825 112	850 116	876 119	901 122	926 126	951 129	977 133	1002 136	444	
<b>300</b>	1027 139	1052 143	1077 146	1102 149	1127 153	1152 156	1177 160	1202 163	1227 166	1252 170	447	
<b>305</b>	1277 173	1302 176	1326 179	1351 183	1376 186	1401 189	1426 193	1450 196	1475 199	1500 203	450	
<b>310</b>	1524 206	1549 209	1573 212	1598 216	1622 219	1647 222	1671 225	1696 229	1720 232	1745 235	452	
<b>315</b>	1769 238	1793 241	1818 245	1842 248	1866 251	1891 254	1915 257	1939 261	1963 264	1987 267	454	
<b>320</b>	2011 270	2036 273	2060 276	2084 280	2108 283	2132 286	2156 289	2180 292	2204 295	2228 298	457	
<b>325</b>	2251 302	2275 305	2299 308	2323 311	2347 314	2371 317	2394 320	2418 323	2442 326	2465 330	459	
<b>330</b>	2489 333	2513 336	2536 339	2560 342	2583 345	2607 348	2631 351	2654 354	2677 357	2701 360	460	
<b>335</b>	2724 363	2748 366	2771 369	2794 372	2818 375	2841 378	2864 381	2888 385	2911 388	2934 391	461	
<b>340</b>	2957 394	2980 397	3004 400	3027 403	3050 406	3073 409	3096 412	3119 414	3142 417	3165 420	462	
<b>345</b>	3188 423	3211 426	3233 429	3256 432	3279 435	3302 438	3325 441	3348 444	3370 447	3393 450	463	
<b>350</b>	3416 453	3438 456	3461 459	3484 462	3506 465	3529 468	3551 470	3574 473	3596 476	3619 479	465	
<b>355</b>	3641 482	3664 485	3686 488	3709 491	3731 494	3753 496	3776 499	3798 502	3820 505	3843 508	465	
<b>360</b>	3865 511	3887 514	3909 517	3931 519	3953 522	3976 525	3998 528	4020 531	4042 534	4064 536	466	
<b>365</b>	4086 539	4108 542	4130 545	4152 548	4174 551	4196 553	4217 556	4239 559	4261 562	4283 565	467	
<b>370</b>	4305 567	4326 570	4348 573	4370 576	4392 579	4413 581	4435 584	4457 587	4478 590	4500 592	467	
<b>375</b>	4521 595	4543 598	4564 601	4586 603	4607 606	4629 609	4650 612	4672 614	4693 617	4714 620	468	
<b>380</b>	4736 623	4757 625	4778 628	4799 631	4821 634	4842 636	4863 639	4884 642	4905 644	4926 647	468	
<b>385</b>	4948 650	4969 653	4990 655	5011 658	5032 661	5053 663	5074 666	5095 669	5116 671	5136 674	468	
<b>390</b>	5157 677	5178 679	5199 682	5220 685	5241 687	5261 690	5282 693	5303 695	5323 698	5344 701	469	
<b>395</b>	5365 703	5385 706	5406 708	5426 711	5447 714	5467 716	5488 719	5508 722	5529 724	5549 727	470	
PACK FLOW LO ΔFUEL = - 0.4 %			PACK FLOW HI OR/ AND CARGO COOL ON ΔFUEL = + 1 %			ENGINE ANTI ICE ON ΔFUEL = + 1.5 %		TOTAL ANTI ICE ON ΔFUEL = + 6 %				

11.1-08FOA330-223 PW4168A 2220000C5L8370 0 018590 0 0 1 1.0 .00 03901 .990 .000 .000 0 FCOM-02-05-30-041-077

Figure C.12 Integrated cruise table for LR at FL390 (part 1) (Operating Manual)



 <b>A330</b> FLIGHT CREW OPERATING MANUAL	<b>FLIGHT PLANNING</b>	2.05.30	P 42
	INTEGRATED CRUISE	SEQ 147	REV 09

<b>INTEGRATED CRUISE</b>											
MAX. CRUISE THRUST LIMITS NORMAL AIR CONDITIONING ANTI-ICING OFF				ISA CG=37.0%		DISTANCE (NM) TIME (MIN)			<b>LR FL 390</b>		
WEIGHT (1000LB)	0	.5	1.0	1.5	2.0	2.5	3.0	3.5	4.0	4.5	TAS (KT)
<b>400</b>	5569 729	5590 732	5610 734	5630 737	5651 740	5671 742	5691 745	5711 747	5731 750	5751 753	470
<b>405</b>	5771 755	5791 758	5811 760	5831 763	5851 765	5871 768	5891 770	5911 773	5931 775	5951 778	471
<b>410</b>	5971 780	5990 783	6010 785	6030 788	6049 790	6069 793	6089 796	6108 798	6128 800	6147 803	471
<b>415</b>	6167 805	6186 808	6206 810	6225 813	6245 815	6264 818	6283 820	6303 823	6322 825	6341 828	471
<b>420</b>	6361 830	6380 833	6399 835	6418 837	6437 840	6456 842	6475 845	6494 847	6513 850	6532 852	471
<b>425</b>	6551 854	6570 857	6589 859	6608 862	6626 864	6645 866	6664 869	6682 871	6701 874	6720 876	471
<b>430</b>	6738 878	6757 881	6776 883	6794 885	6812 888	6831 890	6849 892	6868 895	6886 897	6904 899	471
<b>435</b>	6923 902	6941 904	6959 906	6977 909	6996 911	7014 913	7032 916	7050 918	7068 920	7086 922	471
<b>440</b>	7104 925	7121 927	7139 929	7157 932	7175 934	7193 936	7210 938	7228 941			471
<b>445</b>											
<b>450</b>											
<b>455</b>											
PACK FLOW LO $\Delta$ FUEL = - 0.4 %			PACK FLOW HI OR/ AND CARGO COOL ON $\Delta$ FUEL = + 1 %			ENGINE ANTI ICE ON $\Delta$ FUEL = + 1.5 %			TOTAL ANTI ICE ON $\Delta$ FUEL = + 6 %		

11.1-08FOA330-223 PW4168A 2220000C5LB370 0 018590 0 0 1 1.0 .00 03901 .990 .000 0 FCOM-02-05-30-042-077

Figure C.13 Integrated cruise table for LR at FL390 (part 2) (Operating Manual)

<b>A330</b> FLIGHT CREW OPERATING MANUAL	<b>FLIGHT PLANNING</b>	2.05.30	P 47
	<b>INTEGRATED CRUISE</b>	SEQ 072	REV 07

### CLIMB CORRECTION

The planner must correct the values for the fuel and the time obtained from the integrated cruise tables with the numbers given in the following tables. The tables which are established for M.80, M.82, M.84 and long range speed take into account climbing from the brake release point at 250KT/300KT/M.80.

#### LONG RANGE SPEED

R

<b>CORRECTION ON FUEL CONSUMPTION (1000 lb)</b>													
FL	<b>WEIGHT AT BRAKE RELEASE (1000 lb)</b>												time correctio
	300	320	340	360	380	400	420	440	460	480	500	520	
<b>410</b>	4.7	5.0	5.3	5.5	5.7	5.9	—	—	—	—	—	—	5 min
<b>390</b>	4.5	4.8	5.1	5.3	5.6	5.9	6.1	—	—	—	—	—	5 min
<b>370</b>	4.3	4.6	4.8	5.1	5.4	5.7	6.0	6.2	6.4	—	—	—	5 min
<b>350</b>	4.1	4.4	4.7	4.9	5.2	5.4	5.7	6.0	6.2	6.5	6.5	—	6 min
<b>330</b>	4.0	4.2	4.4	4.7	5.0	5.2	5.4	5.7	6.0	6.3	6.4	6.7	6 min
<b>310</b>	3.8	4.0	4.2	4.5	4.7	5.0	5.2	5.5	5.7	6.0	6.3	6.5	6 min
<b>290</b>	3.5	3.8	4.0	4.2	4.5	4.7	4.9	5.2	5.3	5.7	5.9	6.2	5 min
<b>270</b>	3.3	3.5	3.8	4.0	4.2	4.4	4.6	4.9	5.1	5.4	5.6	5.8	5 min
<b>250</b>	3.1	3.3	3.5	3.7	3.9	4.2	4.3	4.6	4.8	5.0	5.3	5.5	4 min
<b>200</b>	2.6	2.8	2.9	3.1	3.3	3.4	3.4	3.8	4.0	4.2	4.5	4.7	3 min
<b>150</b>	2.1	2.2	2.4	2.5	2.7	2.8	3.0	3.1	3.3	3.5	3.6	3.8	3 min
<b>100</b>	1.5	1.6	1.7	1.8	1.9	2.0	2.2	2.3	2.4	2.5	2.6	2.8	2 min

#### CLIMB TO OPTIMUM FL

R

<b>CORRECTION ON FUEL CONSUMPTION (1000 lb)</b>													
FL	<b>WEIGHT AT BRAKE RELEASE (1000 lb)</b>												time correctio
	300	320	340	360	380	400	420	440	460	480	500	520	
<b>LRC</b>	4.7	5.0	5.3	5.5	5.6	5.9	5.9	6.2	6.2	6.5	6.4	6.5	6 min
<b>M.80</b>	4.7	5.0	5.3	5.6	5.7	5.9	6.0	6.2	6.3	6.5	6.6	6.6	6 min
<b>M.82</b>	4.7	5.0	5.3	5.5	5.8	5.9	6.1	6.2	6.4	6.5	6.6	6.6	6 min
<b>M.84</b>	4.5	4.8	5.0	5.1	5.3	5.4	5.6	5.7	5.9	5.9	6.6	6.1	6 min

### STEP CLIMB CORRECTION

When the flight includes one or more step climbs (2000 feet below FL290, 4000 feet above), apply a correction of 350 lb per step climb to the fuel consumption.

Figure C.14 Climb correction tables (Operating Manual)

<b>A330</b> <small>FLIGHT CREW OPERATING MANUAL</small>	<b>FLIGHT PLANNING</b>		2.05.30	P 48
	<b>INTEGRATED CRUISE</b>		SEQ 072	REV 07

### DESCENT CORRECTION

Correct the fuel and the time values determined in the integrated cruise tables as follows to take into account the descent down to 1500 feet followed by 6 min IFR approach and landing.

### LONG RANGE CRUISE

CORRECTION ON FUEL CONSUMPTION (1000 lb)									
FL	WEIGHT OVERHEAD DESTINATION (1000 lb)								Time Correction
	280	300	320	340	360	380	400	420	
290 and above	1.3	1.4	1.5	1.6	1.8	1.9	2.1	2.2	10 min
270	1.2	1.3	1.5	1.6	1.7	1.8	2.0	2.1	8 min
250	1.2	1.3	1.4	1.5	1.6	1.8	1.9	2.0	
200	1.1	1.2	1.3	1.4	1.5	1.6	1.7	1.8	
150	1.0	1.0	1.1	1.2	1.3	1.4	1.5	1.5	
100	0.8	0.8	0.9	0.9	1.0	1.0	1.1	1.2	

### LRC, M.80, M.82, M.84 FROM OPTIMUM FL

CORRECTION ON FUEL CONSUMPTION (1000 lb)									
280	WEIGHT OVERHEAD DESTINATION (1000 lb)								Time Correction
	300	320	340	360	380	400	420		
1.3	1.5	1.6	1.8	2.0	2.1	2.3	2.4	11 min	

Figure C.15 Descent correction tables (Operating Manual)

<b>A330</b> <small>FLIGHT CREW OPERATING MANUAL</small>	<b>FLIGHT PLANNING</b>	2.05.50	P 3
	ALTERNATE	SEQ 147	REV 09

ALTERNATE PLANNING FROM DESTINATION TO ALTERNATE AIRPORT								
GO-AROUND : 1100 LB - CLIMB : 250KT/300KT/M.80 - CRUISE : LONG RANGE								
DESCENT : M.80/300KT/250KT - VMC PROCEDURE : 350 LB (4MIN)								
REF. LDG WT AT ALT = 310000 LB			ISA			FUEL CONSUMED (LB)		
NORMAL AIR CONDITIONING			CG = 30.0 %			TIME (H.MIN)		
ANTI ICING OFF								
AIR DIST. (NM)	FLIGHT LEVEL					CORRECTION ON FUEL CONSUMPTION (LB/1000LB)		
	230	270	310	350	390	FL230 FL270	FL310 FL350	FL390
<b>150</b>	6376 0.31	6406 0.30				7		0
<b>200</b>	7757 0.39	7667 0.38	7694 0.37	7755 0.36		9	10	0
<b>250</b>	9141 0.47	8930 0.46	8859 0.45	8853 0.43	8875 0.43	11	13	14
<b>300</b>	10527 0.55	10196 0.54	10026 0.53	9952 0.50	9911 0.49	13	15	16
<b>350</b>	11917 1.03	11463 1.02	11196 1.01	11054 0.57	10950 0.56	15	17	18
<b>400</b>	13309 1.12	12733 1.11	12369 1.09	12157 1.04	11990 1.03	16	19	20
<b>450</b>	14704 1.20	14005 1.19	13545 1.17	13263 1.11	13033 1.09	18	21	22
<b>500</b>	16101 1.28	15279 1.27	14723 1.25	14370 1.18	14078 1.16	20	23	24
<b>550</b>	17501 1.36	16555 1.35	15904 1.32	15479 1.25	15126 1.22	22	25	26
<b>600</b>	18904 1.44	17834 1.43	17088 1.40	16589 1.32	16175 1.29	24	27	28
<b>650</b>	20310 1.52	19115 1.51	18274 1.48	17704 1.39	17227 1.36	26	30	31
<b>700</b>	21719 2.00	20398 1.59	19464 1.56	18820 1.46	18281 1.42	28	32	33
<b>750</b>	23130 2.09	21683 2.07	20656 2.04	19939 1.53	19337 1.49	29	34	35
<b>800</b>	24545 2.17	22970 2.15	21850 2.12	21060 2.00	20394 1.55	31	36	37
<b>850</b>	25962 2.25	24259 2.23	23047 2.20	22184 2.07	21454 2.02	33	39	39
<b>900</b>	27382 2.33	25551 2.31	24247 2.28	23309 2.14	22517 2.08	35	41	41
<b>950</b>	28805 2.41	26845 2.40	25450 2.35	24437 2.21	23581 2.15	37	43	44
<b>1000</b>	30230 2.49	28141 2.48	26656 2.43	25568 2.28	24647 2.22	38	46	46
<b>1050</b>	31659 2.57	29440 2.56	27864 2.51	26700 2.35	25715 2.28	40	48	48
<b>1100</b>	33090 3.05	30741 3.04	29076 2.59	27835 2.42	26786 2.35	42	50	50
<b>1150</b>	34525 3.13	32044 3.12	30290 3.07	28973 2.49	27859 2.41	44	53	53
<b>1200</b>	35960 3.21	33349 3.20	31507 3.15	30112 2.56	28935 2.48	45	55	55
<b>PACK FLOW LO</b>		<b>PACK FLOW HI OR/ AND CARGO COOL ON</b>		<b>ENGINE ANTI ICE ON</b>		<b>TOTAL ANTI ICE ON</b>		
ΔFUEL = - 0.4 %		ΔFUEL = + 1 %		ΔFUEL = + 1.5 %		ΔFUEL = + 6 %		

FLIP23D A330-223 PW4168A 2520 03001.3000101100250300 .8001 .00000 350 0300350310 0 485441198361 18590 FCOM-02-05-50-003-077

Figure C.16 Alternate determination tables (Operating Manual)

<b>A330</b> <small>FLIGHT CREW OPERATING MANUAL</small>	<b>FLIGHT PLANNING</b>  <b>GENERAL</b>	2.05.10	P 2
		SEQ 010	REV 06

### MINIMUM RECOMMENDED FUEL REQUIREMENTS

The total fuel quantity required to fly a given sector is the sum of the following quantities:

#### **TAXI FUEL**

Quantity required for startup and taxi. Fuel calculation is based on a consumption of

**25 kg/min** or **55 lb/min**  
 Average quantity (12 minutes) → **300 kg** or **660 lb**

#### **TRIP FUEL**

Fuel required from departure to destination includes the following quantities :

- Takeoff and climb at selected speed.
- Cruise at selected speed.
- Descent from cruising level to 1500 feet above destination airport.
- Approach and landing. Fuel calculation is based on a consumption of

**40 kg/min** or **90 lb/min**  
 Average quantity (6 minute IFR) → **240 kg** or **540 lb**

#### **RESERVE FUEL**

This quantity includes :

##### “En Route” reserve fuel (contingency fuel)

- According to national regulations and company policy (generally based on a percentage of trip fuel).

##### Alternate fuel

- Fuel required to fly from destination to alternate airport.

It includes go-around **500 kg** or **1100 lb** , climb to cruising level, cruise at long range speed, descent and approach procedure.

**160 kg or 360 lb for 4 minutes VFR**

##### Holding Fuel

Calculation of holding fuel should take into account the altitude of the alternate and the landing weight at the alternate, using holding charts of chapter 3.05.25.

A conservative quantity corresponding to 30 minute holding at 1500 feet above alternate airport elevation at green dot speed in the clean configuration is

**2400 kg** or **5300 lb** .

Figure C.17 General information of constants (Operating Manual)

## C.2 Comparison to computed Results of the modified Program

**Table C.1** Comparison of results of LR speed example

Output Summary	unit	calculated results	Operating Manual
<b>Run Number</b>		1	
Ramp Weight	lb	440900	440700
Brake Release Weight	lb	440000	440000
Payload	lb	50500	50500
OEW	lb	259600	259600
HLFC drag reduction	lb	0,00%	
HLFC fuel flow increase	%	0,00%	
Contingency	%	5,0%	5,0%
Range	nm	4381	4380
Trip fuel	lb	109061	110100
Trip time	hr min	09:42	09:38
Block fuel	lb	110361	
Block time	hr min	10:22	
Alternate	nm	250	250
Hold time	hr min	00:30	00:30
<b>Fuel Breakdown</b>			
Start up and taxi	lb	900	700
Trip fuel	lb	109061	110100
Alternate and land	lb	8802	9000
Final reserve (Holding)	lb	4881	5300
Contingency fuel	lb	5453	5500
Additional	lb	0	0
Tankered fuel	lb	1702	0
Total fuel	lb	<b>130800</b>	130600
<b>Trip Fuel Breakdown</b>			
Takeoff, climb to 1500 ft	lb	1791	
Climb to cruise altitude	lb	7763	
Cruise	lb	97801	
Descent to 1500 ft	lb	1205	
Approach & land	lb	500	
<b>Total trip fuel (excl. taxi)</b>	lb	<b>109061</b>	110100

## Appendix D

### Example according to the Operating Manual A330

#### D.1 Example for a fixed Mach number

This example accords to the **Operating Manual** for an aircraft of the version A330. It is established to achieve a greater similarity to conditions fixed in the program used. The necessary input parameters are given in table 5.8 in chapter 5.2.2. A wind correction is left out, since still air conditions are assumed. In the integrated cruise table shown in figures D.1 to D.3 a range of 8693 nm and a time of 1136 min can be found for the start weight of 480,000 lb. All three values are entered the table D.1.

On account of the step climb performed at a gross weight of 454,500 lb, which is apparent because of the change in TAS, the mission is split at this point. This would not have been necessary and has only descriptive reasons. The appropriate range equals to 7792 nm and the time to 1019 min. In the box designated with "1" in table D.1, the differences between the weights, distances and times are calculated, as well as the remaining distance by subtracting the already flown distance from the input range defined at the beginning.

**Table D.1** Cruise fuel and time calculation

Mach number	0.80 opt. FL
Initial Flightlevel:	FL350
Ground Distance:	5000nm
Wind ('-' head/'+' tail)	0 kt
Air distance	5000 nm

FL: 350

Overhead Departure	
Weight:	480000 lb
Distance:	8693 nm
Time:	1136 min

Start of climb segment	
Weight:	454500 lb
Distance:	7792 nm
Time:	1019 min

1	
Fuel:	35500 lb
Distance:	901 nm
Time:	117 min
Remaining Distance:	4099 nm

FL: 390

Begin of second cruise segment	
Weight:	454500 lb
Distance:	7792 nm
Time:	1019 min

Overhead Destination	
Weight:	353717 lb
Distance:	3693 nm
Time:	483 min

2	
Fuel:	100783 lb
Distance:	4099 nm
Time:	536 min
Remaining Distance:	0 nm

Total Values	
Weight overhead departure:	480000 lb
Weight overhead destination:	353717 lb
Fuel:	136283 lb
Time:	653 min

The values from the start of climb segment represent also the weight, distance and time at the begin of the second cruise segment, since the more needed fuel to perform the step climb is considered later. Because the remaining distance at destination must amount to zero, the in the second cruise segment covered distance is equivalent to the remaining distance of 4099 nm. By calculating the difference between this and distance parameter at the begin of this segment, which amounts to 7792 nm, a value of 3693 nm is obtained. With this the appropriate weight and time can be determined from the integrated cruise table from figure D.1. Since the value cannot be found, this must be done by interpolation between to adjacent values, which leads to a time of 483 min and a weight overhead departure of 353,717 lb.

The differences between the weights and times represent the time needed and the fuel used in this second cruise segment and can be entered in the in the box designated with “2” in table D.1. Adding the corresponding values of the boxes “1” and ”2” gives the fuel used and the time needed in performing a cruise over 5000 nm. These values are not very useful, as all other parts of the flight mission are not yet considered. The BRW and the weight overhead destination are used succeeding to carry out the necessary corrections. Both values are listed in table D.2.

**Table D.2** Corrections and calculation of block fuel, payload and flight time

1	(1) MaxTO Weight at BRAKE RELEASE		4	8	0	0
2	Weight Overhead Destination		3	5	3	7
3	- Temperature Correction for CRUISE	-			0	0
4	+ Correction for Air Conditioning (+ for LO, - for HI)	+			0	0
5	- Climb Correction	-			6	5
6	+ TO Altitude Correction	+			0	0
7	- Step Climb Correction	-			0	4
8	= Corrected Weight Overhead Destination	=	3	4	6	8
9	+ DESCENT correction (including 6 min IFR)	+			1	9
10	(2) Landing Weight at Destination	=	3	4	8	7
11	- ALTERNATE Fuel	-			9	3
12	= ALTERNATE Landing Weight	=	3	3	9	4
13	- HOLDING	-			5	3
14	= Weight at END OF HOLDING	=	3	3	4	1
15	TRIP FUEL (1) – (2)		1	3	1	3
16	- “En Route” Reserve	-			6	6
17	(3) ZERO FUEL WEIGHT	=	3	2	7	5
18	- OPERATING WEIGHT EMPTY	-	2	5	9	6
19	= Max Allowable Payload	=		6	7	9

#### BLOCK FUEL CALCULATION

20	Required Fuel (1) – (3)		1	5	2	5
21	+ Taxi	+			0	7
22	= Block Fuel	=	1	5	3	2

#### FLIGHT TIME CALCULATION (H.MIN)

23	Time from integrated cruise table		1	0	5	3
24	+ CLIMB Correction	+		0	0	6
25	+ Descent Correction (including 6 min IFR)	+		0	1	0
26	= Flight Time	=	1	1	0	9



The climb correction term is determined from figure C.14 for a velocity of Mach 0.80 and a BRW of 480,000 lb and amounts to 6,500 lb. Additionally, the step climb is considered by 400 lb, which is the up-rounded value of a proposed amount of 350 lb, also found in figure C.14. Both correction terms are subtracted from the weight overhead destination, since the aircraft engines burn more fuel while performing a climb than performing a cruise. All other corrections of lines 3 to 7 in table D.2 are not necessary on account of the chosen input parameters, which gives a corrected weight overhead destination of 346,800 lb.

Now, the descent correction term is determined from figure C.15, based on the weight overhead destination. An interpolation leads to an amount of about 1,900 lb, which, of course, must be added to calculate the landing weight at destination of 348,700 lb.

Subsequently, the alternate fuel according to the international requirements has to be determined from figure C.16. By assuming that 250 nm flown at FL310 are required, it leads to an amount of 8,859 lb additional fuel needed. However, this value is based on the assumption of an alternate landing weight of 310,000 lb. Therefore, another correction factor is provided in figure C.16, which amounts to 13 in this case and has to be handled in the following way using also the landing weight at destination:

$$348,700 \text{ lb} - 8,859 \text{ lb} = 339,841 \text{ lb} \quad (\text{D-1})$$

$$\left( \frac{339,841 \text{ lb} - 310,000 \text{ lb}}{1,000} \right) \cdot 13 = 388 \text{ lb} \quad (\text{D-2})$$

$$8,859 \text{ lb} + 388 \text{ lb} = \underline{\underline{9,247 \text{ lb}}} \quad (\text{D-3})$$

Thus, an amount of 9,300 lb is considered in the calculation in order to do not neglect about 50 lb fuel. Subtraction of this value leads to a landing weight at alternate of 339,400 lb. Finally, fuel needed for the hold, which is defined as a constant of 5,300 lb in figure C.17, has to be subtracted, which gives an weight at the end of hold of 334,100 lb.

The trip fuel is obviously represented by the difference between BRW and landing weight at destination and equals to 131,300 lb. From this the contingency fuel, here called en-route reserve, can be calculated, which amounts to 5% of the trip fuel, and thus to 6,600 lb. This leads to a ZFW of 327,500 lb. Since the OEW weight is known, the maximum allowable payload for this flight mission is obtained and equals to 67,900 lb.

Eventually, the block fuel and the flight time are determined by applying values, which are constant for this mission and can be found in figures C.14, C.15 and C.17. This results in a flight time of 11:09 hrs and a fuel of 153,200 lb necessary to be taken on-board.

<b>A330</b> FLIGHT CREW OPERATING MANUAL	<b>FLIGHT PLANNING</b>		2.05.30	P 2
	<b>INTEGRATED CRUISE</b>		SEQ 147	REV 09

<b>INTEGRATED CRUISE</b>												
MAX. CRUISE THRUST LIMITS NORMAL AIR CONDITIONING ANTI-ICING OFF			ISA CG=37.0%			DISTANCE (NM) TIME (MIN)		<b>M.80 OPT FL</b>				TAS (KT)
WEIGHT (1000LB)	0	.5	1.0	1.5	2.0	2.5	3.0	3.5	4.0	4.5		
<b>280</b>	0 0	27 4	54 7	80 10	107 14	134 17	160 21	187 24	214 28	240 31	459	
<b>285</b>	267 35	293 38	320 42	346 45	373 49	399 52	426 56	452 59	479 63	505 66	459	
<b>290</b>	531 69	558 73	584 76	610 80	637 83	663 87	689 90	715 94	742 97	768 100	459	
<b>295</b>	794 104	820 107	846 111	872 114	898 117	924 121	950 124	976 128	1002 131	1028 134	459	
<b>300</b>	1054 138	1080 141	1106 145	1132 148	1157 151	1183 155	1209 158	1235 161	1261 165	1286 168	459	
<b>305</b>	1312 172	1338 175	1363 178	1389 182	1414 185	1440 188	1465 192	1491 195	1516 198	1542 202	459	
<b>310</b>	1567 205	1593 208	1618 212	1643 215	1669 218	1694 222	1719 225	1745 228	1770 231	1795 235	459	
<b>315</b>	1820 238	1845 241	1870 245	1896 248	1921 251	1946 254	1971 258	1996 261	2021 264	2046 267	459	
<b>320</b>	2071 271	2096 274	2120 277	2145 281	2170 284	2195 287	2220 290	2244 293	2269 297	2294 300	459	
<b>325</b>	2319 303	2343 306	2368 310	2392 313	2417 316	2442 319	2466 322	2491 326	2515 329	2539 332	459	
<b>330</b>	2564 335	2588 338	2613 342	2637 345	2661 348	2686 351	2710 354	2734 358	2758 361	2783 364	459	
<b>335</b>	2807 367	2831 370	2855 373	2879 376	2903 380	2927 383	2951 386	2975 389	2999 392	3023 395	459	
<b>340</b>	3047 398	3071 402	3095 405	3119 408	3143 411	3166 414	3190 417	3214 420	3238 423	3261 426	459	
<b>345</b>	3285 430	3309 433	3332 436	3356 439	3379 442	3403 445	3426 448	3450 451	3473 454	3497 457	459	
<b>350</b>	3520 460	3543 463	3567 466	3590 469	3613 472	3636 475	3660 479	3683 482	3706 485	3729 488	459	
<b>355</b>	3752 491	3775 494	3798 497	3821 500	3844 503	3867 506	3890 509	3913 512	3936 515	3959 518	459	
<b>360</b>	3982 521	4004 524	4027 527	4050 530	4072 533	4095 535	4118 538	4140 541	4163 544	4185 547	459	
<b>365</b>	4208 550	4230 553	4253 556	4275 559	4297 562	4320 565	4342 568	4364 571	4386 574	4408 576	459	
<b>370</b>	4430 579	4452 582	4475 585	4497 588	4515 590	4533 593	4555 596	4577 598	4598 601	4620 604	459	
<b>375</b>	4642 607	4664 610	4686 613	4707 616	4729 618	4751 621	4772 624	4794 627	4816 630	4837 633	459	
<b>380</b>	4859 635	4880 638	4902 641	4923 644	4945 647	4966 649	4988 652	5009 655	5031 658	5052 661	459	
<b>385</b>	5073 663	5095 666	5116 669	5137 672	5158 675	5180 677	5201 680	5222 683	5243 686	5264 688	459	
<b>390</b>	5285 691	5307 694	5328 697	5349 699	5370 702	5391 705	5412 708	5433 710	5454 713	5474 716	459	
<b>395</b>	5495 719	5516 721	5537 724	5558 727	5578 729	5599 732	5620 735	5641 738	5661 740	5682 743	459	
PACK FLOW LO ΔFUEL = - 0.4 %			PACK FLOW HI OR/ AND CARGO COOL ON ΔFUEL = + 1 %			ENGINE ANTI ICE ON ΔFUEL = + 1.5 %			TOTAL ANTI ICE ON ΔFUEL = + 7 %			

11.1-08FOA330-223 PW4168A 22700000C5LB370 0 018590 0 0 1.0. 0. 00 0 01.800.000.000 0 FCOM-GO 02-05-30-002-077

Figure D.1 Integrated cruise table for M0.80 opt. FL (part 1) (Operating Manual)

 <b>A330</b> <small>FLIGHT CREW OPERATING MANUAL</small>	<b>FLIGHT PLANNING</b>	2.05.30	P 3
	<b>INTEGRATED CRUISE</b>	SEQ 147	REV 09

<b>INTEGRATED CRUISE</b>												
MAX. CRUISE THRUST LIMITS NORMAL AIR CONDITIONING ANTI-ICING OFF				ISA CG=37.0%		DISTANCE (NM) TIME (MIN)		<b>M.80 OPT FL</b>				TAS (KT)
WEIGHT (1000LB)	0	.5	1.0	1.5	2.0	2.5	3.0	3.5	4.0	4.5	TAS (KT)	
<b>400</b>	5702 746	5723 748	5743 751	5764 754	5785 756	5805 759	5825 762	5846 764	5866 767	5886 770	459	
<b>405</b>	5907 772	5927 775	5947 778	5967 780	5988 783	6008 786	6028 788	6046 791	6061 793	6080 795	459	
<b>410</b>	6100 798	6120 800	6140 803	6160 806	6180 808	6200 811	6220 813	6240 816	6260 819	6280 821	459	
<b>415</b>	6299 824	6319 826	6339 829	6359 831	6378 834	6398 837	6418 839	6438 842	6457 844	6477 847	459	
<b>420</b>	6496 849	6516 852	6536 855	6555 857	6575 860	6594 862	6614 865	6633 867	6653 870	6672 872	459	
<b>425</b>	6691 875	6711 878	6730 880	6750 883	6769 885	6788 888	6808 890	6827 893	6846 895	6865 898	459	
<b>430</b>	6885 900	6904 903	6923 905	6942 908	6961 910	6980 913	7000 915	7019 918	7038 920	7057 923	459	
<b>435</b>	7076 925	7095 928	7114 930	7133 933	7152 935	7170 938	7189 940	7208 943	7227 945	7246 947	459	
<b>440</b>	7265 950	7283 952	7302 955	7321 957	7340 960	7358 962	7377 965	7395 967	7414 969	7433 972	459	
<b>445</b>	7451 974	7470 977	7488 979	7507 982	7525 984	7543 986	7562 989	7580 991	7599 994	7617 996	459	
<b>450</b>	7635 998	7652 1001	7667 1002	7683 1005	7701 1007	7719 1009	7737 1012	7755 1014	7774 1016	7792 1019	459	
<b>455</b>	7810 1021	7828 1023	7846 1026	7864 1028	7882 1031	7900 1033	7918 1035	7936 1038	7954 1040	7972 1042	461	
<b>460</b>	7990 1045	8008 1047	8026 1049	8043 1052	8061 1054	8079 1056	8097 1058	8115 1061	8133 1063	8150 1065	461	
<b>465</b>	8168 1068	8186 1070	8204 1072	8221 1075	8239 1077	8257 1079	8274 1082	8292 1084	8310 1086	8327 1088	461	
<b>470</b>	8345 1091	8362 1093	8380 1095	8397 1098	8415 1100	8432 1102	8450 1104	8467 1107	8485 1109	8502 1111	461	
<b>475</b>	8520 1113	8537 1116	8555 1118	8572 1120	8589 1123	8607 1125	8624 1127	8641 1129	8659 1132	8676 1134	461	
<b>480</b>	8693 1136	8710 1138	8727 1141	8745 1143	8762 1145	8779 1147	8796 1149	8813 1152	8830 1154	8847 1156	461	
<b>485</b>	8864 1158	8881 1161	8898 1163	8915 1165	8932 1167	8949 1169	8966 1172	8983 1174	9000 1176	9017 1178	461	
<b>490</b>	9034 1180	9051 1183	9067 1185	9084 1187	9101 1189	9118 1191	9134 1193	9151 1196	9168 1198	9184 1200	461	
<b>495</b>	9201 1202	9218 1204	9234 1206	9251 1209	9267 1211	9281 1212	9294 1214	9310 1216	9327 1218	9343 1221	461	
<b>500</b>	9359 1223	9376 1225	9392 1227	9409 1229	9425 1231	9441 1233	9458 1235	9474 1237	9491 1240	9507 1242	465	
<b>505</b>	9523 1244	9540 1246	9556 1248	9572 1250	9588 1252	9605 1254	9621 1256	9637 1258	9653 1261	9669 1263	465	
<b>510</b>	9686 1265	9702 1267	9718 1269	9734 1271	9750 1273	9766 1275	9782 1277	9798 1279	9815 1281	9831 1283	465	
<b>515</b>	9847 1285	9863 1288	9879 1290	9895 1292	9911 1294	9927 1296	9943 1298	9958 1300	9974 1302	9990 1304	465	
PACK FLOW LO			PACK FLOW HI OR/ AND CARGO COOL ON			ENGINE ANTI ICE ON			TOTAL ANTI ICE ON			
ΔFUEL = - 0.4 %			ΔFUEL = + 1 %			ΔFUEL = + 1.5 %			ΔFUEL = + 7 %			

11.1-08FOA330-223 PW4168A 2270000C5LB370 0 018590 0 0 1 1.0 0 .00 0 01 .800 .000 .000 0 FCOM-GO 02-05-30-003-077

Figure D.2 Integrated cruise table for M0.80 opt. FL (part 2) (Operating Manual)

 <b>A330</b> FLIGHT CREW OPERATING MANUAL	<b>FLIGHT PLANNING</b>		2.05.30	P 4
	INTEGRATED CRUISE		SEQ 147	REV 09

INTEGRATED CRUISE												
MAX. CRUISE THRUST LIMITS NORMAL AIR CONDITIONING ANTI-ICING OFF				ISA CG=37.0%		DISTANCE (NM) TIME (MIN)		<b>M.80 OPT FL</b>				
WEIGHT (1000LB)	0	.5	1.0	1.5	2.0	2.5	3.0	3.5	4.0	4.5	TAS (KT)	
<b>520</b>	10006 1306	10022 1308	10038 1310	10054 1312	10070 1314	10085 1316	10101 1318	10117 1320	10133 1322	10149 1324	465	
<b>525</b>	10164 1326	10180 1328	10196 1331	10212 1333	10227 1335	10243 1337	10259 1339	10274 1341	10290 1343	10305 1345	465	
<b>530</b>	10321 1347	10337 1349	10352 1351	10368 1353	10383 1355	10399 1357	10414 1359	10430 1361	10445 1363	10460 1365	465	
<b>535</b>	10476 1367										469	
<b>540</b>												
<b>545</b>												
<b>550</b>												
PACK FLOW LO $\Delta$ FUEL = - 0.4 %			PACK FLOW HI OR/ AND CARGO COOL ON $\Delta$ FUEL = + 1 %			ENGINE ANTI ICE ON $\Delta$ FUEL = + 1.5 %			TOTAL ANTI ICE ON $\Delta$ FUEL = + 7 %			

11.1-08FOA330-223 PW4168A 22700000C5LB370 0 018590 0 0 1 1.0 .00 0 01 .800 .000 .000 0 FCDM-GO 02-05-30-004-077

Figure D.3 Integrated cruise table for M0.80 opt. FL (part 3) (Operating Manual)

## D.2 Comparison to computed Results of the modified Program

**Table D.3** Comparison of results of fixed Mach number example

<b>Output Summary</b>	<b>unit</b>	<b>calculated results</b>	<b>Operating Manual</b>
<b>Run Number</b>		1	
Ramp Weight	lb	480900	480700
Brake Release Weight	lb	480000	480000
Payload	lb	67900	67900
OEW	lb	259600	259600
HLFC drag reduction	lb	0,00%	
HLFC fuel flow increase	%	0,00%	
Contingency	%	5,0%	5,0%
Range	nm	5000	5000
Trip fuel	lb	130893	131300
Trip time	hr min	11:04	11:09
Block fuel	lb	132193	
Block time	hr min	11:44	
Alternate	nm	250	250
Hold time	hr min	00:30	00:30
<b>Fuel Breakdown</b>			
Start up and taxi	lb	900	700
Trip fuel	lb	130893	131300
Alternate and land	lb	9176	9300
Final reserve (Holding)	lb	5387	5300
Contingency fuel	lb	6545	6600
Additional	lb	0	0
Tankered fuel	lb	499	0
Total fuel	lb	<b>153400</b>	153200
<b>Trip Fuel Breakdown</b>			
Takeoff, climb to 1500 ft	lb	1972	
Climb to cruise altitude	lb	8379	
Cruise	lb	118805	
Descent to 1500 ft	lb	1237	
Approach & land	lb	500	
<b>Total trip fuel (excl. taxy)</b>	lb	<b>130893</b>	131300

## Appendix E

### Airspeed conversions

The following equations are based on the unit knots for the airspeeds and according to **Boeing (1989)**

Determination of Mach number from other airspeed information:

from CAS:

$$M = \sqrt{5 \left[ \left( \frac{1}{d} \left\{ \left[ 1 + 0.2 \left( \frac{CAS}{661.4786} \right)^2 \right]^{3.5} - 1 \right\} + 1 \right)^{\frac{1}{3.5}} - 1 \right]}$$

from EAS:

$$M = \frac{EAS}{661.4786} \sqrt{\frac{1}{d}}$$

from TAS:

$$M = \frac{v}{661.4786 \sqrt{q}}$$

Determination of calibrated air speed (CAS) from other airspeed information:

from Mach number:

$$CAS = 1479.1 \sqrt{\left[ \left( d \left[ \left( 0.2M^2 + 1 \right)^{3.5} - 1 \right] + 1 \right)^{\frac{1}{3.5}} - 1 \right]}$$

from EAS:

$$CAS = 1479.1 \sqrt{\left[ \left( d \left\{ \left[ 1 + \frac{1}{d} \left( \frac{EAS}{1479.1} \right)^2 \right]^{3.5} - 1 \right\} + 1 \right)^{\frac{1}{3.5}} - 1 \right]}$$

from TAS:

$$CAS = 1479.1 \sqrt{\left[ \left( d \left\{ \left[ 1 + \frac{1}{q} \left( \frac{v}{1479.1} \right)^2 \right]^{3.5} - 1 \right\} + 1 \right)^{\frac{1}{3.5}} - 1 \right]}$$

Determination of equivalent air speed (EAS) from other airspeed information:

from Mach number:  $EAS = 661.4786M \sqrt{d}$

from CAS: 
$$EAS = 1479.1 \sqrt{d \left[ \left( \frac{1}{d} \left[ 1 + 0.2 \left( \frac{CAS}{661.4786} \right)^2 \right]^{3.5} - 1 \right) + 1 \right]^{\frac{1}{3.5}} - 1}$$

from TAS:  $EAS = v \sqrt{s} = v \sqrt{\frac{d}{s}}$

Determination of equivalent air speed (EAS) from other airspeed information:

from Mach number:  $v = 661.4786 M \sqrt{q}$

from CAS: 
$$v = 1479.1 \sqrt{q \left[ \left( \frac{1}{d} \left[ 1 + 0.2 \left( \frac{CAS}{661.4786} \right)^2 \right]^{3.5} - 1 \right) + 1 \right]^{\frac{1}{3.5}} - 1}$$

from EAS:  $v = \frac{EAS}{\sqrt{s}} = EAS \sqrt{\frac{q}{d}}$

# Appendix F

## Units conversions

(Young, 1999)

Length:	1 in = 2.54 cm
	1 ft = 0.3048 m
	1 nm = 1.852 km
Area:	1 inch <sup>2</sup> = 6.4516 cm <sup>2</sup>
	1 ft <sup>2</sup> = 9.2902 · 10 <sup>-2</sup> m <sup>2</sup>
Volume:	1 ft <sup>3</sup> = 2.832 · 10 <sup>-2</sup> m <sup>3</sup>
Mass:	1 lb = 0.4536 kg
	1 slug = 14.59 kg
Density:	1 slug/ft <sup>3</sup> = 515.4 kg/m <sup>3</sup>
Speed:	1 ft/sec = 0.3048 m/sec
	1 kt = 0.5144 m/sec
	1 nm = 1 kt = 1.852 km/hr
Force:	1 lb = 4.448 N
Pressure:	1 lb/in <sup>2</sup> = 1 N/m <sup>2</sup>



# Appendix G

## ISA Table and Basic Data

Table G.1 ISA Table (Young, 2000)

Height (ft)	Theta	Temp (K)	Temp (C)	Delta	Pressure (Pa)	Pressure (lb/ft <sup>2</sup> )	Sigma	Density (kg/m <sup>3</sup> )	Density slugs/ft <sup>3</sup>	a (m/s)	a (ft/s)	a (kts)
0	1,0000	288,15	15,00	1,0000	101325	2116,22	1,0000	1,2250	2,377E-03	340,3	1116,5	661,5
1000	0,9931	286,17	13,02	0,9644	97717	2040,85	0,9711	1,1896	2,308E-03	339,1	1112,6	659,2
2000	0,9862	284,19	11,04	0,9298	94213	1967,68	0,9428	1,1549	2,241E-03	337,9	1108,7	656,9
3000	0,9794	282,21	9,06	0,8962	90812	1896,64	0,9151	1,1210	2,175E-03	336,8	1104,9	654,6
4000	0,9725	280,23	7,08	0,8637	87511	1827,70	0,8881	1,0879	2,111E-03	335,6	1101,0	652,3
5000	0,9656	278,24	5,09	0,8320	84307	1760,79	0,8617	1,0555	2,048E-03	334,4	1097,1	650,0
6000	0,9587	276,26	3,11	0,8014	81200	1695,89	0,8359	1,0239	1,987E-03	333,2	1093,2	647,7
7000	0,9519	274,28	1,13	0,7716	78185	1632,94	0,8106	0,9930	1,927E-03	332,0	1089,3	645,4
8000	0,9450	272,30	-0,85	0,7428	75262	1571,89	0,7860	0,9629	1,868E-03	330,8	1085,3	643,0
9000	0,9381	270,32	-2,83	0,7148	72428	1512,70	0,7620	0,9334	1,811E-03	329,6	1081,4	640,7
10000	0,9312	268,34	-4,81	0,6877	69682	1455,33	0,7385	0,9046	1,755E-03	328,4	1077,4	638,3
11000	0,9244	266,36	-6,79	0,6614	67020	1399,74	0,7156	0,8766	1,701E-03	327,2	1073,4	636,0
12000	0,9175	264,38	-8,77	0,6360	64441	1345,87	0,6932	0,8491	1,648E-03	326,0	1069,4	633,6
13000	0,9106	262,39	-10,76	0,6113	61943	1293,70	0,6713	0,8224	1,596E-03	324,7	1065,4	631,2
14000	0,9037	260,41	-12,74	0,5875	59524	1243,18	0,6500	0,7963	1,545E-03	323,5	1061,4	628,8
15000	0,8969	258,43	-14,72	0,5643	57182	1194,27	0,6292	0,7708	1,496E-03	322,3	1057,3	626,4
16000	0,8900	256,45	-16,70	0,5420	54915	1146,93	0,6090	0,7460	1,448E-03	321,0	1053,3	624,0
17000	0,8831	254,47	-18,68	0,5203	52722	1101,12	0,5892	0,7218	1,401E-03	319,8	1049,2	621,6
18000	0,8762	252,49	-20,66	0,4994	50600	1056,80	0,5699	0,6981	1,355E-03	318,5	1045,1	619,2
19000	0,8694	250,51	-22,64	0,4791	48548	1013,94	0,5511	0,6751	1,310E-03	317,3	1041,0	616,8
20000	0,8625	248,53	-24,62	0,4595	46563	972,49	0,5328	0,6527	1,266E-03	316,0	1036,8	614,3
21000	0,8556	246,54	-26,61	0,4406	44645	932,43	0,5150	0,6308	1,224E-03	314,8	1032,7	611,9
22000	0,8487	244,56	-28,59	0,4223	42791	893,72	0,4976	0,6095	1,183E-03	313,5	1028,6	609,4
23000	0,8419	242,58	-30,57	0,4046	41001	856,32	0,4807	0,5888	1,143E-03	312,2	1024,4	606,9
24000	0,8350	240,60	-32,55	0,3876	39271	820,19	0,4642	0,5686	1,103E-03	311,0	1020,2	604,4
25000	0,8281	238,62	-34,53	0,3711	37601	785,31	0,4481	0,5489	1,065E-03	309,7	1016,0	601,9
26000	0,8212	236,64	-36,51	0,3552	35989	751,64	0,4325	0,5298	1,028E-03	308,4	1011,7	599,4
27000	0,8144	234,66	-38,49	0,3398	34433	719,15	0,4173	0,5112	9,919E-04	307,1	1007,5	596,9
28000	0,8075	232,68	-40,47	0,3250	32932	687,81	0,4025	0,4931	9,568E-04	305,8	1003,2	594,4
29000	0,8006	230,70	-42,45	0,3107	31485	657,58	0,3881	0,4754	9,226E-04	304,5	999,0	591,9
30000	0,7937	228,71	-44,44	0,2970	30090	628,43	0,3741	0,4583	8,893E-04	303,2	994,7	589,3
31000	0,7869	226,73	-46,42	0,2837	28745	600,34	0,3605	0,4417	8,570E-04	301,9	990,3	586,8
32000	0,7800	224,75	-48,40	0,2709	27449	573,28	0,3473	0,4255	8,256E-04	300,5	986,0	584,2
33000	0,7731	222,77	-50,38	0,2586	26201	547,21	0,3345	0,4097	7,950E-04	299,2	981,7	581,6
34000	0,7662	220,79	-52,36	0,2467	24999	522,11	0,3220	0,3944	7,654E-04	297,9	977,3	579,0
35000	0,7594	218,81	-54,34	0,2353	23842	497,96	0,3099	0,3796	7,366E-04	296,5	972,9	576,4
36000	0,7525	216,83	-56,32	0,2243	22729	474,71	0,2981	0,3652	7,086E-04	295,2	968,5	573,8
36089	0,7519	216,65	-56,50	0,2234	22632	472,68	0,2971	0,3639	7,062E-04	295,1	968,1	573,6
37000	0,7519	216,65	-56,50	0,2138	21663	452,43	0,2844	0,3483	6,759E-04	295,1	968,1	573,6
38000	0,7519	216,65	-56,50	0,2038	20646	431,20	0,2710	0,3320	6,442E-04	295,1	968,1	573,6
39000	0,7519	216,65	-56,50	0,1942	19677	410,97	0,2583	0,3164	6,140E-04	295,1	968,1	573,6
40000	0,7519	216,65	-56,50	0,1851	18754	391,68	0,2462	0,3016	5,851E-04	295,1	968,1	573,6
41000	0,7519	216,65	-56,50	0,1764	17874	373,30	0,2346	0,2874	5,577E-04	295,1	968,1	573,6
42000	0,7519	216,65	-56,50	0,1681	17035	355,78	0,2236	0,2739	5,315E-04	295,1	968,1	573,6
43000	0,7519	216,65	-56,50	0,1602	16236	339,09	0,2131	0,2611	5,066E-04	295,1	968,1	573,6
44000	0,7519	216,65	-56,50	0,1527	15474	323,18	0,2031	0,2488	4,828E-04	295,1	968,1	573,6
45000	0,7519	216,65	-56,50	0,1455	14748	308,01	0,1936	0,2371	4,601E-04	295,1	968,1	573,6

**Table G.2** Basic data for ISA -Table Calculation (Young, 2000)

<b>Temperature</b>	<b>value</b>	<b>unit</b>
At sea-level pressure		
T <sub>0</sub> =	288,15	K
In the troposphere		
theta = 1 - (L/T <sub>0</sub> )*h		
L =	0,0019812	K/ft
In the stratosphere		
T =	216,65	K
theta =	0,751865	
<b>Pressure</b>	<b>value</b>	<b>unit</b>
At sea-level pressure		
p <sub>0</sub> =	101325	Pa
p <sub>0</sub> =	2116,217	lb/ft <sup>2</sup>
In the troposphere		
delta = (1-a1*h) <sup>a2</sup>		
a1 =	6,87559E-06	
a2 =	5,25588	
In the stratosphere		
delta = a3*e <sup>(a4-a5h)</sup>		
a3 =	0,223361	
a4 =	1,73457	
a5 =	4,80635E-05	
<b>Density</b>	<b>value</b>	<b>unit</b>
sigma = delta/theta		
sea-level		
rho <sub>0</sub> =	1,225	kg/m <sup>3</sup>
rho <sub>0</sub> =	0,002377	slugs/ft <sup>3</sup>
<b>Speed of Sound</b>	<b>value</b>	<b>unit</b>
sea-level		
a <sub>0</sub> =	340,294	m/s
a <sub>0</sub> =	1116,45	ft/s
a <sub>0</sub> =	661,4786	knots